

Aus der Institut Experimentelle Neurologie der Klinik für Neurologie
der Medizinischen Fakultät Charité – Universitätsmedizin Berlin

DISSERTATION

Involvement of histone acetylation in neuroprotection against
brain ischemic injury

zur Erlangung des akademischen Grades
Doctor of Philosophy in Medical Neurosciences
(PhD in Medical Neurosciences)

vorgelegt der Medizinischen Fakultät
Charité – Universitätsmedizin Berlin

von

Ferah Yildirim

aus Antakya, der Türkei

Gutachter: 1. Prof. Dr. med A. Meisel
2. Prof. Dr. R. Stumm
3. Prof. Dr. R. Veltkamp

Datum der Promotion: 22. 02. 2010

Acknowledgements

I would like to

–sincerely thank my supervisors Prof Dr. Andreas Meisel and Prof Dr. Matthias Endres for giving me the opportunity to work with them on this exciting topic. I am grateful for their support, advice and patience.

–thank Prof Dr. Ulrich Dirnagl for his continuous support and precious advice.

–special thanks to Dr Christoph Harms, Dr Golo Kronenberg and Dr Julian Bösel, from whom I have learnt a lot not only during my PhD but already during my MSc Thesis project.

–thank my friends and colleagues Jan Klohs, Miguel Lopes, Joao Paulo Capela, Florin Gandor, Christel Bonnas, Nicolas Coquery, Ana Ferreira, Dr. Juri Katchanov, Ryan Cordell, Dr Jens Dreier, Martina Füchtemeier, Dr. Hendrik Harms, Takeesha Roland, Vincent Prinz, Dr. Juliane Klehmet, Dr. Karen Gertz, ShengBo Ji and Anja Kahl, who made the life in the lab easy and fun.

–thank the lab members Dr Dorette Freyer, Renate Gusinda, Claudia Muselmann, Marco Foddis, Dirk Megow, Sabine Cho, who at various stages have been helpful technically and scientifically.

–thank Prof. Dr. Josef Priller and Prof Dr. Ute Lindauer for their advice.

–thank our collaborators Dr Klaus Fink in Bonn, Dr Angel Barco, Roman Olivares and Eva Benito in Spain.

–thank Jesus Hernandez for his neverending support, care and encouragement.

–thank my mother, my father, my sister and my brothers for being there for me...Without their endless love and support this work would not have been possible.

This list would grow much larger, if I were to include every single person who has been helpful during my PhD thesis project. I apologize to those whose names are not mentioned. Thanks to all of you. Special thanks to the International Graduate Program Medical Neuroscience of the Charite-Universitätsmedizin Berlin, Germany.

Table of contents

Abbreviations.....	1
1 Summary.....	4
2 Introduction.....	6
2.1 Cerebral ischemia.....	6
2.1.1 Pathophysiology of cerebral ischemia.....	6
2.1.1.1 Excitotoxicity and ionic imbalance.....	7
2.1.1.2 Oxidative and nitrosative stress.....	7
2.1.1.3 Apoptosis.....	8
2.1.1.4 Inflammation.....	8
2.2 Endogenous neuroprotection and ischemic preconditioning in brain.....	10
2.2.1 Ischemic preconditioning/tolerance.....	10
2.2.2 The phenomenon ischemic preconditioning also exists in humans.....	11
2.2.3 Mechanisms of ischemic preconditioning/tolerance.....	11
2.3 Epigenetics.....	12
2.3.1 Nucleosome.....	13
2.3.2 Epigenetic modifications.....	14
2.3.3 Histone acetylation.....	15
2.3.4 Histone acetyltransferase (HAT) families.....	16
2.3.5 Histone deacetylase (HDAC) families.....	17
2.3.6 Regulation of histone acetyltransferase and deacetylase enzyme activities.....	17
2.3.7 Histone acetylation homeostasis.....	18
2.3.8 Pharmacological manipulation of histone acetyltransferase and deacetylase enzyme activities.....	19
2.3.9 Epigenetic mechanisms and neuroprotection against cerebral ischemia.....	20
2.4 Hypotheses.....	21
3 Materials and methods.....	23
3.1 Materials.....	23
3.1.1 Cell culture media and supplements.....	23
3.1.2 Chemicals.....	23
3.1.3 Antibodies, reagents and kits.....	25
3.1.4 Tools & Equipment.....	26
3.1.5 Animals.....	27

3.2 Methods	28
3.2.1 Primary Neuronal Cell Cultures	28
3.2.2 Pre-treatment with Trichostatin A	29
3.2.2.1 Pre-treatment of primary cortical cultures with Trichostatin A	29
3.2.2.2 Pre-treatment of mice with Trichostatin A	29
3.2.3 Injury Paradigms	29
3.2.3.1 Combined oxygen-glucose deprivation (OGD) as injury paradigm in vitro	29
3.2.3.2 Middle cerebral artery occlusion (MCAo) as injury paradigm in vivo	30
3.2.4 Ischemic preconditioning paradigms	31
3.2.4.1 Combined oxygen-glucose deprivation (OGD) as ischemic preconditioning stimulus in vitro	31
3.2.4.2 Middle cerebral artery occlusion (MCAo) as ischemic preconditioning stimulus in vivo	31
3.2.5 Cell Death Assays	32
3.2.5.1 Lactate Dehydrogenase (LDH) assay	32
3.2.5.2 Propidium Iodide staining of dead cells	32
3.2.5.3 MTT reduction test	33
3.2.6 Phalloidin Staining	33
3.2.6.1 Phalloidin Staining of primary cortical cultures	33
3.2.6.2 Phalloidin Staining of mouse brain slices	33
3.2.7 Measurement of intracellular Ca²⁺ in primary cortical cultures	34
3.2.8 Assessment of mitochondrial membrane potential by TMRE Assay	34
3.2.9 Western immunoblotting	35
3.2.9.1 Western immunoblotting of proteins from primary cortical cultures	35
3.2.9.2 Western immunoblotting of proteins from mouse brain	36
3.2.10 ELISA-based Histone Acetyltransferase (HAT) Activity Assay	36
3.2.11 Immunochemical staining	37
3.2.11.1 Immunocytochemistry of primary cortical cultures	37
3.2.11.2 Immunohistochemistry of mouse brain slices	38
3.2.12 Neurological Scoring of Mice- Determination of functional deficits	38

3.2.13 Measurement of physiological variables.....	39
3.2.14 Determination of brain lesion size.....	39
3.1.15 Statistical evaluation.....	39
4 Results.....	40
4.1 Histone acetylation and neuronal ischemic injury.....	40
4.1.1 Histone acetylation levels decrease in neurons following injurious combined oxygen-glucose deprivation.....	40
4.1.2 CREB-binding protein (CBP) is rapidly depleted in neurons following injurious combined oxygen-glucose deprivation.....	41
4.1.3 Curcumin, a CBP's HAT activity inhibitor, exacerbates injury by combined oxygen-glucose deprivation.....	43
4.1.4 CBP-deficient neurons are more susceptible to injury by combined oxygen-glucose deprivation.....	45
4.2 Histone acetylation and brain ischemic preconditioning.....	47
4.2.1 Brief non-injurious ischemia protect mice brain against following severe middle cerebral artery occlusion.....	47
4.2.2 Brief sub-lethal ischemia protects neuronal cultures against following severe combined oxygen-glucose deprivation.....	48
4.2.3 Ischemic preconditioning enhances histone acetylation levels in rat primary cortical cultures and in mice brain.....	49
4.2.4 Ischemic preconditioning enhances histone acetyltransferase (HAT) activity in rat primary cortical cultures.....	52
4.3 Neuroprotection by Trichostatin A (TSA) pre-treatment.....	53
4.3.1 Trichostatin A pre-treatment protects neuronal cultures against ischemic injury.....	53
4.3.2 Trichostatin A pre-treatment protects mice against brain ischemic injury.....	54
4.3.3 Trichostatin A pre-treatment increases histone acetylation levels in vitro in rat primary cortical cultures and in vivo in mice brain.....	56
4.3.4 Enhancement of histone acetylation by Trichostatin A renders neurons more resistant to ischemic injury.....	58
4.3.5 Trichostatin A up-regulates gelsolin expression in neurons and in mice brain..	61
4.3.6 Trichostatin A confers actin filament remodelling.....	64

4.3.7 Trichostatin A reduces intracellular calcium overload caused by ischemic injury.....	66
4.3.8 Trichostatin A prevents loss of mitochondrial membrane potential caused by ischemic injury.....	67
4.3.9 Trichostatin A pre-treatment does not protect gelsolin-deficient mice against brain ischemic injury.....	69
4.3.10 TSA confers actin remodelling in wild-type but not in gelsolin-deficient mice brain.....	70
5 Discussion.....	72
5.1 Histone acetylation and neuronal ischemic injury.....	72
5.1.1 Histone acetylation and CREB-binding protein (CBP) levels rapidly decrease in neurons following ischemic injury.....	72
5.1.2 Loss of CREB-binding protein (CBP) is causally associated to extent of damage caused by neuronal ischemia.....	73
5.2 Histone acetylation and brain ischemic injury.....	74
5.2.1 Brief ischemia protects mice brain against subsequent ischemic injury.....	74
5.2.2 Brief ischemia protects neuronal cultures against subsequent ischemic injury..	75
5.2.3 Mechanisms of brain ischemic preconditioning.....	76
5.2.4 Involvement of histone acetylation in brain ischemic preconditioning.....	77
5.3 Neuroprotection by Trichostatin A pre-treatment.....	78
5.3.1 Histone deacetylase inhibitors are already in clinical use.....	79
5.3.2 HDAC inhibition in experimental models of neurodegenerative and psychiatric diseases.....	79
5.3.3 Induction of cell death vs. cell protection by HDAC inhibitors.....	80
5.3.4 Trichostatin A protects against cerebral ischemia.....	82
5.3.5 Other HDAC inhibitors are also beneficial against cerebral ischemia.....	83
5.3.6 Induction of gelsolin by TSA and subsequent down-stream events.....	85
5.3.7 Other gene targets of HDAC inhibitors.....	86
6 Conclusion.....	88
7 References.....	90
Curriculum Vitae.....	112
Publications and Presentations.....	113
Eidesstattliche Erklärung.....	115

Index of figures

Figure 1: Damaging cascades of events after focal cerebral ischemia.....7

Figure 2: Depiction of the major pathophysiological events evoked by cerebral ischemic injury.....9

Figure 3: Major post-translational histone modifications.....14

Figure 4: Illustration of euchromatin and heterochromatin.....16

Figure 5: Pharmacological inhibition of histone acetyltransferase (HAT) and histone deacetylase (HDAC) enzymes.....20

Figure 6: Histone acetylation levels decrease in neurons after exposure to injurious combined oxygen-glucose deprivation.....40

Figure 7: CBP is depleted in neurons following injurious oxygen-glucose deprivation.....42

Figure 8: Curcumin exacerbates neuronal damage caused by oxygen-glucose deprivation...44

Figure 9: Primary cortical cultures from CBP-deficient mice are more susceptible to injury by oxygen-glucose deprivation.....46

Figure 10: Ischemic preconditioning protects mice brain against injury by middle cerebral artery occlusion and reperfusion.....48

Figure 11: Ischemic preconditioning protects cortical neurons against combined oxygen-glucose deprivation.....49

Figure 12: Histone acetylation levels are increased in rat cortical neurons and in mice brain following ischemic preconditioning.....51

Figure 13: Histone acetyltransferase activity is increased in cortical neurons after ischemic preconditioning.....52

Figure 14: Trichostatin A pretreatment protects primary cortical cultures against combined oxygen-glucose deprivation.....54

Figure 15: Trichostatin A pre-treatment protects mice from middle cerebral artery occlusion and reperfusion.....55

Figure 16: Trichostatin A enhances histone acetylation in cortical cultures and in mice brain.....57

Figure 17: Trichostatin A enhances histone acetylation levels in cortical neurons.....59

Figure 18: Trichostatin A up-regulates gelsolin expression in cortical cultures and in mice brain.....62

Figure 19: Effects of Trichostatin A on filamentous actin.....65

Figure 20: Trichostatin A decreases calcium influx following combined oxygen-glucose deprivation.....66

Figure 21: Trichostatin A decreases loss of mitochondrial membrane potential following combined oxygen/glucose deprivation.....68

Figure 22: Trichostatin A does not protect gelsolin knockout mice against MCAo/reperfusion.....70

Figure 23: Effects of Trichostatin A on filamentous actin levels in mice brain tissue.....71

For my parents

Abbreviations

Acetyl CoA	Acetyl Coenzyme A
ADP	Adenosine diphosphate
AMP	Adenosine monophosphate
AMPA	α -amino-3-hydroxy-5-methyl-4-isoxazole propionic acid
ATP	Adenosine triphosphate
ATPase	Adenosine triphosphatase
BCA	Bicinchoninic acid
Bcl-2	B-cell leukemia 2
Bcl-xL	B-cell leukemia XL
BDNF	Brain derived neurotrophic factor
BSA	Bovine serum albumin
CAMK-IV	Calcium-calmodulin-dependent protein kinase
CNS	Centre Nervous System
CRE	cAMP response element
CREB	cAMP response element binding protein
CBP	CREB-binding protein
DIV	Day in vitro
DNA	Deoxyribonucleic acid
DNase	Deoxyribonuclease
DTT	Dithiothreitol
EDTA	Ethylendiaminetetraacetic acid
EGTA	Ethylene glycol tetraacetic acid
ELISA	Enzyme Linked Immunosorbent Assay
E2F	E2 (adenoviral protein) factor
FCS	Foetal calf serum
FDA	US Food and Drug Administration
GFAP	Glial fibrillary acidic protein
HIF	Hypoxia inducible factor
HIV-tat	Human immunodeficiency virus-transactivator of transcription protein
HSP70	Heat shock proteins 70

iNOS	Inducible nitric oxide synthase
IL-1	Interleukin-1
LDH	Lactate dehydrogenase
LTP	Long term potentiation
MAP2	Microtubule associated protein 2
MABP	Mean arterial blood pressure
MAPK	Mitogen-activating protein kinase
MCAo	Middle cerebral artery occlusion
MeCP2	Methyl-CpG-binding protein 2
mRNA	Messenger ribonucleic acid
MSc	Master of Science
MTT	Thiazolyl blue tetrazolium bromide
NBM	Neurobasal medium
NeuN	Neuronal nuclear protein
NFkb	Nuclear factor kappa B
NMDA	N-methyl D-aspartate
NO	Nitric oxide
OGD	Oxygen-glucose deprivation
OD	Optic density
PaO ₂	Partial pressure of arterial oxygen
PaCO ₂	Partial pressure of arterial carbon dioxide
PBS	Phosphate buffered saline
PCAF	p300/CBP associated factor
PKA	Protein kinase A
RNA	Ribonucleic Acid
ROS	Reactive oxygen species
SOD	Superoxide dismutase
SAHA	Suberanilohydroxamic acid
SDS-PAGE	Sodium dodecyl sulphate-polyacrylamide gel electrophoresis
SP-1	Stimulatory protein-1
TAFII250	TATA box binding protein associated factor II 250
TGF-beta	Tranforming growth factor-beta
TIA	Transient ischemic attack

TLR	Toll-like receptor
TNF-alpha	Tumor necrosis factor-alpha
TMRE	Tetramethylrhodamine ethyl ester
TSA	Trichostatin A
VEGF	Vascular endothelial cell growth factor
VPA	Valproic acid

1 SUMMARY

Histone acetylation is a master epigenetic switch for active gene expression processes, and is therefore considered as a diagnostic feature of ongoing gene expression activities. Aberrant histone acetylation patterns and/or impaired function of histone acetylation machinery were recently linked to manifestation of numerous neurodegenerative conditions such as Huntington's disease, Alzheimer's disease and amyotrophic lateral sclerosis. This PhD thesis work shows loss of histone acetylation patterns in neurons following ischemic injury, and further, it demonstrates protection against cerebral ischemic injury by enhancement of histone acetylation by two different neuroprotective strategies: Ischemic preconditioning and Trichostatin A pre-treatment. Histone acetylation and histone acetyltransferase (HAT) enzyme CREB-binding protein (CBP) levels were rapidly decreased in neurons after ischemic injury. Suppression of histone acetylation, by genetic as well as by pharmacological means, exacerbated the neuronal damage by ischemic injury, suggesting that histone acetylation balance is a determinant factor for neuronal susceptibility to ischemic insult. In contrast to injurious ischemia, ischemic preconditioning enhanced histone acetylation levels in rat primary cortical cultures as well as in mice brain, and proved significant neuroprotection against cerebral ischemia. Enhanced histone acetylation levels were accompanied by increased HAT enzyme activity in neuronal cells after ischemic preconditioning. Histone deacetylase (HDAC) inhibitor Trichostatin A (TSA) increased histone acetylation levels and conferred neuroprotection against cell culture as well as animal models of cerebral ischemia. TSA up-regulated anti-apoptotic and anti-excitotoxic protein gelsolin expression in neuronal cultures and in mice brain, and the down-stream protective pathways involved dynamic actin remodelling, reduction in intracellular calcium overload and stabilisation of mitochondrial membrane potential. TSA did not protect gelsolin knockout mice against brain ischemic injury, underscoring gelsolin's integral role for TSA-induced neuroprotection against cerebral ischemic damage. Altogether, these results not only show a causal involvement of histone hypoacetylation in the pathophysiological cascades after ischemic injury, but they also demonstrate that histone acetylation enhancement by ischemic preconditioning and by TSA pre-treatment confers robust protection against cerebral ischemic injury. Histone acetylation enhancement indicates increased transcriptional activity as in the case of neuroprotective gene expression during the acquisition of ischemia tolerance. On the other hand, loss of histone acetylation probably reflects the loss of neuronal genomic fertility during pathological

progression. Thus, enhancement of histone acetylation appears as an attractive avenue for development of novel treatment strategies for the reduction of brain injury following cerebral ischemia. Given that currently there is no effective treatment for stroke, results of this PhD thesis suggests that HDAC inhibitors like TSA should be evaluated for their potential use for clinical trials in stroke patients. Alternatively, CBP activators and/or agents that increase CBP stabilization might be promising neuroprotective drugs.

2 INTRODUCTION

2.1 CEREBRAL ISCHEMIA

Ischemic stroke, is the third leading cause of death and a major cause of long-lasting disability in industrially developed countries, only surpassed by heart disease and cancer. It is a pathological condition resulting from occlusion or hemorrhage of blood vessels supplying oxygen and essential nutrients to the brain. In all cases, stroke ultimately induces death and/or dysfunction of brain cells, as well as neurological impairments that reflect the location and size of the ischemic brain area. Even though a large number of compounds have been proven to reduce ischemic injury in experimental animal models, clinical trials have reported disappointing results because of toxic side effects. At present the only FDA (US Food and Drug Administration) approved treatment is to provide tissue plasminogen activator (tPA) to re-open occluded blood vessels, however, due to a narrow time-window of 4,5 hours after the stroke onset (Hacke, Kaste et al., 2008; ECASS III), this treatment is only appropriate for a very small number of patients. Thus, research on the discovery of novel mechanisms and the development of new drugs for treating cerebral ischemia are imperative.

2.1.1 Pathophysiology of cerebral ischemia

Cerebral ischemic event triggers a set of complex pathological mechanisms eventually leading to death and/or dysfunction of brain cells. Excitotoxicity and ionic imbalance, oxidative/nitrosative stress, inflammation and apoptosis are some of the ischemia-induced pathophysiological processes, each of which has a distinct time frame, some occurring over minutes, others over hours and days, causing injury to neurons, glia and endothelial cells (Dirnagl et al., 1999; Lo et al., 2003; Gonzalez et al., 2006). Within the core of the ischemic area, where blood flow is most severely restricted, excitotoxic and necrotic cell death occurs within minutes. In the periphery of the ischemic area, where collateral blood flow can buffer the full effects of the stroke, the degree of ischemia and the timing of reperfusion determine the outcome for individual cells. In this ischemic penumbra cell death occurs less rapidly via mechanisms such as apoptosis and inflammation (Dirnagl et al., 1999; Gonzalez et al., 2006).

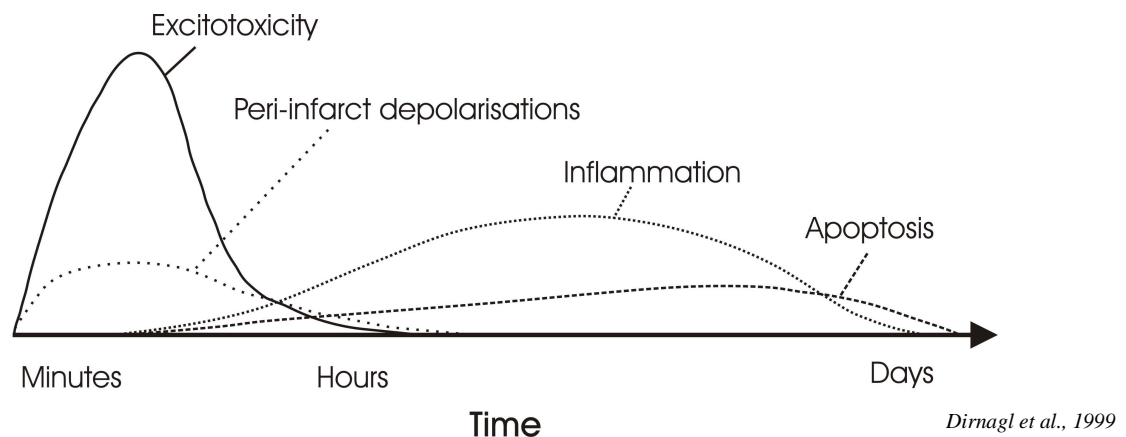


Figure 1 Damaging cascades of events after focal cerebral ischemia. Temporal evolution of the cascades and the impact of each pathological event on final outcome are reflected by the x- and y-axes, respectively.

2.1.1.1 Excitotoxicity and ionic imbalance

After ischemia, Na^+/K^+ -ATPase and Ca^{2+} -ATPase, which are vitally important ion pumps found on the plasma membrane of neurons, can no longer function due to energy depletion. Their impaired functions cause neuronal plasma membrane depolarization, release of potassium into the extracellular space and entry of sodium and calcium into the cells (Caplan et al., 2000). Consequently, calcium dependent proteases, lipases and DNases become active, eventually leading to catabolism and death of many cells in the ischemic core. Furthermore, membrane depolarization results in neurotransmitter release, most prominently the release of the excitatory neurotransmitter glutamate, which plays a central role in the pathology of cerebral ischemia (Simon et al., 1984). Increase in synaptic glutamate concentration over-activates its receptors, N-methyl-D-aspartate (NMDA) and α -amino-3-hydroxy-5-methyl-4-isoxazolepropionic acid (AMPA) and metabotropic glutamate (mGlu) receptors, which in return cause further membrane depolarization and greater calcium influx, exacerbating excitotoxicity (Liu et al., 2006; Peng et al., 2006; Bruno et al., 2001).

2.1.1.2 Oxidative and nitrosative stress

Unlike other organs, the brain is especially vulnerable to reactive oxygen species due to

neurons having relatively low levels of endogenous antioxidants (Coyle and Puttfarcken, 1993). High levels of intracellular calcium, sodium and ADP induce mitochondria to produce deleterious levels of reactive oxygen species, and consequently overly abundant oxygen radicals cause the destruction of cellular macromolecules and participate in signaling mechanisms that result in apoptotic cell death (Halliwell, 1994; Sugawara and Chan, 2003; Gonzalez et al., 2006). Moreover, there is a surge in production of superoxide, NO and peroxynitrate, following reperfusion. Thrombolytic therapy has a 4,5 hour time window of efficacy. Part of the reason for this limited time window is that the surge in production of free radicals associated with delayed reperfusion brings a second wave of oxidative and nitrosative stress that increases the risk of brain hemorrhage and edema.

2.1.1.3 Apoptosis

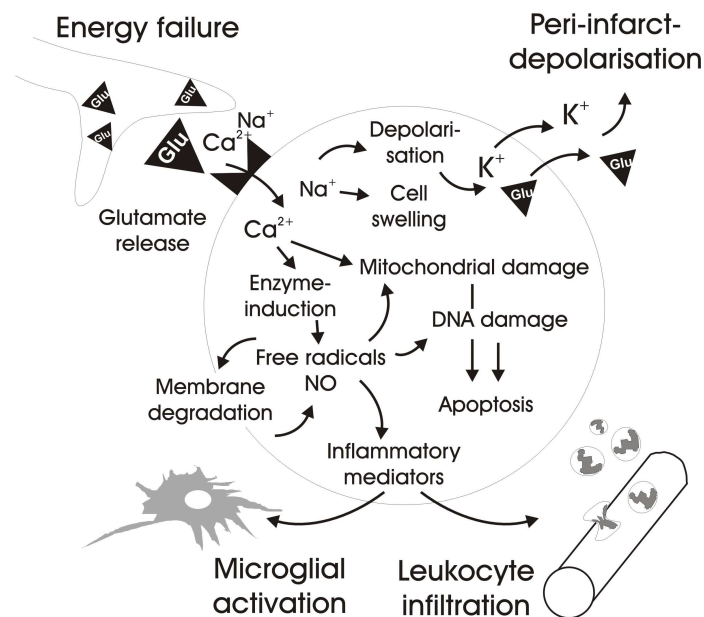
Mild ischemic injury preferentially induces cell death via an apoptotic-like mechanism rather than necrosis. Because the ischemic penumbra sustains milder injury and preserves ATP, apoptosis predominates in this region (Gonzalez et al., 2006). Triggers of apoptosis include ionic imbalance, oxygen free radicals, death receptor ligation, DNA damage and protease activation. Cytochrome c release from the outer mitochondrial membrane, an event which is promoted or prevented by bcl-2 family of proteins, initiates the intrinsic apoptotic cascade. In addition, extrinsic apoptosis pathway, which could be activated by inflammatory signals such as TNF family of ligands, is also operative after ischemia (del Zoppo, 1997; del Zoppo et al., 2000). Eventually, downstream effector caspases are activated targeting the substrates that dismantle the cell by cleaving homeostatic, cytoskeletal, repair, metabolic and cell signalling proteins (Namura et al., 1998).

2.1.1.4 Inflammation

Inflammation contributes to cerebral ischemic injury. Effects of individual components of the inflammatory cascade, however, can be beneficial depending on the stage of tissue injury, the magnitude of the response and whether the inflammatory component also activates neuroprotective pathways (Bruce et al., 1996; Nawashiro et al., 2000; Zhang et al.,

2000). After stroke immune cells can gain access to brain parenchymal tissue (Ross et al., 2007).

Infiltration of bone marrow-derived cells into the ischemic brain persists for weeks following stroke, and while the initial infiltration leads to worsening of tissue damage and exacerbation of neurological deficits, subsequent aspects of the infiltration such as the phagocytosis of debris and the release of cytokines that promote glial scar formation could be crucial for effective wound healing. On the other hand, numerous cytokines and chemokines are produced by activated endothelial cells, microglia, neurons, platelets, leukocytes, and fibroblasts and contribute to ischemic brain injury (Gong et al., 1998; Huang et al., 2006). In particular, IL-1, TNF- α and toll-like receptors (TLRs) are important inflammatory factors with detrimental effects for stroke outcome (Huang et al., 2006; Zaremba et al., 2001; Lehnardt et al., 2007; Cao et al., 2007; Ziegler et al., 2007). In contrast, TGF- β was reported to play a neuroprotective role in the pathogenesis of stroke (Wiessner et al., 1993).



Dimagl et al., 1999

Figure 2 Depiction of the major pathophysiological events evoked by cerebral ischemic injury. Glutamate excitotoxicity, peri-infarct depolarisations, oxidative/nitrosative stress, apoptosis and inflammation contribute to injury following brain ischemia.

2.2 ENDOGENOUS NEUROPROTECTION AND ISCHEMIC PRECONDITIONING IN BRAIN

Since the advent of recombinant thrombolytic agents, re-canalizing the occluded vessel and reversing the ischemia in stroke patients has become feasible and was proven to be beneficial if performed within 4.5 hours of stroke onset (Hacke, Kaste et al., 2008). However due to the narrow time-window of 4.5 hours, this treatment is only applicable for a very small number of patients. On the bench side, even though a large number of compounds have been so far proven to reduce ischemic injury in experimental animal models, clinical trials have reported disappointing results because of toxic side effects. Today, effective measures to protect neurons exposed to ischemia are still fragmentary. Thus, research for gaining new insights into endogenous neuroprotection, how brain protects itself against injury, has become crucial. If induction of ischemic preconditioning/tolerance could be mimicked and further accelerated by a drug treatment, that is safe and effective, this could tremendously improve the treatment of stroke.

2.2.1 Ischemic preconditioning/tolerance

Ischemic preconditioning or ischemic tolerance is described as a brief episode of sub-lethal ischemia which renders the brain resistant to subsequent, longer and severe ischemic insults. Ischemic preconditioning represents endogenous protection and is probably a fundamental cell/organ response to certain types or levels of injury. The terms 'tolerance' and 'preconditioning' were introduced for the first time by Janoff in 1964 (Janoff et al., 1964), and ever since, the phenomenon of ischemic preconditioning has been observed in numerous organs such as brain (Dahl et al., 1964; Kitagawa et al., 1990) and heart (Murry et al., 1986; Meldrum et al., 1997) as well as in a wide range of species like the gerbil (Kirino et al., 1991; Kato et al., 1991), the rat (Liu et al., 1992; Nishi et al., 1993; Simon et al., 1993) and the mouse (Wu et al., 2001). Amongst various brain regions, hippocampus, cerebral cortex, basal ganglia and thalamus were often reported to acquire ischemic tolerance (Kitagawa et al., 1991). Measurement of cerebral blood flow showed that such tolerance was not accompanied by an improvement of regional tissue perfusion during or after the ischemic episode that induced tolerance (Matsushima and Hakim, 1995; Chen et al., 1996; Barone et al., 1998).

Therefore, the state of ischemic tolerance seems to be based on the alteration of neurons themselves at the cellular level.

2.2.2 The phenomenon ischemic preconditioning also exists in humans

An analogous process is believed to exist in human: Previous transient ischemic attacks (TIA) are associated with better clinical outcome after subsequent stroke. In 1999, Blanco presented a study demonstrating how transient ischemic attacks prior to fatal stroke could induce ischemic tolerance (Blanco et al., 1999). In 26 patients with previous ipsilateral TIA 72 hours prior to ischemic stroke, the Canadian Stroke Scale on admission, at 48 hours, at 7 days and at 3 months was significantly better than that recorded in the group without TIA. Furthermore, more neurological deterioration and bigger infarct volumes were found in the group without previous TIA. Another retrospective case-control study in 148 stroke patients, with and without preceding TIA, showed that TIA before stroke was an independent predictor of mild stroke (Canadian Neurological Scale score ≥ 6.5) (Weih et al., 1999). Similar results were observed in more recent retrospective analyses (Moncayo et al., 2000; Arboix et al., 2004). Wegener demonstrated that initial diffusion lesions tended to be smaller and final infarct volumes were significantly reduced in patients with previous TIA (Wegener et al., 2004).

2.2.3 Mechanisms of ischemic preconditioning/tolerance

Mechanisms of ischemic preconditioning could be grouped into three components according to the temporal profile of their development. The first component is the stress sensor/signalling component that can detect various stressful conditions and convert the information into intracellular signals. Hypoxia inducible factor (HIF), oxygen sensitive ion channels, potassium channels, calcium and sodium channel families control cellular responses for hypoxia in neurons as well as in many other cell types and belong to the sensor/signalling component of tolerance development (Kemp et al., 2007). Once the danger is detected by the cell, an appropriate cellular response is coordinated by the transducer component, which includes various kinases such as p38 mitogen activated protein kinase (MAPK) (Nishimura et al., 2003) and extracellular regulated kinases (ERK) (Jones and Bergeron, 2004), as well as

transcription factors like signal transducer and activator of transcription (STATs) (Digicaylioglu et al., 2001), cyclic AMP response-element binding-protein (CREB) (Meller et al., 2005) and nuclear factor kappa B (NF- κ B) (Digicaylioglu et al., 2001). Lastly, the effector component represents the executive mediators of protection: Reactive oxygen species (ROS) scavenger superoxide dismutase (SOD) (Danielisova et al., 2005), anti-apoptotic protein Bcl-2 (Liu et al., 2002), vascular endothelial growth factor (VEGF) (Bernaudin et al., 2002), nitric oxide (NO) and hexokinase-2 are some of the most reported mediators of neuroprotection conferred by ischemic preconditioning (Kirino et al., 2002; Dirnagl et al., 2003).

Ischemic preconditioning-induced neuroprotection may be the result of a combination of different cellular and molecular pathways, with a net outcome of counteracting pathophysiological cascades triggered by lethal ischemic insult. Ischemic tolerance thus reflects a fundamental change in the cellular response to injury that shifts the outcome from cell death to cell survival (Dirnagl et al., 2003). In fact, Stenzel-Poore, with a substantial series of genome-wide gene expression analysis study, suggested that preconditioning may lead to a fundamental reprogramming of the transcriptional response to ischemic injury, ultimately conferring neuroprotection (Stenzel-Poore et al., 2003; Stenzel-Poore et al., 2004; Stenzel-Poore et al., 2007). Although transcription factors, such as HIF, CREB and NF- κ B are already known to be driving neuroprotective gene expression upon an ischemic preconditioning stimulus, we are today more aware that apart from the transcription factors and DNA sequence, regulation of such transcriptional activity requires the cooperation of a third party, namely epigenetic alterations of the DNA and histones. Indeed, these modifications crucially regulate the accessibility of cognate regulatory DNA elements for transcription machinery. Recent years have witnessed the emergence of growing evidence supporting an integral role for epigenetic mechanisms in neuronal gene expression, yet involvement of these mechanisms in brain ischemic preconditioning and neuroprotection is mostly unknown.

2.3 EPIGENETICS

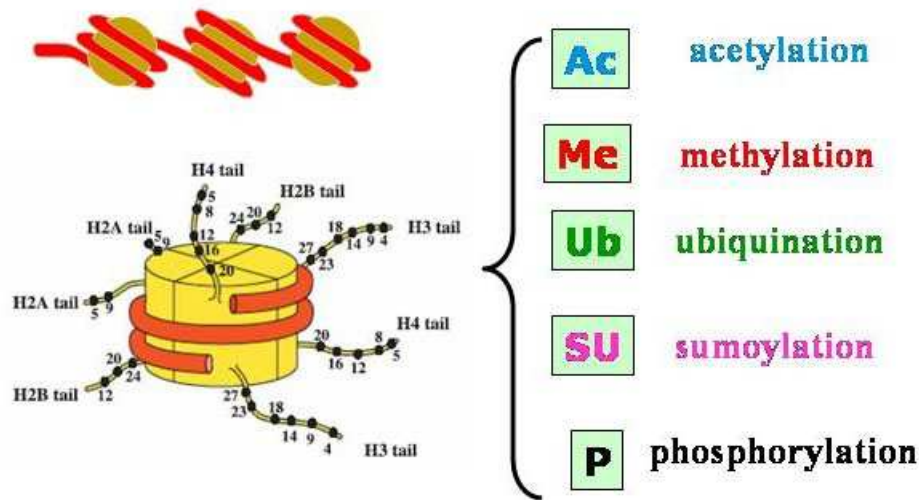
Epigenetics is conventionally defined as all mitotically and meiotically heritable changes in gene expression patterns which are not coded in DNA sequence. Another

definition, which includes the dynamic nature of chromatin modifications that are not necessarily heritable but still result in changes in gene expression, describes epigenetics as the structural adaptation of chromatin regions to register, signal or perpetuate altered activity states (Bird et al., 2007). Epigenetic mechanisms define a cell's identity by regulating its characteristic pattern of gene expression and mainly include DNA methylation, RNA associated post-transcriptional gene silencing and covalent modifications of histones, which constitute nucleosomes, the basic subunits of the highly-ordered chromatin structure.

2.3.1 Nucleosome

The nucleosome core particle is the fundamental unit of chromatin structure in all eukaryotes. It is an octamer, containing two copies of each of the four histone proteins, H2A, H2B, H3, H4, and around which 146 bp of DNA is wrapped in $1\frac{3}{4}$ superhelical turns (Luger et al., 1997). Wrapping of DNA around the nucleosome results in an approximately sevenfold reduction in its length. Although this is only a small reduction in DNA length in comparison to the several-thousand-fold length reduction necessary for compaction into metaphase chromosomes, it is highly likely to be an essential initial step that enables higher-order chromatin structure to assemble (Grunstein et al., 1992).

All core histone proteins have a similar structure with an N-terminal domain, a globular domain and a C-terminal domain. It has been known for many years that the histone N-terminal tails are exposed on the surface of the nucleosome and that selected amino acid residues could be subjected to a variety of enzyme-catalyzed, posttranslational modifications. These include acetylation of lysines, phosphorylation of serines, and methylation of lysines and arginines, and addition of small peptide ubiquitin. The current epigenetics defines the nucleosome and its modified tail domains not solely as a structural packer of DNA but a carrier of epigenetic information that determines both how genes are expressed and how their expression patterns are maintained from one cell generation to the next.



chemistry.gsu.edu/faculty/Zheng

Figure 3 Major post-translational histone modifications. Acetylation, methylation, ubiquitination, sumoylation and phosphorylation of histones are the most investigated posttranslational histone modifications and they play essential roles in gene expression regulation in physiological as well as in disease states.

2.3.2 Epigenetic modifications

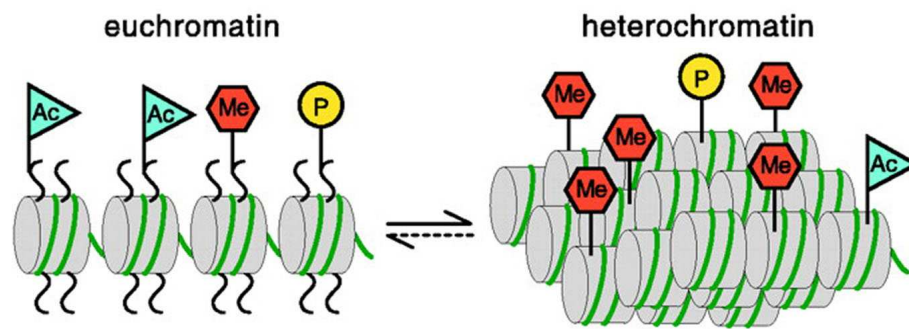
Covalent histone modifications, DNA methylation and RNA-associated post-transcriptional gene silencing have been so far the most investigated modifications that carry epigenetic information. The histone tail modifications are likely to act in concert with the rather more widely known mediator of chromatin structure and gene expression, namely methylation of cytosine residues in CpG dimers through the action of DNA methyltransferases. Long-term silencing, as found in imprinted genes or the female inactive X chromosome, is generally associated with relatively high levels of CpG methylation. Current knowledge on the exact mechanism(s) by which CpG methylation leads to gene silencing is still fragmentary, yet there is evidence that, histone modifications are also involved. The methyl DNA-binding protein MeCP2 can bind histone deacetylases, thereby targeting them to methylated DNA and resulting in local histone deacetylation and suppression of transcription (Bird et al., 2002). Conversely, experiments in the filamentous fungus *Neurospora crassa* have shown that DNA methylation is dependent upon methylation of histone H3 lysine 9 (Tamaru et al., 2001). Recent studies have shed light on the complexity of epigenetic information that could possibly be carried in the histone tails. Currently, there are 50 different acetylated isoforms of the four

core histones (H2B, H3, and H4 have 16 each and H2A has two). These isoforms can be modified further by methylation of selected lysines and arginines (H3 and H4) and phosphorylation of serine (H3, H4, H2B). Moreover, methylation can be attachment of one, two, or three methyl groups, and there are other modifications, such as ubiquitination and ADP-ribosylation (Hansen et al., 1998). The total number of possible histone isoforms, carrying different combinations of tail modifications, that can mark the nucleosome surface, can reach a total sum of many thousands. This vast information carrying potential of histone tail modifications have given rise to the concept of a histone code (Strahl et al., 2000; Jenuwein et al., 2001) or an epigenetic code (Turner et al., 2000), which is expected to be much more sophisticated than the genetic code carried in DNA sequence.

2.3.3 Histone acetylation

Studies on histone acetylation were the first association between a histone tail modification and a particular functional state of chromatin (Allfrey et al., 1963). Transcriptionally active chromatin fractions were enriched in acetylated histones (Pogo et al., 1966; Hebbes et al., 1988), whereas regions of transcriptionally silent heterochromatin were found to be underacetylated (Jeppesen et al., 1993). Histone acetylation therefore is a diagnostic feature of transcriptionally active chromatin sites. Acetylation of the histone tails result in loss of positive charge, thereby weaker affinity for DNA binding. Consequently, chromatin becomes more open and conducive to transcription. Nevertheless, more sophisticated and multi-layered epigenetic mechanisms are also known to be involved and that the functional effects of tail modifications are likely to depend on the specific amino acids that are modified. It is now known that specific tail modifications are recognised and bound by distinct proteins, which in return recruit protein complexes associated to either repressive or permissive transcriptional events.

The setting of specific patterns of histone acetylation, residue-specific modifications, reflects the specificities of histone acetyltransferase (HAT) or deacetylase (HDAC) enzymes. Both HATs and HDACs constitute extensive enzyme families and are often found as a catalytic subunit in multiprotein complexes whose other components confer genomic targeting and other capabilities (Ng et al., 2000; Grant et al., 1999).



Jenuwein et al., 2001

Figure 4 Illustration of euchromatin and heterochromatin. These accessible or condensed nucleosome fibers contain posttranslationally modified histones with acetylated (Ac), methylated (Me) and phosphorylated N-terminals

2.3.4 Histone acetyltransferase (HAT) families

Histone acetyltransferases (HATs) are the group of enzymes which transfer the acetyl moiety from acetyl coenzyme A (acetyl Co A) onto one or more lysine residues contained within the N-terminal tails of histone proteins. Sequence analysis of HAT proteins reveal that they fall into distinct families that show high sequence similarity within families but poor to no sequence similarity between families (Kuo et al., 1998). Each HAT family appears to have a distinct substrate preference, and different families tend to appear in different functional contexts. Gcn5/PCAF, MYST, TAFII250 and Creb-binding protein (CBP)/p300 are some of the most studied HAT families so far. Among those, CBP/p300 family, including CBP and its close homologue P300, is fundamentally important in various signal modulated transcriptional events (Eckner et al., 1994). The ability of CBP/p300 to enhance transcription is believed to be accomplished in two modes. First, by acting as a bridging factor thus recruiting the RNA polymerase II holoenzyme via interaction with general transcription factors (Manteuffel-Cymborowska et al., 1999) and, second, by acetylation of histones via their HAT activity (Ogryzko et al., 1996). Nucleosomal histones H3 and H4 are the preferred substrates (Schiltz et al., 1999). Both CBP and p300 proteins were shown to interact with a diverse set of sequence-specific transcription factors such as E2F, p53, MyoD, c-Myb and HIV-tat (Snowden et al, 1998). Homozygous knockout mice of either CBP or p300 display, among several other malformations, defects in neural tube closing and are embryonic lethal (Yao et

al., 1998). Despite the sequence similarity, both CBP and p300 have non-overlapping functions, such that both proteins are required for normal development.

2.3.5 Histone deacetylase (HDAC) families

Classification of mammalian histone deacetylases (HDACs) is based upon similarity to their yeast homologs. HDACs 1, 2, 3, and 8 comprise the class I HDAC family. In general, these HDACs are expressed ubiquitously, consist primarily of a deacetylase domain and almost exclusively exhibit a nuclear localization. Class II HDACs are made up of two subgroups: class IIa HDACs include HDACs 4, 5, 7, and 9, class IIb HDACs consists of HDACs 6 and 10. The additional non-catalytic region of class II HDACs is believed to facilitate protein interactions and therefore class II HDACs are thought to display a wider range of interaction partners. All members of class II HDACs are observed both in the cytoplasm and nucleus (de Ruijter et al., 2003).

2.3.6 Regulation of histone acetyltransferase and deacetylase enzyme activities

Like most other signaling components of cellular response, signal induced activity of HATs and HDACs are regulated mainly by phosphorylation. In addition to the recruitment of HATs to transcriptional complexes, phosphorylation enhances their acetyltransferase activity and facilitates transactivation of target promoters. Important in neuronal context, during activity-dependent CBP engagement and after N-methyl-D-aspartate (NMDA) treatment, CBP was phosphorylated at serine 301 in a CAMK-IV-dependent manner (Impey et al., 2002). Type-I PKA and p42/p44 MAPK were also reported to phosphorylate CBP (Liu et al., 1998). Regulation of HDACs, on the other hand, may broadly be divided into two categories involving each of the two classes of mammalian HDACs. A general mode of regulation for HDAC class-I proteins involves association with proteins that modulate their deacetylase activity and recruitment to genomic arena, whereas class-II HDACs are regulated by sub-cellular compartmentalization, where active nucleocytoplasmic trafficking delimits the availability of these enzymes for epigenetic utilization. Both these processes are dependent on

signal-induced phosphorylation events which might result in different functional outcome in the case for each specific HDAC enzyme (de Ruijter et al., 2003).

2.3.7 Histone acetylation homeostasis

The histone acetylation machinery, which consists of HAT and HDAC enzyme families, is one of the ultimate regulatory switches of gene expression. In addition to their involvement in transcriptional regulation, HAT–HDAC system involves in the modulation of other chromatin-associated processes like replication, site-specific recombination and DNA repair, thereby plays a major role in determining the overall cell fate. Regulation of transcription may require exchange of HDAC complexes with those containing HAT activities. This kinetic balance between HAT and HDAC enzymatic activities in steady-state cells confers stability to the cellular homeostasis by coordinating gene expression and repression on both temporal and spatial basis and is therefore referred to as ‘acetylation homeostasis’ underscoring the vitality of regulated histone acetylation for maintaining cellular homeostasis. Perturbations in the acetylation balance have been associated with aetiopathologies of various human diseases, including multiple leukemias (Gayther et al., 2000; Kouzarides et al., 1999; Carapeti et al., 1999; Redner et al., 1999).

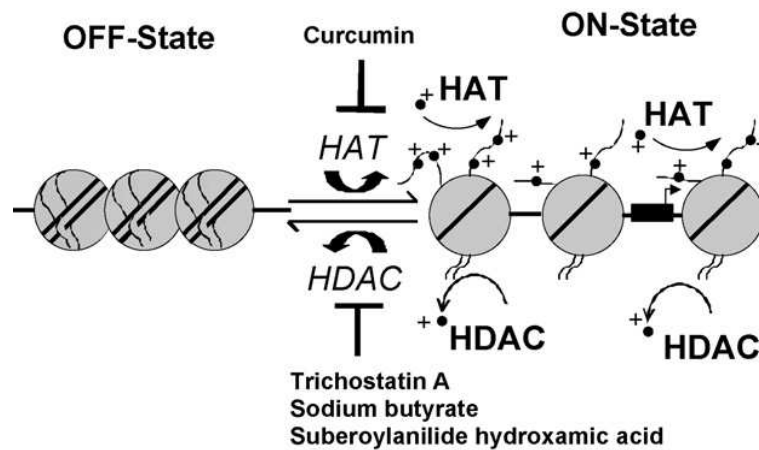
In neurons, as in other types of cells, histone acetylation equilibrium is maintained very stringently and any perturbation in the harmony between the HAT and HDAC dose and activity is not appreciated. It is now evident that histone acetylation balance is dramatically impaired during neurodegenerative conditions and neurodegeneration-coupled HAT loss could be the main molecular event underpinning the forfeiture of neuronal acetylation homeostasis. Among all HATs, loss of CBP appears to be pivotal in facilitating neurodegenerative cascade of events, partly because of its ability to regulate transcription factor CREB, which has been well-documented to display neuroprotective functions (Lonze et al., 2002; Lonze et al., 2002; Jin et al., 2001). Upon their translocation into nucleus, polyglutamine containing neurotoxins selectively enhanced ubiquitination and degradation of CBP (Nucifora et al., 2001; Jiang et al., 2003). CBP’s proteosomal degradation was also reported during Alzheimer’s disease (AD) progression (Marambaud et al., 2003). Furthermore, caspase-6-dependent CBP proteolysis was demonstrated in low K^+ shock model

of neurodegeneration (Rouaux et al., 2003), as well as in Alzheimer brain. The same authors also reported decrease in p300 protein levels during some neurodegenerative conditions.

2.3.8 Pharmacological manipulation of histone acetyltransferase and deacetylase activities

Like many enzymes, the enzyme families that modify core histones or reorganize chromatin structure are susceptible to pharmacological inhibition. Since these enzymes regulate patterns of gene expression by targeting selected genes or chromosome regions, the therapeutic potential of such inhibitors is enormous, particularly for treating cancers or other diseases which manifest aberrant patterns of gene expression. The enzymes most closely studied to date are the HDACs, for which a wide range of inhibitors are currently available. Some of these agents have proven to be remarkably effective at selectively inhibiting the growth of human tumour cells (Marks et al., 2001). In October 2006, the US Food and Drug Administration (FDA) approved the first drug of this new class, SAHA, vorinostat (1, Zolinza, Merck) for the treatment of cutaneous T cell lymphoma. HDAC inhibitors are categorized in different classes based on their chemical structures (de Ruijter et al., 2003). The various classes of HDAC inhibitors include hydroxamates, short chain fatty acids, cyclic peptides and benzamides. Trichostatin A (TSA), suberoyl anilide bishydroxamide (SAHA), scriptaid, pyroxamide and oxamflatin are examples of hydroxamates. Among hydroxamates, TSA was the first to be characterized 19 years ago (Yoshida et al., 1990). TSA inhibits both class I and class II HDACs and due to its high potency as an HDAC inhibitor, effective in nanomolar concentrations, TSA has been used as the core chemical structure for synthesis of new HDAC inhibitors (Furumai et al., 2001). Crystal structure studies of hydroxamates, such as TSA and SAHA have revealed that these inhibitors work by binding to the zinc ion in the HDAC active site and abolishing the deacetylase activity (Finnin et al., 1999).

Despite the substantial progress made in the study of HDAC inhibitors, very little has so far been done regarding pharmacological manipulation of HAT activity. Amongst the very few HAT inhibitors, garcinol and curcumin were shown to penetrate cellular membranes and inhibit acetylation of histones in vivo (Balasubramanyam et al., 2003; Balasubramanyam et al., 2003; Lau et al., 2000).



Taniura et al., 2007

Figure 5 Pharmacological inhibition of histone acetyltransferase (HAT) and histone deacetylase (HDAC) enzymes. HAT inhibition by curcumin or HDAC inhibition by Trichostatin A, respectively, results in closed – off- or open –on- local chromatin environment for transcriptional events.

2.3.9 Epigenetic mechanisms and neuroprotection against cerebral ischemia

Our group has previously demonstrated that aberrant DNA methylation is associated with augmented brain injury after mild middle cerebral artery occlusion (MCAo) in mice (Endres et al., 2000). Suppression of DNA methylation, by genetic as well as by pharmacological means, conferred resistance to ischemia. Furthermore, single dose intracerebroventricular Trichostatin A administration shortly before ischemia onset proved significant neuroprotection against mild MCAo in mice. With this study, our group not only convincingly documented the ability of DNA demethylating and histone acetylation enhancing agents to ameliorate the brain ischemic damage, but also evidenced that various epigenetic mechanisms could be indeed involved in pathophysiological cascades following mild brain ischemia. In primary mouse cortical cultures subjected to hypoxia, HAT enzyme CBP was selectively expressed in cells with morphologically intact cell nuclei, and not in cells with condensed or fragmented nuclei indicative of irreversibly damaged neurons, supporting a role for transcriptional activation by CREB and CBP in neuronal cell-survival programs following cerebral ischemia (Jin et al., 2001). A number of studies have so far successfully manipulated neuronal vulnerability by influencing the dose and/or enzymatic

activity of histone acetyltransferases (HATs) and histone deacetylases (HDACs), thus focusing on the importance of balanced acetylation status in neuronal vitality. Oxidative stress, reported to be associated with many neurodegenerative diseases, including Alzheimer's disease (AD), Parkinson's disease, Huntington's disease (HD), stroke, multiple sclerosis and Friedreich's ataxia, failed to induce neuronal apoptosis when cells were treated with HDAC inhibitors (Ryu et al., 2003). Similarly, HDAC inhibitors like TSA and suberoylanilide hydroxamic acid (SAHA) arrest polyglutamine toxicity (McCampbell et al., 2001; Steffan et al., 2001). Yet, in the context of cerebral ischemia, whether balanced function of histone acetylation machinery thus histone acetylation homeostasis is impaired in neurons following ischemic injury, and whether protective properties of HDAC inhibitors against cerebral ischemia is through restoration of aberrant histone acetylation levels is still not known. Furthermore, in relation to brain ischemic preconditioning transcription factor CREB is known to drive neuroprotective gene expression, however involvement of its co-activator CBP and histone acetylation events in these processes remains to be investigated.

2.4 HYPOTHESES

Throughout my PhD thesis project I have focused on the following questions:

1 Does ischemic injury impair histone acetylation pattern and/or histone acetylation machinery in neuronal cells?

Aberrant histone acetylation levels and loss HAT enzyme CBP were previously associated to deterioration processes during numerous neurodegenerative conditions. In my PhD thesis project, I investigated whether neuronal histone acetylation and CBP protein levels were also impaired following ischemic injury. I further tested whether suppression of CBP protein availability/function alters neuronal susceptibility to ischemia.

2 Does ischemic preconditioning enhance histone acetylation levels in neuronal cells?

Scientific output in recent years define histone acetylation as a master epigenetic mechanism for the regulation of gene expression, and enhanced histone acetylation patterns could be referred as diagnostic signature of on-going active gene expression events. It is presently well-known that acquisition of ischemic tolerance in brain, in most parts, is dependent on novel neuroprotective gene expression. Yet, current knowledge on epigenetic involvement in brain ischemic preconditioning phenomenon is poor. Here, I examined whether histone acetylation levels were enhanced in neuronal cultures and in mice brain after ischemic preconditioning stimuli. I further investigated if HAT enzyme activity was altered in neurons following preconditioning ischemia.

3 Does histone acetylation enhancement by Trichostatin A confer neuroprotection against ischemic injury, and what are the mechanisms involved?

Increasing number of scientific work has so far underscored a multi-facet beneficial role of HDAC inhibitors against various neurodegenerative conditions. In the cerebral ischemia context, our group has previously demonstrated that single dose intracerebroventricular Trichostatin A administration shortly before ischemia onset proved significant neuroprotection against mild ischemic injury in mice. Here, I investigated whether Trichostatin A provides neuroprotection against cerebral ischemia through its HDAC inhibitory function and further characterized mechanisms of neuroprotection by Trichostatin A.

3 MATERIALS AND METHODS

3.1 Materials

3.1.1 Cell culture media and supplements

Product	Supplier
B27 Supplement	Gibco (Karlsruhe, Germany)
Collagen-G solution	Biochrom (Berlin, Germany)
D-(+)-glucose	Sigma (Taufkirchen, Germany)
Dulbecco's phosphate-buffered saline (DPBS)	Biochrom (Berlin, Germany)
Foetal calf serum (FCS)	Biochrom (Berlin, Germany)
Foetal calf serum, Gold (FCS.Gold)	PAA (Linz, Austria)
Glutamate	Sigma (Taufkirchen, Germany)
HEPES	Biochrom (Berlin, Germany)
Insulin (Insuman Rapid)	Sanofi Aventis (Frankfurt, Germany)
L-Glutamin	Biochrom (Berlin, Germany)
MEM-Earle	Biochrom (Berlin, Germany)
Neurobasal medium (NBM)	Gibco (Karlsruhe, Germany)
Penicillin/ Streptomycin	Biochrom (Berlin, Germany)
Poly-L-Lysin	Biochrom (Berlin, Germany)

3.1.2 Chemicals

Product	Supplier
Ammonium persulphate (NH ₄) ₂ S ₂ O ₈	Sigma (Taufkirchen, Germany)
β-mercaptoethanol	Merck (Darmstadt, Germany)
β-NADH	Sigma (Taufkirchen, Germany)
Bromphenol blue	Sigma (Taufkirchen, Germany)
Calcium chloride (CaCl ₂)	Sigma (Taufkirchen, Germany)

Coomassie brilliant blue G	Fluka (Munich, Germany)
Curcumin	Sigma (Schnelldorf, Germany)
Dimethylsulphoxide (DMSO)	Sigma (Taufkirchen, Germany)
Dipotassium phosphate (K_2HPO_4)	Sigma (Taufkirchen, Germany)
DTT	Bio-mol (Hamburg, Germany)
EDTA	Sigma (Taufkirchen, Germany)
Ethanol	J.T. Baker (Deventer, Holland)
EGTA	Sigma (Taufkirchen, Germany)
Fluo-4 AM dye	Molecular Probes, Invitrogen (Karlsruhe, Germany)
Glycerol	Merck (Darmstadt, Germany)
Glycine	Sigma (Taufkirchen, Germany)
Harris haematoxylin (Papanicolaou solution 1a)	Merck (Darmstadt, Germany)
Hydrochloric acid (HCl)	Sigma (Taufkirchen, Germany)
Isofluorane (Forene)	Abbott (Switzerland)
ImmunoFluor Mounting Medium	ICN Biochemicals (Costa Mesa, CA, USA)
Isopentane	Roth (Karlsruhe, Germany)
Kodak Biomax Light-1 X-ray films	Sigma (Taufkirchen, Germany)
LumiGLO reagent and peroxide	NEB (Frankfurt a. M., Germany)
Lauryl sulphate (SDS)	Sigma (Taufkirchen, Germany)
LDH-standard TruCal-U	Greiner, DiaSys (Flacht, Germany)
Magnesium chloride ($MgCl_2$)	Serva (Heidelberg, Germany)
Magnesium sulphate, heptahydrate	Sigma (Taufkirchen, Germany)
Methanol	Roth (Karlsruhe, Germany)
Milk powder (blocking grade)	Roth (Karlsruhe, Germany)
Monosodium phosphate (NaH_2PO_4)	Sigma (Taufkirchen, Germany)
Monopotassium phosphate (KH_2PO_4)	Sigma (Taufkirchen, Germany)
Nonidet P 40 (NP40)	Sigma (Steinheim, Germany)
Paraformaldehyde	Merck (Darmstadt, Germany)
Ponceau S solution	Sigma (Taufkirchen, Germany)
Potassium chloride (KCl)	Sigma (Taufkirchen, Germany)
Potassium dihydrogenphosphate (KH_2PO_4)	Merck (Darmstadt, Germany)

Potassium monohydrogenphosphate (K ₂ HPO ₄)	Merck (Darmstadt, Germany)
Potassium monohydrogenphosphate trihydrate (K ₂ HPO ₄ 3H ₂ O)	Merck (Darmstadt, Germany)
Propidium iodide	Sigma (Steinheim, Germany)
Rotiphorese gel (30% acrylamid, 0,8% bisacrylamid)	Sigma (Taufkirchen, Germany)
Sodium bicarbonate (NaHCO ₃)	Sigma (Taufkirchen, Germany)
Sodium chloride (NaCl)	Roth (Karlsruhe, Germany)
Sodium deoxycholate (C ₂₄ H ₃₉ NaO ₄)	Sigma (Taufkirchen, Germany)
Sodium fluoride (NaF)	Sigma (Taufkirchen, Germany)
Sodium orthovanadate (Na ₃ VO ₄)	Sigma (Taufkirchen, Germany)
Sodium pyruvate (CH ₃ COCOONa)	Sigma (Taufkirchen, Germany)
Sulphuric acid (H ₂ SO ₄)	
TEMED	Sigma (Taufkirchen, Germany)
Thiazolyl blue tetrazolium bromide (MTT)	Sigma (Taufkirchen, Germany)
Thimerosal	Sigma (Schnelldorf, Germany)
Trichostatin A (TSA) (T8552)	Sigma (Schnelldorf, Germany)
Trizma-base	Sigma (Steinheim, Germany)
Trizma-HCl	Sigma (Taufkirchen, Germany)
TMRE	Molecular Probes, Invitrogen (Karlsruhe, Germany)
Trypsin/EDTA	Biochrom (Berlin, Germany)
Tween-20	Sigma (Taufkirchen, Germany)

3.1.3 Antibodies, reagents and kits

Product	Supplier
Alexa 488 phalloidin dye	Invitrogen (Karlsruhe, Germany)
BCA protein assay kit (23225)	Pierce, Bonn (Germany)
BCA protein assay kit, reducing agent compatible (23250)	Pierce (Bonn, Germany)

Donkey anti-goat HRP-linked (sc-2020)	Santa Cruz (Santa Cruz, CA, USA)
Donkey anti-rabbit HRP-linked (NA934)	GE Healthcare (Buckinghamshire, UK)
Goat anti-actin HRP-linked (sc-1616)	Santa Cruz (Santa Cruz, CA, USA)
Goat Anti-rabbit HRP-conjugate (12-348) (ELISA)	Millipore (Schwalbach/Ts.,Germany)
HAT assay kit (17-289)	Millipore (Schwalbach, Germany)
Hoechst 33258, bis-benzimide	Sigma (Taufkirchen, Germany)
LumiGlo, enhanced chemiluminesce (ECL) Reagent	New England Biolabs (Frankfurt am Main, Germany)
Mouse anti NeuN	Chemicon (Temecula, CA, USA)
Prec Plus Std Kaleidoscope	Bio-rad (Munich, Germany)
Protease inhibitor cocktail	Roche (Mannheim, Germany)
Rabbit anti-acetylated histone H2B (07-373)	Millipore (Schwalbach/Ts.,Germany)
Rabbit anti-acetylated histone H3 (06-599)	Millipore (Schwalbach/Ts.,Germany)
Rabbit anti-acetylated histone H4 (06-598; 06-866)	Millipore (Schwalbach/Ts.,Germany)
Rabbit anti-acetylated histone H4 (AHP418)	Serotec (Duesseldorf, Germany)
Rabbit anti-acetyl-Lysin (06-933 for WB; 07-129 for ELISA)	Millipore (Schwalbach/Ts.,Germany)
Rabbit anti-CBP (A-22) (sc-369)	Santa Cruz (Santa Cruz, CA, USA)
Rabbit anti-histone H4 (05-858)	Millipore (Schwalbach/Ts.,Germany)
Rabbit anti microtubule associated protein 2 (MAP2) (AB5622)	Millipore (Schwalbach/Ts.,Germany)
Rabbit anti murine gelsolin	Dr Kwiatkowski (Harvard Medical School, Boston, MA, USA)
Sytox Green, nucleic acid stain	Invitrogen (Karlsruhe, Germany)

3.1.4 Tools and equipment

Product	Supplier
Blotting chamber	Trans-Blot Semi-Dry Transfer Cell, Biorad (Munich, Germany)

Cell culture incubator	Nuair, COTECH (Berlin, Germany)
Centrifuge, Universal 30 RF	Thermo Electron (Oberhausen, Germany)
Cryostat, Cryo-Star HM 560	MICROM International (Walldorf, Germany)
Criterion cassettes	Bio-rad (Munich, Germany)
Criterion precast gel, 4-20%	Bio-rad (Munich, Germany)
Cytofluor reader	CytoFluor II, PerSeptive Biosystems (Framingham, MA, USA)
Electrophoresis chamber	Criterion, Biorad (Munich, Germany)
Fluorescent microscope, DMRA2	Leica (Wetzlar, Germany)
Inverted contrasting microscope, DM IL	Leica (Wetzlar, Germany)
Multi-well cell culture plates	Falcon (Franklin Lakes, NJ, USA)
Nitrocellulose membrane	Bio-rad (Munich, Germany)
OGD chamber, Concept 400	Ruskinn Technologies (Bridgend, UK)
pH metre, pH100	VWR International (Darmstadt, Germany)
Plate reader	MRX Revelation, Thermo Labsystems (Dreieich, Germany)
Power supply, Power Pack 200	Bio-rad (Munich, Germany)
Sonicator, Sonorex Super 10P	Bandelin Electronic (Berlin, Germany)
Streptavidin coated microwell plate (20-183)	Upstate, Millipore (Schwalbach, Germany)
Whatman paper	Biometra (Göttingen, Germany)

3.1.5 Animals

Animal	Supplier
C57Bl/6 mouse	Charles River Laboratories (Sulzfeld, Germany)
CBP ^{+/-} mouse (E16-17) (F2 of C57BL/6J and DBA background)	Dr. Barco (Institute for Neuroscience, Alicante, Spain)
Gsn ^{-/-} mouse (mixed 129/SV×C57Bl/6 background)	Dr. Fink (Institute for Pharmacology and Toxicology, Bonn, Germany)
129SV mouse	Charles River Laboratories (Sulzfeld, Germany)

Wistar rat (E17-18)

Forschungseinrichtungen für experimentelle
Medizin (FEM), Charite (Berlin, Germany)

3.2 Methods

3.2.1 Primary Neuronal Cell Cultures

Culture plates were pre-treated by incubation with poly-L-lysine (5 µg/ml in PBS w/o) for 1 hour at room temperature, rinsed with PBS and incubated with collagen coating medium (modified Eagle's medium supplemented with 5% FCS GOLD, 1% Pen/Strep, 10 mM HEPES and 0.03 w/v collagen G) for 1 hour at 37°C. After rinsing of plates twice with PBS, cortical cells were plated in 24-well plates (for OGD experiments) or in six-well plates (for Western Immunoblotting experiments) in wells in starter medium, at a density of 200,000 cells/cm²; 300,000 cells/well for 24-well plates and 1,500,000 cells/well for 6-well plates. For immunocytochemistry, cells were seeded on glass cover slips in 24-well plates. Cultures were kept at 36.5°C and 5% CO₂, and were fed every four day, from the fourth day in vitro (DIV 4) on with cultivating medium (starter medium without glutamate) by replacing half of the medium. All experiments were carried out between DIV 8-DIV 10 and condition of the cultures was assessed by light microscopy, prior to experiments.

In our primary cortical cell culture system, as previously demonstrated by immunocytochemistry (using antibodies against glial fibrillary acidic protein for astrocytes, OX42 for microglia, NeuN for neurons and choline acetyl transferase for cholinergic neurons), neuronal purity was always higher than 90% until DIV 14; Less than 10% astrocytes until DIV 14 and less than 1% microglia until DIV 28 was present in our near-pure neuronal cultures (Lautenschlager et al., 2000).

It should be noted that sister cultures were used within every individual in vitro experiment carried out during this PhD thesis project, i.e OGD vs. OGD control cultures. All culture plates were handled in the same manner regarding the routine cell culture procedures. Cortical cells were plated in 24-well plates for OGD experiments and in 6-well plates for western immunoblotting due to the ease of experimental handling.

3.2.2 Pre-treatment with Trichostatin A

3.2.2.1 Pre-treatment of primary cortical cultures with Trichostatin A

TSA was dissolved in 0.01% ethanol to generate a 3 mM stock solution, with subsequent dilutions in medium to reach final concentrations of 25–500 nM. TSA was applied to cortical neuronal cell cultures on in vitro day 8 (DIV 8) for varying durations (from 6 hours to 24 hours) according to experimental planning, or for 12 or 24 h before OGD. Vehicle-treated cultures received 0.01% ethanol in medium.

3.2.2.2 Pre-treatment of mice with Trichostatin A

Animal experiments were performed according to institutional and international guidelines. All surgical procedures were approved by the local authorities. Male 129/SV wildtype mice (18–22 g, BfR, Germany), and gelsolin (*gsn*)^{-/-} along with *gsn*^{+/+} mice (both in a mixed 129/SV × C57Bl/6 background because the gelsolin null-state is not viable in a pure C57Bl6 background, see (Endres et al., 1999) were housed with ad libitum food and water access. TSA was obtained from Sigma-Aldrich, dissolved in 50 µl dimethyl sulfoxide and injected intraperitoneally (i.p.) at a dose of 1 or 5 mg kg⁻¹ body weight for 14 days. Control (i.e., vehicle) mice were daily i.p. injected with the identical volume of dimethyl sulfoxide.

3.2.3 Injury Paradigms

3.2.3.1 Combined oxygen-glucose deprivation (OGD) as injury paradigm in vitro

Animal experiments were performed according to institutional and international guidelines. All surgical procedures were approved by the local authorities. As the paradigm of ischemic injury, we used combined oxygen-glucose deprivation (OGD) which is a widely used model to study neuronal ischemia in vitro. 24-well plates were used for OGD and OGD experiments were performed between on DIV 8 and DIV10. Length of OGD experiments were between 30 min to 60 min for ischemic preconditioning experiments, whereas for injurious ischemia it lasted for 120min to 180 min. In all experimental paradigms, however, the procedure was as following; Culture medium was removed from cells and preserved. Cells were rinsed twice

with warmed PBS, placed in OGD chamber (a humidified, temperature controlled (36±/−0.5°C) chamber at PO₂ < 2mmHg). PBS was replaced by warmed balanced salt solution (BSS₀), which was put into the chamber 6-12 hours prior to the performance of the OGD experiment. OGD was terminated by taking the culture plates out of the OGD chamber and replacing BSS₀ by warmed conditioned medium (of 50% fresh cultivating medium and 50% the preserved cell culture medium (Bruer et al. 1997; Harms et al. 2004). Subsequently, culture plates were returned to normoxic cell culture incubator. OGD control, sister cultures went under the same washing and experimental procedures, except that they were maintained in the normoxic cell culture incubator after replacing the PBS by BSS₂₀ for the same duration as OGD, followed by return of the conditioned medium. The condition of the cells at various time points after OGD was determined morphologically by phase contrast microscopy. At various time points after OGD, aliquots of the medium were saved for the analysis of LDH activity and/or subsequent propidium iodide (PI) staining of cells or MTT reduction test were carried out.

3.2.3.2 Middle cerebral artery occlusion (MCAo) as injury paradigm in vivo

Animal experiments were performed according to institutional and international guidelines. All surgical procedures were approved by the local authorities. Mice were anesthetized for induction with 1.5% isoflurane and maintained in 1.0% isoflurane in 70% N₂O and 30% O₂ using a vaporizer. Ischemia experiments were essentially performed as described ([Endres et al., 1999] and [Endres et al., 2000]). In brief, brain ischemia was induced with an 8.0 nylon monofilament coated with a silicone resin/hardener mixture (Xantopren M Mucosa and Activator NF Optosil Xantopren, Haereus Kulzer, Germany). The filament was introduced into the left internal carotid artery up to the anterior cerebral artery. Thereby, the middle cerebral artery and anterior choroidal arteries were occluded. Filaments were withdrawn after 30 min or 1 hour to allow reperfusion. Regional cerebral blood flow (rCBF) measured using laser-Doppler-flowmetry (Perimed, Jarfälla, Sweden) fell to less than 20% during ischemia and returned to approximately 100% within 5 min after reperfusion in either group (P > 0.05). Core temperature during the experiment was maintained at 36.5 °C ± 0.5 °C with a feed-back temperature control unit. As control, sham-operated mice underwent identical surgery but did not have the filament inserted.

3.2.4 Ischemic preconditioning paradigms

3.2.4.1 Brief combined oxygen-glucose deprivation (OGD) as ischemic preconditioning stimulus in vitro

As the paradigm of ischemic preconditioning in vitro, I exposed primary cortical cultures to brief period of combined oxygen-glucose deprivation (OGD) for 30 min to 1 hour. Cells were seeded out in 24-well plates and ischemic preconditioning experiments were performed between DIV 8 and DIV 9. The experimental procedure was as following; Culture medium was removed from cells and preserved. Cells were rinsed twice with warmed PBS and placed in OGD chamber (a humidified, temperature controlled ($36\pm 0.5^{\circ}\text{C}$) chamber at $\text{PO}_2 < 2\text{mmHg}$). In the chamber, PBS was replaced by warmed balanced salt solution (BSS_0), which was put into the chamber 6-12 hours prior to the performance of the experiment. The experiment was terminated by taking the culture plates out of the OGD chamber and replacing BSS_0 by warmed conditioned medium (mixture of fresh cultivating medium [50%] and the preserved cell culture medium [50%]) (Bruer et al. 1997; Harms et al. 2004). Subsequently, culture plates were returned to normoxic cell culture incubator. Control, sister cultures went under the same washing and experimental procedures, except that they were maintained in the normoxic cell culture incubator after replacing the PBS by BSS_{20} for the same duration as for the experiment, followed by return of the conditioned medium. The condition of the cells at various time points after OGD was determined morphologically by phase contrast microscopy. At 24 hours after the preconditioning, LDH activity in the medium was measured to ensure that the ischemic preconditioning itself was not injurious to neuronal cultures.

3.2.4.2 Brief middle cerebral artery occlusion (MCAo) as ischemic preconditioning stimulus in vivo

Mice were anesthetized for induction with 1.5% isoflurane and maintained in 1.0% isoflurane in 70% N_2O and 30% O_2 using a vaporizer. Brain ischemic preconditioning was induced with an 8.0 nylon monofilament coated with a silicone resin /hardener mixture (Xantopren M Mucosa and Activator NF Optosil Xantopren, Haereus Kulzer, Germany) by

introduction of the filament into the left internal carotid artery up to the anterior cerebral artery. Thereby, the middle cerebral artery and anterior choroidal arteries were occluded.

Filaments were withdrawn after 5 min to allow reperfusion. Core temperature during the experiment was maintained at $36.5\text{ }^{\circ}\text{C} \pm 0.5\text{ }^{\circ}\text{C}$ with a feed-back temperature control unit. As control, sham-operated mice underwent identical surgery but did not have the filament inserted.

3.2.5. Cell Death Assays

3.2.5.1 Lactate Dehydrogenase (LDH) assay

We assessed neuronal injury by the measurement of LDH in the medium by means of a kinetic photometric assay (at 340 nm) (Koh and Choi, 1987) at 24 h after the injury paradigm. Lactate dehydrogenase (LDH), which is a cytosolic enzyme present in most eukaryotic cells, releases into culture medium upon cell death due to damage of plasma membrane. The increase of the LDH activity in culture supernatant is, therefore proportional to the number of lysed cells. The LDH assay measures the reduction in co-factor β -NADH used in the LDH-driven reaction, at the excitation wave-length of 340nm. Accordingly, 50 μ l of culture media were pipetted into 96-well plates and mixed with 200 μ l of β -NADH solution (0.15 mg/ml in 1x LDH buffer). Measurement was started rapidly after addition of the reaction substrate pyruvate (50 μ l of 22.7 mM pyruvate-solution). Optical density was measured at 340 nm using a microplate reader, by 10 counts with 30 sec intervals, followed by calculation of results using a LDH-standard (Greiner).

3.2.5.2 Propidium Iodide staining of cells

PI staining of neuronal cell cultures was performed as described previously (Harms et al. 2004). Briefly, cortical neurons were incubated for 1 min with 0.02 mg/ml PI (stock solution, 1 mg/ml; 1: 50) in medium with gentle shaking, and rinsed once with PBS. Conditioned medium was reapplied and phase contrast and fluorescent pictures were taken immediately using an inverse fluorescence microscope with a digital camera (Leica Microsystems,

Wetzlar, Germany). Cell counts were performed from merged phase contrast micrographs and red fluorescent pictures stained with PI. Neurons with dendrites which did not show any PI-positive signal in their nuclei were designated as intact, viable neurons. Mean intact neurons in 16 representative high-power fields were counted.

3.2.5.3 MTT reduction test

In addition to LDH assay and MTT reduction test, we also assessed neuronal viability after the injury paradigm by MTT reduction test. It is a standard cell vitality test which relies on the reduction of yellow MTT dye (3-(4,5-Dimethylthiazol-2-yl)-2,5-diphenyltetrazolium bromide) to insoluble purple formazan crystals by a mitochondrial enzyme of living cells. Briefly, cortical cells were incubated for 30 min at 37°C with 0.05 mg/ml Thiazolyl blue (Sigma), followed by addition of 10% SDS in 0.01 M HCl for lysing of the formazan crystals. After an interval of one day, optical density was measured at 550 nm in a plate-reader (Thermo LabSystems, MRX).

3.2.6 Phalloidin Staining

3.2.6.1 Phalloidin Staining of primary cortical cultures

Phalloidin staining was essentially performed as described previously (Harms et al. 2004). Briefly, cells were fixed for 10 min in 4% paraformaldehyde in PBS and subsequently membranes were permeabilized by treatment with 0.1% Triton-X-100 in PBS for 5 min. Cells were then incubated in Alexa 488 phalloidin dye at a concentration of 1 U / 200 µL PBS for 20 min, washed twice with PBS and prepared for microscopy using ImmunoFlour Mounting Medium (ICN). Images were acquired using a Leica Fluorescence Microscope with a 100× oil immersion objective. After the taking of photomicrographs, methanol extraction of phalloidin was carried out for (semi)quantitative measurements of phalloidin-bound F-actin levels. Fluorescence intensity was measured at 485-nm excitation and 530-nm emission wavelength in a Cytofluor reader (CytoFluor II, PerSeptive Biosystems, Framingham, MA, USA).

3.2.6.2 Phalloidin Staining of mouse brain slices

Phalloidin staining was essentially performed as described previously (Harms et al., 2004). Briefly, brain sections were fixed in 4% paraformaldehyde in 0.1 M phosphate buffer for 10 min and then permeabilized by treatment with 0.1% Triton X-100 in PBS. Sections were then incubated in Alexa 488 phalloidin at a concentration of 200 μ l PBS/ unit over 20 min and washed twice in PBS.

3.2.7 Measurement of intracellular Ca^{2+} in primary cortical cultures

Intracellular free Ca^{2+} -levels were assessed semi-quantitatively according to Minta et al. (1989) by loading cells with 5 μ M of cell-permeant fluorescent calcium-indicator dye Fluo-4 AM for 45 min at room temperature. Dye loading was carried out either during or after exposure of the cortical cultures to combined oxygen–glucose deprivation. Subsequently, cells were rinsed three times with PBS and the fluorescent signal was measured using a multi-well fluorescence plate reader (CytoFluor II, PerSeptive Biosystems, Framingham, MA, USA). Data are presented as difference in relative fluorescence units (RFUs) between indicated treatments and controls or % of relative fluorescence of controls.

3.2.8 Assessment of mitochondrial membrane potential by TMRE Assay

Tetramethyl rhodamine ethyl ester (TMRE) (Molecular Probes) was used to assess mitochondrial membrane potential as described (Heiskanen et al., 1999). The membrane potential-dependent dye tetramethylrhodamine ethyl ester (TMRE; Molecular Probes, Invitrogen) selectively stains for mitochondria with an intact membrane, as described previously (Cregan et al., 2002). An interval of 24 h after the injury paradigm, TMRE was added (100nM) into the cell culture medium, incubated at 37°C for 40 min and replaced with fresh cultivating medium. To assess mitochondrial TMRE uptake, fluorescence photomicrographs were taken, followed by measurement of fluorescence signal in a multi-well fluorescence plate reader at an excitation wave-length of 530 nm and an emission wave-length of 594 nm.

3.2.9 Western immunoblotting

3.2.9.1 Western immunoblotting of proteins from primary cortical cultures

For total cellular protein extraction, cortical cells were lysed in ristocetin-induced platelet agglutination (RIPA) buffer [50 mM Tris pH 7.4, 150 mM NaCl, 0.1% w/v sodium dodecyl sulphate (SDS), 1% w/v Triton X-100, 1% w/v sodium deoxycholate and protease inhibitor cocktail (Roche)] (100 μ l RIPA buffer was used per well of 6 well-plate), incubated on ice for 15 min and clarified at 12 000 \times g for 5 min at 4°C. Supernatants were collected and stored at -80°C for later use. For extraction of nuclear proteins, cortical cells were lysed in cell lysis (CL) buffer [10 mM HEPES, 2 mM magnesium chloride, 1 mM EDTA, 1 mM EGTA, 10 mM potassium chloride, 1 mM dithiothreitol (DTT), 10 mM sodium fluoride, 0.1 mM sodium vanadate, 1% Nonidet P 40, protease inhibitor cocktail (Roche)] (100 μ l CL buffer was used per well of 6 well-plate), incubated on ice for 15 min and clarified at 12 000 \times g for 1 min. Supernatants were collected as cytoplasmic protein fraction and stored at -80°C for later use. Pellets were further used for extraction of nuclear proteins in nuclear lysis (NL) buffer [25 mM HEPES, 500 mM sodium chloride, 5 mM magnesium chloride, 10 mM sodium fluoride, 1 mM dithiothreitol (DTT), 10% glycerol, 0.2% Nonidet P 40, protease inhibitor cocktail (Roche)], incubated on ice for 10 min, sonicated for 1 min at 4°C and clarified at 12 000 \times g for 5 min. Supernatants were collected and stored at -80°C for later use. Twenty micrograms of cell or nuclear lysate were denatured by boiling in equal volume of sample buffer (4% SDS, 20% glycerol, 10% 2-mercaptoethanol, 0.004% bromphenol blue and 0.125 M Tris HCl pH 6.8) for 5 min. Samples were electrophoretically separated using 4–20% gel for SDS-PAGE, transferred onto nitrocellulose membranes, blocked in blocking buffer (5% w/v milk in PBS) for 1 h at room temperature. Primary antibodies (0.2 to 1 μ g/ml) were incubated in blocking buffer overnight at 4 °C on a rotary platform with gentle agitation. Membranes were subsequently probed with secondary HRP-conjugated anti-mouse, anti-rabbit IgG or anti-goat antibodies (diluted 1:5000) in blocking buffer for 1 h at room temperature on a rotary platform with gentle agitation. Equal loading was confirmed by probing the membranes with anti-actin (1:1000, Santa Cruz) and anti-histone H4 (1:1000 Upstate) antibodies. Detection was carried out using the enhanced chemiluminescence assay (Cell Signaling Technologies). For negative controls, primary antibodies were omitted which revealed no visible staining.

3.2.9.2 Western immunoblotting of proteins from mouse brain

For total cellular protein extraction, mice brains were lysed in ristocetin-induced platelet agglutination (RIPA) buffer [50 mM Tris pH 7.4, 150 mM NaCl, 0.1% w/v sodium dodecyl sulphate (SDS), 1% w/v Triton X-100, 1% w/v sodium deoxycholate and protease inhibitor cocktail (Roche)] (100 ml RIPA buffer was used per brain hemisphere), incubated on ice for 15 min and clarified at 12 000 ×g for 5 min at 4°C. Supernatants were collected and stored at -80°C for later use. For extraction of nuclear proteins, mice brains were lysed in cell lysis (CL) buffer [10 mM HEPES, 2 mM magnesium chloride, 1 mM EDTA, 1 mM EGTA, 10 mM potassium chloride, 1 mM dithiothreitol (DTT), 10 mM sodium fluoride, 0.1 mM sodium vanadate, 1% Nonidet P 40, protease inhibitor cocktail (Roche)] (1ml CL buffer was used per brain hemisphere), incubated on ice for 15 min and clarified at 12 000 ×g for 1 min. Supernatants were collected as cytoplasmic protein fraction and stored at -80°C for later use. Pellets were further used for extraction of nuclear proteins in nuclear lysis (NL) buffer [25 mM HEPES, 500 mM sodium chloride, 5 mM magnesium chloride, 10 mM sodium fluoride, 1 mM dithiothreitol (DTT), 10% glycerol, 0.2% Nonidet P 40, protease inhibitor cocktail (Roche)], incubated on ice for 10 min, sonicated for 3 x 15 sec at on ice and clarified at 12 000 ×g for 5 min. Supernatants were collected and stored at -80°C for later use. Twenty micrograms of cell or nuclear lysate were denatured by boiling in equal volume of sample buffer (4% SDS, 20% glycerol, 10% 2-mercaptoethanol, 0.004% bromphenol blue and 0.125 M Tris HCl pH 6.8) for 5 min. Samples were electrophoretically separated using 4–20% SDS-PAGE, transferred onto nitrocellulose membranes, blocked in blocking buffer (5% w/v milk in PBS) for 1 h at room temperature. Primary antibodies (0.2 to 1 µg/ml) were incubated in blocking buffer overnight at 4 °C on a rotary platform with gentle agitation. Membranes were subsequently probed with secondary HRP-conjugated anti-rabbit IgG or anti-goat antibodies (diluted 1:5000) in blocking buffer for 1 h at room temperature on a rotary platform with gentle agitation. Equal loading was confirmed by probing the membranes with anti-actin (1:1000, Santa Cruz) and anti-histone H4 (1:1000 Upstate) antibodies. Detection was carried out using the enhanced chemiluminescence assay (Cell Signaling Technologies). For negative controls, primary antibodies were omitted which revealed no visible staining.

3.2.10 ELISA-based Histone Acetyltransferase (HAT) Activity Assay

Nuclear proteins from primary cortical cultures were extracted using the same protocol as utilized for western immunoblotting analysis of proteins. Accordingly, cells were lysed in cell lysis (CL) buffer [10 mM HEPES, 2 mM magnesium chloride, 1 mM EDTA, 1 mM EGTA, 10 mM potassium chloride, 1 mM dithiothreitol (DTT), 10 mM sodium fluoride, 0.1 mM sodium vanadate, 1% Nonidet P 40, protease inhibitor cocktail (Roche)] (100 μ l CL buffer was used per well of 6 well-plate), incubated on ice for 15 min and clarified at 12 000 \times g for 1 min. Supernatants were collected as cytoplasmic protein fraction and stored at -80°C for later use. Pellets were further used for extraction of nuclear proteins in nuclear lysis (NL) buffer [25 mM HEPES, 500 mM sodium chloride, 5 mM magnesium chloride, 10 mM sodium fluoride, 1 mM dithiothreitol (DTT), 10% glycerol, 0.2% Nonidet P 40, protease inhibitor cocktail (Roche)], incubated on ice for 10 min, sonicated for 1 min at 4°C and clarified at 12 000 \times g for 5 min. Supernatants were collected and stored at -80°C for later use. wells of a streptavidin coated strip plate were pre-coated with 100 μ l of 1 μ g/ml reconstituted histone H4 (Catalog # 12-405) for 30 minutes at room temperature, washed 5 times with TBS and blocked with 200 μ l of 3% BSA for 30 minutes at 30°C . Subsequently, 50 μ l of HAT reaction cocktails, which include HAT assay buffer, 100 μ M acetyl-CoA, dd-water and 5 μ g nuclear extract, were added into each well and incubated for 20 min at 30° a rotary platform with gentle agitation. After washing with TBS, 100 μ l of 1:250 anti-acetyl-Lysine antibody was added into the wells in blocking solution, incubated for 1.5 hours at room temperature, followed by washing and incubation with 100 μ l of 1:5,000 Goat Anti-Rabbit IgG, HRP conjugate in blocking solution for 30 minutes at room temperature. TMB Substrate Mixture (100 μ l per well) was used to generate HRP-based colorimetric signal, which was measured subsequently in a plate reader at a wavelength of 450nm.

3.2.11 Immunochemical staining

3.2.11.1 Immunocytochemistry of primary cortical cultures

For immunocytochemical analysis of primary cortical cultures, cells were seeded onto glass cover slips, fixed with 4% paraformaldehyde in PBS for 10 min, permeabilized with 0.1% Triton-X in PBS (8.5 min) and exposed to blocking solution (PBS containing 5% donkey serum and 0.2% Tween-20) for 1 h at room temperature (22°C). Cultures were incubated with

primary antibodies raised against Map-2 (1 : 250), murine gelsolin (1 : 100) or acetylated histone H4 (1 : 250), separately for 60 min at room temperature (22°C), with subsequent rinsing with PBS and development with donkey secondary antibodies conjugated with FITC, rhodamine X for 45 min at room temperature (22°C) (1 : 250). DNA counterstaining was performed with Hoechst 33258 for 5 min at room temperature (22°C) at a final concentration of 2 µg/ml in H₂O, followed by extensive washing in H₂O and preparation for microscopy using ImmunoFluor Mounting Medium (ICN Biochemicals, Costa Mesa, CA, USA). Images were acquired using a Leica fluorescence microscope with a × 40 oil immersion microscope and a digital camera.

3.2.11.2 Immunohistochemistry of mouse brain slices

Animals were deeply anesthetized and perfused transcardially with 4% paraformaldehyde in 0.1 M phosphate buffer. Tissue was essentially processed as described previously ([Katchanov et al., 2001] and [Kronenberg et al., 2005]). Briefly, after postfixation for 48 h in 4% paraformaldehyde brains were transferred to 30% sucrose in 0.1 M phosphate buffer for dehydration. Forty micrometers of coronal sections were cut from a dry ice-cooled block on a sliding microtome (Leica, Bensheim, Germany) and cryoprotected. Sections were stained free floating with antibodies diluted in Tris-buffered saline containing 3% donkey serum and 0.1% Triton X-100 ([Katchanov et al., 2001] and [Gertz et al., 2006]). Immunostaining followed the peroxidase method with biotinylated secondary antibodies (all: 1:500, Jackson ImmunoResearch Laboratories, West Grove, PA), ABC Elite reagent (Vector Laboratories, Burlingame, CA) and diaminobenzidine (Sigma) as chromogen. For immunofluorescence FITC-, RhodX- or Cy5-conjugated secondary antibodies were all used at a concentration of 1:250. Fluorescent sections were coverslipped in polyvinyl alcohol with diazabicyclooctane (DABCO) as anti-fading agent. Images were recorded using a Leica fluorescence microscope with a 40× oil immersion objective and a digital camera.

3.2.12 Neurological Scoring of Mice- Determination of functional deficits

Animals were scored for neurological sensory–motor deficits from 0 (no deficit) to 3 (severe deficit) with minor modifications as described (Bederson et al., 1986). The rater was naïve to the treatment groups.

3.2.13 Measurement of physiological variables

In randomly selected animals, the left femoral artery was cannulated with a PE 10 catheter for blood pressure, heart rate and blood gas determination as described previously (Endres et al., 1999). Arterial blood samples were analyzed for pH, arterial oxygen pressures, and partial pressures of carbon dioxide.

3.2.14 Determination of brain lesion size

Animals were sacrificed at 24 h after brain ischemia. Brains were snap-frozen in isopentane for cryostat sectioning. Ischemic lesion size was measured by computer-assisted volumetry of serial 20 μm -thick hematoxylin stained brain coronal cryostat sections (2 mm apart). Lesion volume was determined by summing the volumes of each section directly or indirectly using the following formula: contralateral hemisphere (mm^3) – undamaged ipsilateral hemisphere (mm^3). The difference between direct and indirect lesion volumes is likely to be accounted for by brain swelling.

3.1.15 Statistical evaluation

Data were pooled from at least two to three representative experiments and presented as mean \pm SEM or mean \pm SD. For statistical analysis Student's t-test (lesion volumes), ANOVA on ranks (cell viability after OGD in CBP-deficient cultures and Bederson deficit scores) test and one-way ANOVA followed by Tukey's post hoc (for all the other data, *i.e.* cell viability, calcium and mitochondrial membrane potential data) were utilized as applicable (SigmaSTAT statistical software). $P < 0.05$ was considered statistically significant.

4 RESULTS

4.1 HISTONE ACETYLATION AND NEURONAL ISCHEMIC INJURY

4.1.1 Histone acetylation levels decrease in neurons following injurious combined oxygen-glucose deprivation

Impaired histone acetyltransferase (HAT) enzyme activity and consequent aberrant histone acetylation status were implicated in pathophysiology of numerous neurodegenerative diseases (Jin et al., 2001; Rouaux et al., 2003; Jiang et al., 2003). Here, my aim was to investigate whether histone acetylation patterns alter in neurons also following ischemic injury. For this purpose, rat primary cortical cultures were exposed to injurious combined oxygen glucose deprivation (OGD) for 2 to 3 hours, and nuclear proteins were extracted at the termination of OGD as well as at 1, 12 and 24 hours after the ischemic damage. Protein samples were subsequently subjected to sodium dodecyl sulphate-polyacrylamide gel electrophoresis (SDS-PAGE), followed by western immunoblotting using antibodies against acetyl-histone H4 and acetyl-histone H3. Acetylation loss of both histone H4 and histone H3 was evident at all time points examined after OGD (Figure 6). In OGD control cultures histone acetylation levels maintained consistent at all time points. Anti-actin antibody was employed for the demonstration of equal protein loading.

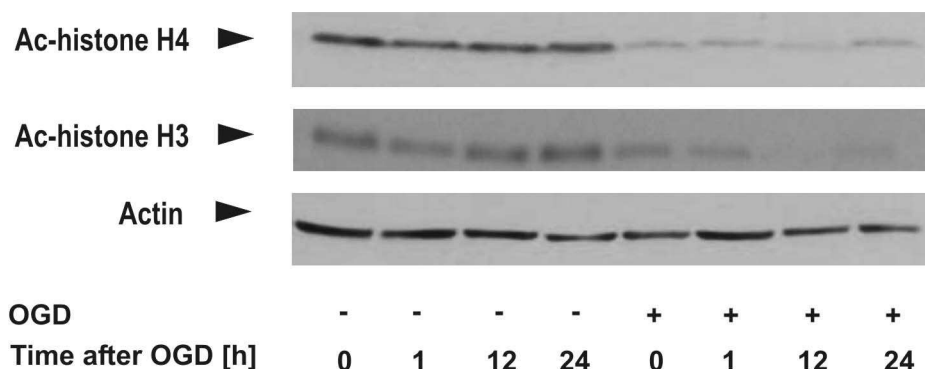


Figure 6 Histone acetylation levels decrease in neurons after exposure to injurious combined oxygen-glucose deprivation. Primary cortical neurons underwent a damaging OGD for 2 to 3 hours. Subsequently nuclear protein extraction was carried out at different time points after the ischemic insult. 20 µg of protein was

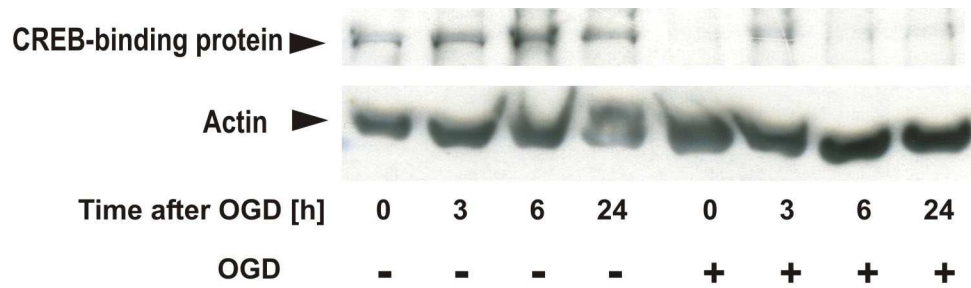
subjected to sodium dodecyl sulphate-polyacrylamide gel electrophoresis (SDS-PAGE) and membranes were incubated with antibodies against acetyl-histone H4, acetyl-histone H3 and actin. The image represents the results of three independent experiments.

4.1.2 CREB-binding protein (CBP) is rapidly depleted in neurons following injurious combined oxygen-glucose deprivation

Loss of CBP protein has been suggested to occur in different neurodegenerative disease models including Huntington's and Alzheimer's Diseases (Nucifora et al., 2001, Jiang et al., 2003, Marambaud et al., 2003). CBP was particularly targeted by caspase 6 at the very early stages of neuronal apoptosis in an in vitro oxidative stress model (Rouaux et al., 2003). To investigate whether CBP protein levels are altered also following neuronal ischemic injury, rat primary cortical cultures were exposed to combined oxygen glucose deprivation (OGD) for 2 to 3 hours, and nuclear proteins were subsequently extracted at the termination of OGD as well as at 3, 6 and 24 hours time intervals after the ischemic damage. Samples were subjected to SDS-PAGE protein electrophoresis, followed by western immunoblotting using an antibody against CBP. Loss of CBP protein was evident at all time points examined after OGD (Figure 7A). Whilst there was a weak CBP band at 3 hours after OGD, no detection was obtained either at 6 or 24 hours. In control cultures, CBP protein bands were consistently present at all time points of protein extraction following OGD. Actin antibody was employed for the demonstration of equal protein loading.

In addition, immunocytochemical stainings were carried out on rat primary cortical cultures after their exposure to injurious OGD. Cultures were fixated immediately after the ischemic insult and an antibody directed against CBP was used for immunocytochemistry, as well as Sytox Green staining for nucleic acids (green). In agreement with the western immunoblotting data, photomicrographs revealed a decrease in CBP protein (red) levels in neurons following injurious OGD (Figure 7B). CBP protein was no longer evident particularly in neurons with prominent apoptotic morphology (see arrows).

A



B

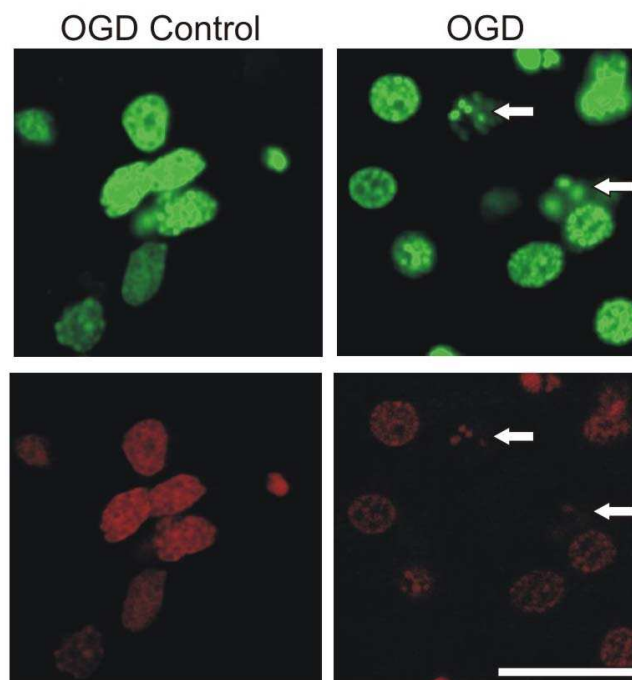


Figure 7 CBP is depleted in neurons following injurious oxygen-glucose deprivation. (A, B) Primary cortical neurons underwent injurious OGD. (A) Subsequently, nuclear protein extraction was carried out at different time points after the ischemic insult. 20 μ g of protein was subjected to sodium dodecyl sulphate-polyacrylamide gel electrophoresis (SDS-PAGE) and membranes were incubated with antibodies against CREB-binding protein (CBP) and actin. (B) For immunocytochemistry, cortical cells were fixated immediately after OGD. Nuclear staining (green), CBP (red). Scale bar, 30 μ m. The images are representative results of three independent experiments.

4.1.3 Curcumin, a CBP's HAT activity inhibitor, exacerbates injury by combined oxygen-glucose deprivation

Having shown CBP's rapid depletion following injurious OGD, we next investigated whether CBP' HAT function is associated to neuronal susceptibility to ischemic damage in vitro. For this purpose, curcumin, an inhibitor of CBP's HAT activity was employed (Balasubramanyam et al., 2003). Rat primary cortical cultures on in vitro day 9 (DIV9) underwent an injurious combined oxygen-glucose deprivation (OGD) of 2 to 3 hours. Neurons were continuously treated with curcumin both during and after OGD until the assessment of cellular damage. Twenty-four hours after OGD, lactate dehydrogenase (LDH) release into the medium was measured as an indirect measurement of cell death. In addition, MTT test was employed as a life/death assay.

OGD caused injury to cortical cultures, by means of increased LDH release into the medium. However, the injury was further enhanced by 4 μ M and 16 μ M curcumin treatment of cultures (Figure 8A). Noteworthy, curcumin treatment by itself did not result in any basal toxicity in sister cultures under normoxic conditions (data not shown). These data was also supported by MTT test. Measurement of MTT 24 hours after OGD revealed further reduction in neuronal survival by curcumin treatment of cortical cultures following injurious OGD (Figure 8B).

To demonstrate that Curcumin has indeed the expected effect on histone acetylation, primary cortical cultures were treated with curcumin at doses of 1, 4 and 16 μ M for 12 hours, nuclear proteins were extracted, followed by western immunoblotting using antibodies against acetyl-histone H4 and acetyl-histone H3. Acetylation levels of histone H4 as well as histone H3 were reduced with the increasing doses of Curcumin, the decrease being evident particularly at 4 and 16 μ M doses (Figure 8C). Actin antibody was employed for the demonstration of equal protein loading.

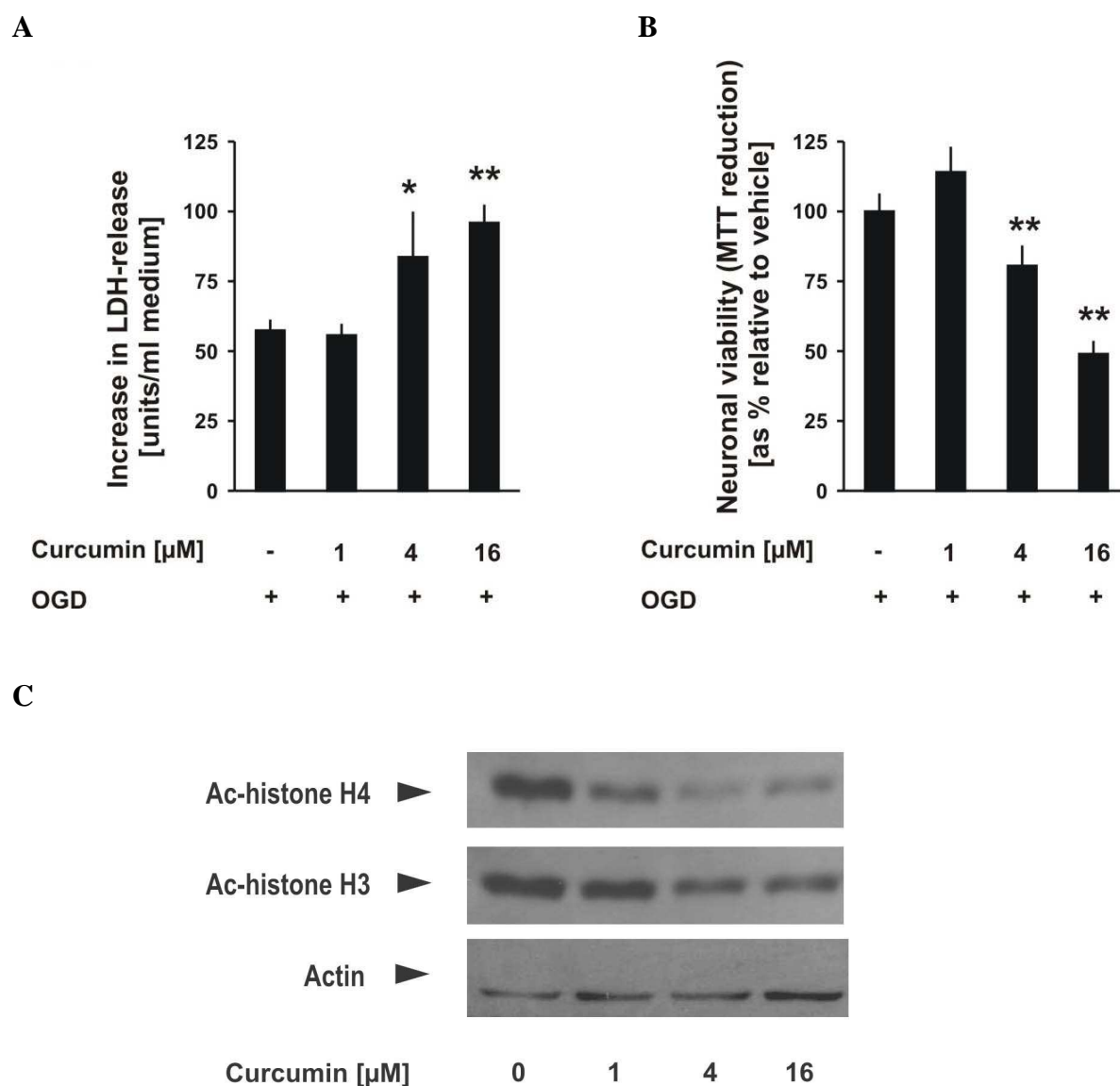


Figure 8 Curcumin exacerbates neuronal damage caused by oxygen-glucose deprivation. (A, B) Primary cortical neurons were subjected to injurious OGD and were treated with curcumin both during and after the ischemic insult. (A) At 24 hours after OGD, release of lactate dehydrogenase (LDH) into the culture medium was measured as an indirect marker of cell death. Data are presented as the increase in LDH release relative to sister cultures in normoxic conditions. (B) At 24 hours after OGD, MTT reduction test was carried out to measure cell viability. Data are presented as percentage in comparison to vehicle-treated cultures. * $p < 0.05$ and ** $p < 0.001$ versus vehicle. (C) Primary cortical neurons were treated with curcumin at doses of 1, 4 and 16 μM for 12 hours, nuclear proteins were subsequently extracted and 20 μg of protein was subjected to sodium dodecyl sulphate-polyacrylamide gel electrophoresis (SDS-PAGE). Membranes were incubated with antibodies against acetyl-histone H4, acetyl-histone H3 and actin. The image represents the results of two independent experiments.

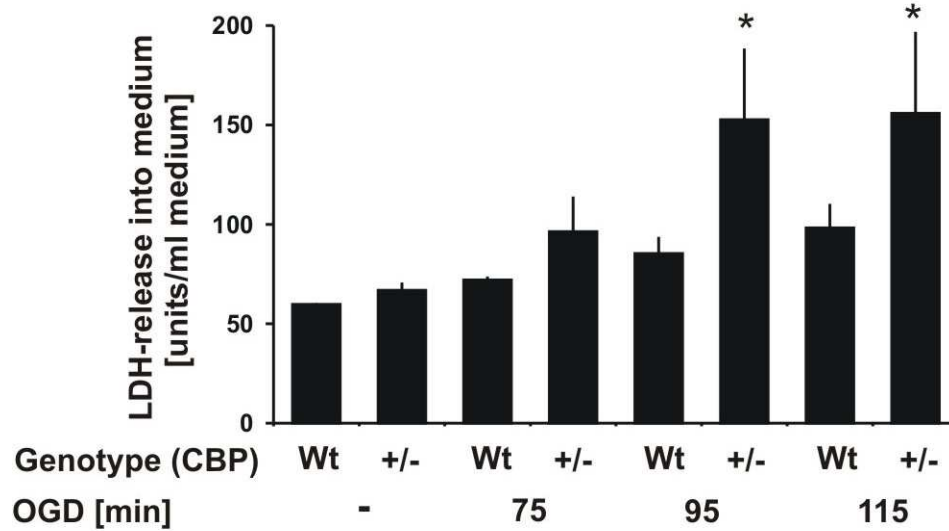
4.1.4 CBP-deficient neurons are more susceptible to injury by combined oxygen-glucose deprivation

To test whether CBP's restrained function is indeed causally linked to increased susceptibility to ischemic damage, we performed experiments utilizing primary cortical cultures from CBP +/- (CBP-deficient) mice. Cultures from wild-type as well as from CBP-deficient mice underwent injurious OGD for different durations of 1 hour 15 minutes to 1 hour 55 minutes on in vitro day 9 (DIV9). According to personal experience, murine cortical neurons show more sensitivity to damage compared to cortical neurons from rat, therefore the duration of OGD was reduced to yield similar cellular damage and comparable increases in LDH levels. Twenty-four hours after OGD, lactate dehydrogenase (LDH) release into the medium was measured as an indirect measurement of cell death. In addition, phase-contrast photomicrographs were taken to visualise the results.

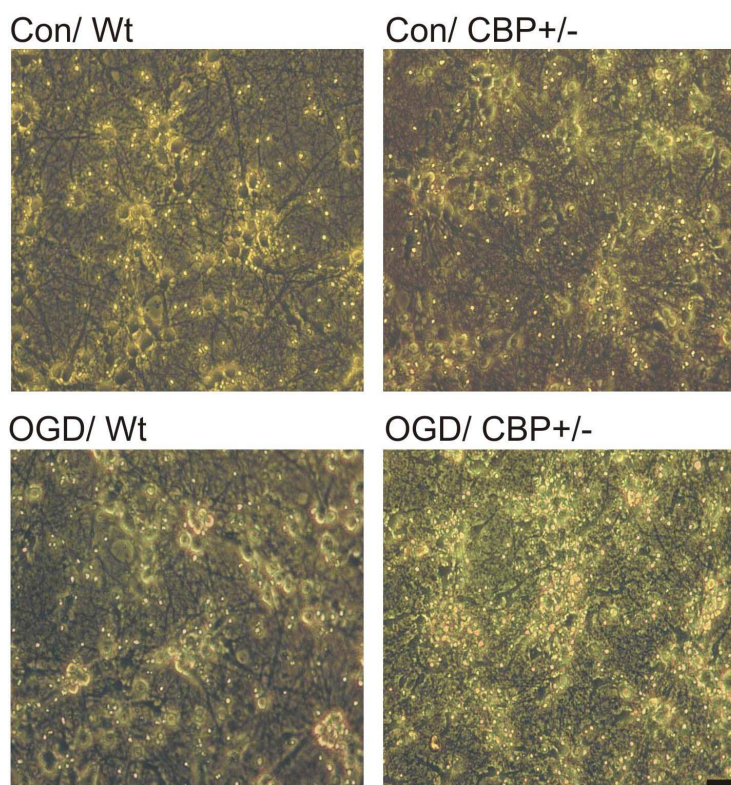
Increasing durations of OGD increased severities of injury to cortical cultures, as measured in the release of LDH into the culture medium. Injury was further exacerbated in primary cortical cultures partially deficient in CBP compared to wild-type cultures, reaching statistical significance particularly after longer OGD durations (1 hour 35 minutes and 1 hour 55 minutes) (Figure 9A). As seen in OGD control conditions, cortical cultures of the two genotypes had similar basal LDH levels, indicating that cellular health under normoxic conditions were comparable. These data were also supported by phase-contrast photomicrographs, showing higher injury in CBP-deficient cultures after OGD in comparison to wild-type cultures. The photomicrographs presented were taken from the control cultures and cultures exposed to the highest OGD duration of 1 hour 55 minutes (Figure 9B).

To study whether CBP deficiency has indeed the expected effect on histone acetylation levels, nuclear proteins were extracted from CBP +/- and wild-type cultures and western immunoblotting was carried out using antibodies against acetyl-histone H4 and acetyl-histone H3. Acetylation levels of both histones H4 and histone H3 were clearly reduced in CBP-deficient neuronal cultures (Figure 9C). Actin antibody was employed for the demonstration of equal protein loading.

A



B



C

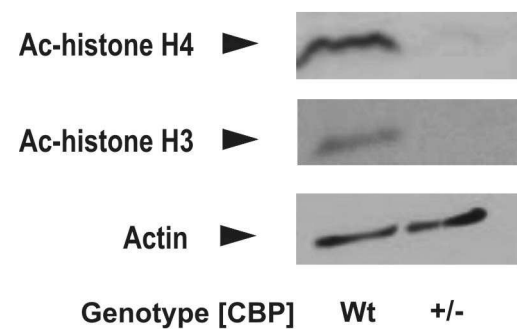


Figure 9 Primary cortical cultures from CBP-deficient mice are more susceptible to injury by oxygen-glucose deprivation. (A, B) Primary cortical neurons were prepared from CBP-deficient (CBP +/-) mice or wildtype (wt) littermates. Cultures were subjected to 1 hour 15 min to 1 hour 55 min combined oxygen-glucose deprivation (OGD). (A) Twenty-four hours after OGD, release of lactate dehydrogenase (LDH) into the culture medium was measured as an indirect marker of cell death. (B) Subsequently representative phase-contrast

photomicrographs were taken. At baseline (in normal conditions) there was no difference between wt and CBP +/- cultures, in regard to LDH release into medium. * $P < 0.01$ for CBP-deficient *vs.* corresponding wild-type culture; One-way ANOVA on ranks. (C) Nuclear proteins were extracted from CBP-deficient as well as from wild-type cultures, 20 μg of protein was subjected to sodium dodecyl sulphate-polyacrylamide gel electrophoresis (SDS-PAGE) and membranes were incubated with antibodies against acetyl-histone H4, acetyl-histone H3 and actin. The image represents the results of two independent experiments. Scale bar, 30 μm .

4.2 HISTONE ACETYLATION AND BRAIN ISCHEMIC PRECONDITIONING

4.2.1 Brief non-injurious ischemia protect mice brain against following severe middle cerebral artery occlusion

Ischemic preconditioning in brain is described as brief ischemic episode protecting brain against subsequent prolonged otherwise lethal ischemic insult. In my project, a so-called “focal-focal” model was employed as an *in vivo* model of ischemic preconditioning. Accordingly, mice underwent a 5 minutes filamentous occlusion of left middle cerebral artery (MCAo), which was not injurious (data not presented). Following an interval of 24 hours, the same artery was occluded for 30 minutes as the injurious ischemic attack. Animals were sacrificed after a reperfusion period of 24 hours, and brains were snap-frozen. Cryostat sectioning of the brains, Hematoxylin staining of the sections and determination of cerebral lesion volumes by computer-assisted volumetry on serial coronal sections were carried out subsequently.

Short (5 minutes) left MCAo 24 hours prior to severe (30 minutes) left MCAo conferred significant reduction in cerebral infarct volumes (figure 10A and B). Similar results were obtained when lesion volumes were corrected for brain oedema (data not shown). Figure 10B confirms that preconditioned mice had smaller cerebral lesion areas in all anterior to posterior coronal brain sections, with the exception of the most anterior area. Despite the reduction in the brain lesion size, a difference between preconditioned *vs.* sham mice was not evident in Bederson neurological sensorimotor deficit scores at 24 hours after the ischemic stroke (data not presented).

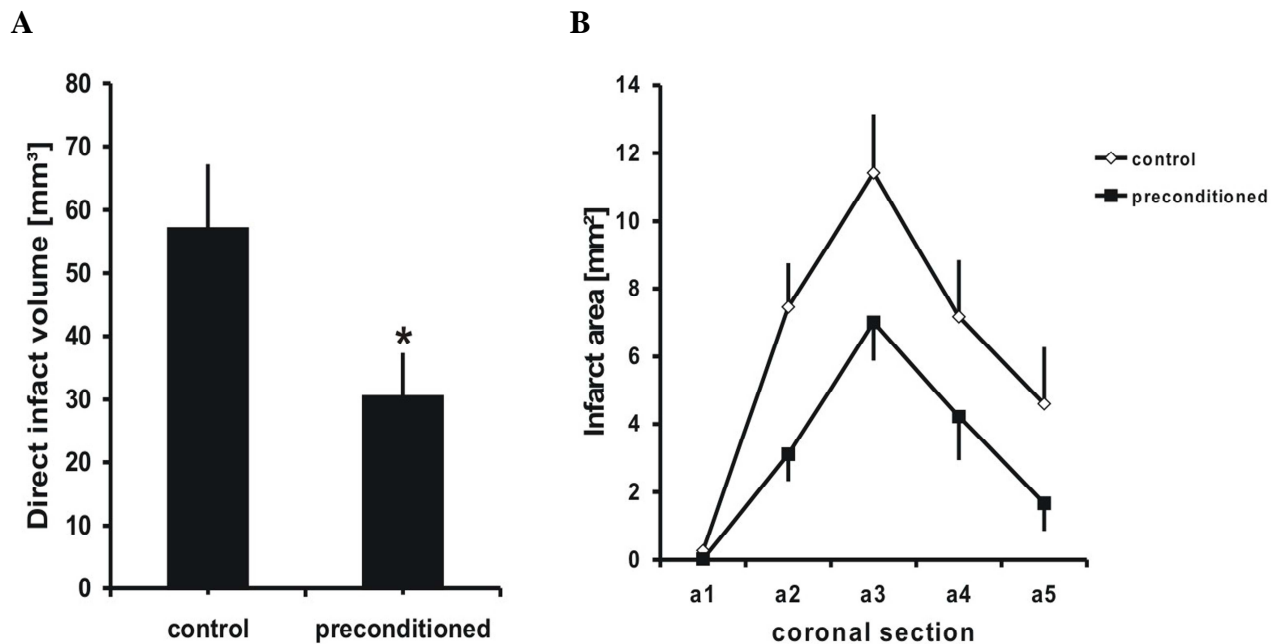


Figure 10 Ischemic preconditioning protects mice brain against injury by middle cerebral artery occlusion and reperfusion. The effect of previous 5 min filamentous MCA occlusion on cerebral infarct volume (A) and areas (B) following 30 minutes filamentous MCA occlusion and 24 hours of reperfusion, compared with not-preconditioned C57Bl/6 mice. Brain lesion volumes were determined quantitatively on 20 μ m thick, hematoxylin-stained brain cryostat sections as described before (Endres et al., 1999); n=10 animals per groups; Student's t-test; * P <0.05.

4.2.2 Brief sub-lethal ischemia protects neuronal cultures against following severe combined oxygen-glucose deprivation

Rat primary cortical cultures were subjected to a short episode of combined oxygen-glucose deprivation (OGD), ranging from 30 minutes to 1 hour on in vitro day 8 (DIV 8), as the preconditioning stimulus. After an interval period of 48 hours, preconditioned as well as control sister cultures were exposed to severe OGD, as the injurious ischemia. Lactate dehydrogenase (LDH) assay and MTT test were employed as cellular death/viability assays.

As presented in figure 11A, OGD caused increase in LDH release into the medium significantly reduced when the cultures had previously undergone a short ischemic episode. Results obtained from MTT test also showed that OGD caused decrease in neuronal viability, and this decrease was partly prevented by ischemic preconditioning (figure 11B).

The protective effect was abrogated when the time interval between ischemic preconditioning OGD was shorter than 24 hours (data not shown). Ischemic preconditioning by itself did not cause a significant increase in LDH release (data not shown).

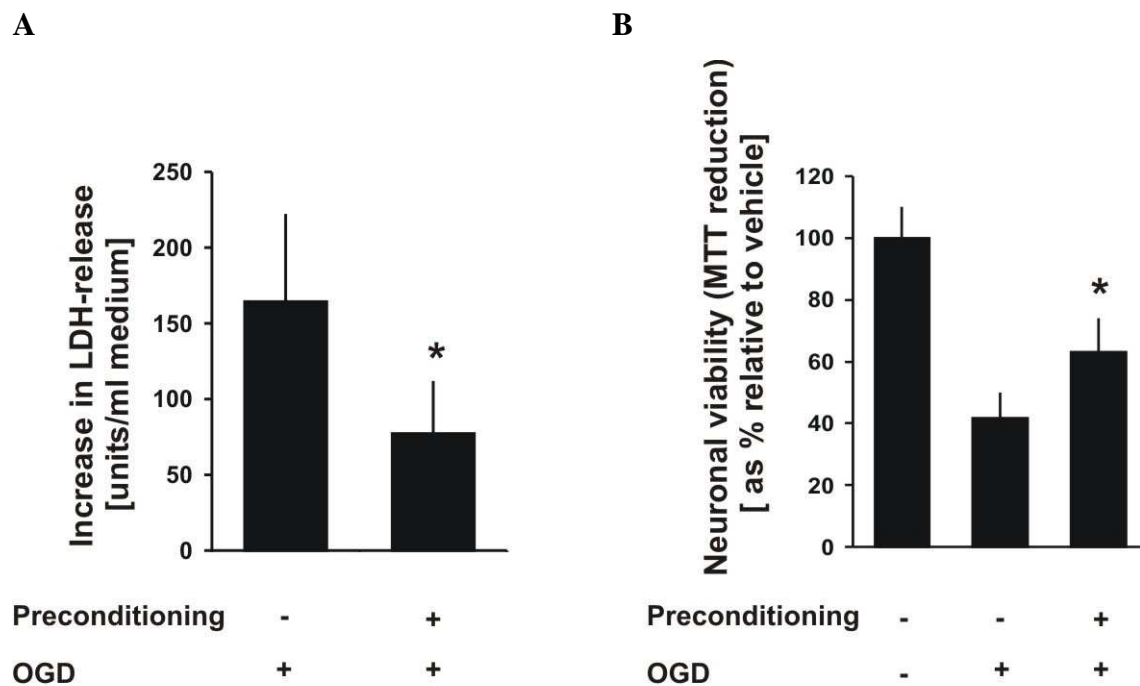


Figure 11 Ischemic preconditioning protects cortical neurons against combined oxygen-glucose deprivation (OGD). (A, B) Primary cortical neurons were exposed to a brief oxygen-glucose deprivation on in vitro day 8 (DIV 8) and 48 hours afterwards subjected to damaging OGD of 2 to 3 hours. (A) At 24 hours after OGD, release of lactate dehydrogenase (LDH) into the culture medium was measured as an indirect marker of cell death. Data is presented as the increase in LDH release, after the subtraction of LDH values of sister cultures in normoxic conditions. * $P < 0.001$ vs. vehicle. (B) At 24 hours after OGD, MTT mitochondrial viability test was carried out as a cellular life/death assay. Data is presented as percentage relative to sister cultures in normoxic conditions, which represents 100 % neuronal viability. * $P < 0.001$ vs. preconditioning control.

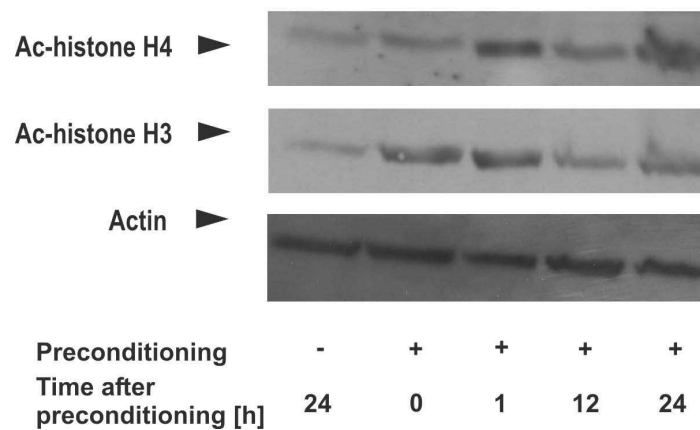
4.2.3 Ischemic preconditioning enhances histone acetylation levels in rat primary cortical cultures and in mice brain

It is widely accepted that ischemic preconditioning in brain is mostly dependent on novel gene expression and that histone acetylation is an ultimate switch for active gene expression processes. After establishing experimental models of ischemic preconditioning,

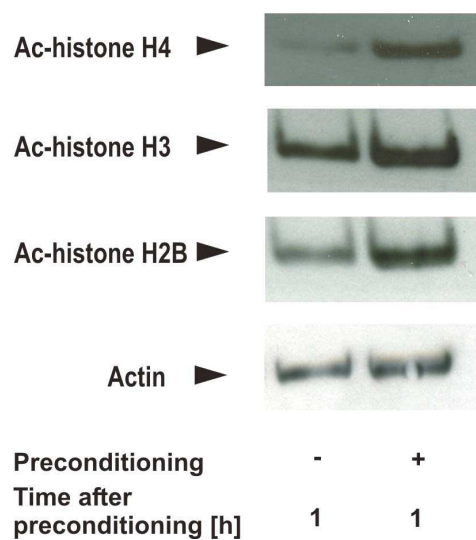
we next aimed at testing whether ischemic preconditioning stimulus alters histone acetylation levels. *In vitro*, rat primary cortical cultures were subjected to a short episode of OGD, as the preconditioning stimulus, followed by extraction of nuclear proteins at the termination of OGD as well as at 1 hour, 12 hours and 24 hours after the preconditioning stimulus. Protein samples were subjected to SDS-PAGE and acetylation of histone H4 and histone H3 were determined by western immunoblotting. Figure 12A demonstrates a dynamic alteration of histone H4 and histone H3 acetylation in cortical cultures upon exposure to the ischemic preconditioning stimulus. Enhancement of histone H4 acetylation displayed a biphasic pattern: It was most prominent at 1 hour and 24 hours, and was less pronounced, though still evident, at 12 hours after the preconditioning stimulus. Increase in histone H3 acetylation, on the other hand, was most evident at immediately and 1 hour after the preconditioning ischemia. In another set of experiments, we examined histone acetylation changes at 1 hour after ischemic preconditioning and observed enhancement of histone H4, histone H3 as well as histone H2B acetylation levels (Figure 12B). Anti-actin antibody was employed for the demonstration of equal loading.

In vivo, mice were sacrificed after reperfusion intervals of 1 hour, 6 hours and 18 hours, following 5 minutes left middle cerebral artery occlusion (MCAo). Whole hemisphere nuclear protein extracts were subjected to SDS-PAGE and acetylated histone H4 levels as well as that of histone H3 and histone H2B were determined by western immunoblotting. Figure 12C demonstrates enhancement of histone H3 and histone H2B acetylation levels 1 hour after preconditioning MCAo. Increase in histone H3 and histone H2B acetylation levels were similar in both ipsilateral, in which middle cerebral artery was occluded, and also in contralateral hemisphere, which did not experience any arterial occlusion. Histone H4 acetylation, on the other hand, did not differ in preconditioned *vs.* control brains. No change in histone acetylation level was detected for any of the three histones at later time points, 6 or 18 hours, following ischemic preconditioning stimulus *in vivo* (data not shown). Anti-actin antibody was employed for the demonstration of equal loading.

A



B



C

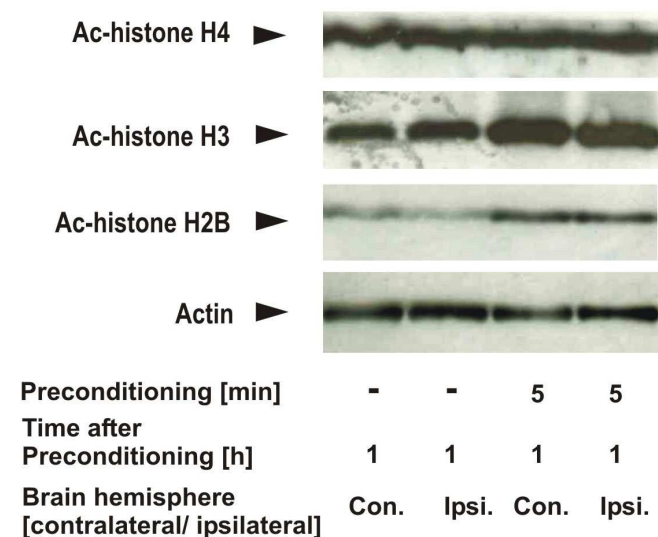


Figure 12 Histone acetylation levels are increased in rat cortical neurons and in mice brain following ischemic preconditioning. (A, B) Rat primary cortical neurons underwent a brief period of oxygen-glucose deprivation (OGD) and subsequently nuclear protein extraction was carried out for western immunoblotting at different time points after the preconditioning stimulus. Twenty μg of protein was subjected to SDS-PAGE and membranes were incubated with antibodies against Ac-histone H4, Ac-histone H3, Ac-histone H2B and actin after stripping and reprobing the same membrane. (C) Immunoblots show the effect of 5 min filamentous MCA occlusion on histone acetylation in both ipsilateral and contralateral brain hemispheres of mice, 1 hour after the preconditioning stimulus. Twenty μg brain lysate was subjected to SDS-PAGE and acetylation of histone H4, Ac-histone H3, Ac-histone H2B was analyzed by Western immunoblotting. Images are representative of three independent experiments.

4.2.4 Ischemic preconditioning enhances histone acetyltransferase (HAT) activity in rat primary cortical cultures

Having demonstrated increased histone acetylation patterns following ischemic preconditioning in vitro as well as in vivo, we next tested whether histone acetyltransferase activity is enhanced in neuronal cultures after ischemic preconditioning as acetylation reaction of histones is driven by members of histone acetyltransferase (HAT) family. An ELISA-based enzyme activity assay was employed to measure total cellular histone acetyltransferase activity. Primary cortical cultures were subjected to a short episode of OGD, as the preconditioning stimulus, followed by extraction of nuclear proteins at 1 hour. Using 5 μg of nuclear proteins total cellular HAT activity was measured on histone H4 coated microwell plates and an antibody against acetyl-lysine residues was employed to recognise acetylation of histone H4. Subsequent to incubation with a secondary antibody and development of HRP reaction, measurement of optic density at 450 nm revealed increase in overall histone acetyltransferase activity in rat primary cortical cultures 1 hour after their exposure to preconditioning ischemia (figure 13).

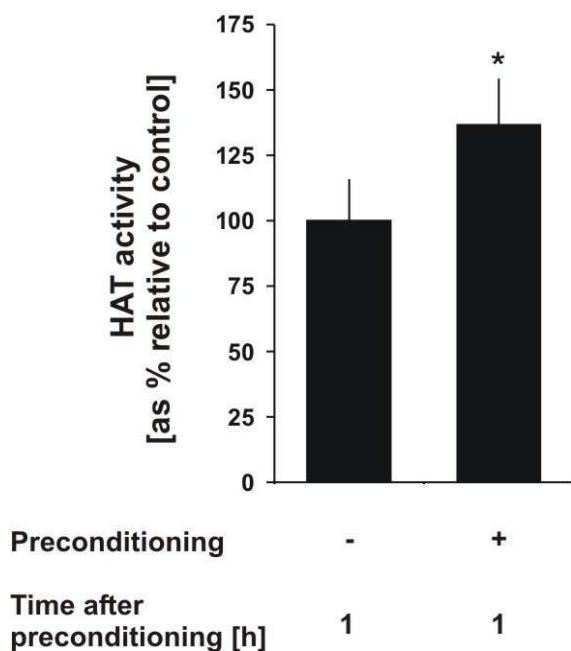


Figure 13 Histone acetyltransferase activity is increased in cortical neurons after ischemic preconditioning. Primary cortical neurons underwent a brief period of oxygen-glucose deprivation (OGD) and subsequently nuclear protein extraction was carried out at 1 hour for ELISA-based enzyme activity assay. Five μg nuclear protein was used to measure total HAT activity on histone H4 coated microwell plates. Data was pooled from three independent experiments, and presented as the percentage relative to not-preconditioned control samples. Values (mean \pm SD) in OD at 450nm are 145.8 \pm 22.9 and 199 \pm 25.7. * P < 0.05 preconditioned vs. control sample.

4.3 NEUROPROTECTION BY TRICHOSTATIN A (TSA) PRE-TREATMENT

4.3.1 Trichostatin A pre-treatment protects neuronal cultures against ischemic injury

Our aim was to test whether enhancing histone acetylation by the potent HDAC inhibitor Trichostatin A (TSA) protect primary cortical cultures against combined oxygen-glucose deprivation (OGD). For this purpose, rat primary cortical cultures were pre-treated with 300nM TSA for 12 or 24 hours and then subjected to 120 min - 150 min OGD on in vitro day 9 (DIV9), along with the vehicle treated cultures. Twenty-four hours later, cultures were stained with propidium iodide (pi) dye to quantify cell death. Photomicrographs were taken subsequently and dead vs. living cells were counted. While healthy cells are spared, propidium iodide dye penetrates into dead cells through fragmented cellular membranes and marks the genetic material of dead cells.

Exposure of primary cortical cultures to OGD resulted in marked reduction in the number of living cells, yet neurons were significantly protected when they were treated with 300nM TSA prior to OGD (Figure 14A). Representative photomicrographs are presented in figure 14B. Pre-treatment regimes with lower doses of TSA and for shorter durations did not afford neuroprotection (data not shown). Pre-treatment regime of 300nM TSA for 12 or 24 hours did not cause any basal toxicity to primary cortical cultures. Approximately 30 percent cell death observed in OGD control cultures, similar both in vehicle and TSA treated, represents normally occurring cell death in culture conditions.

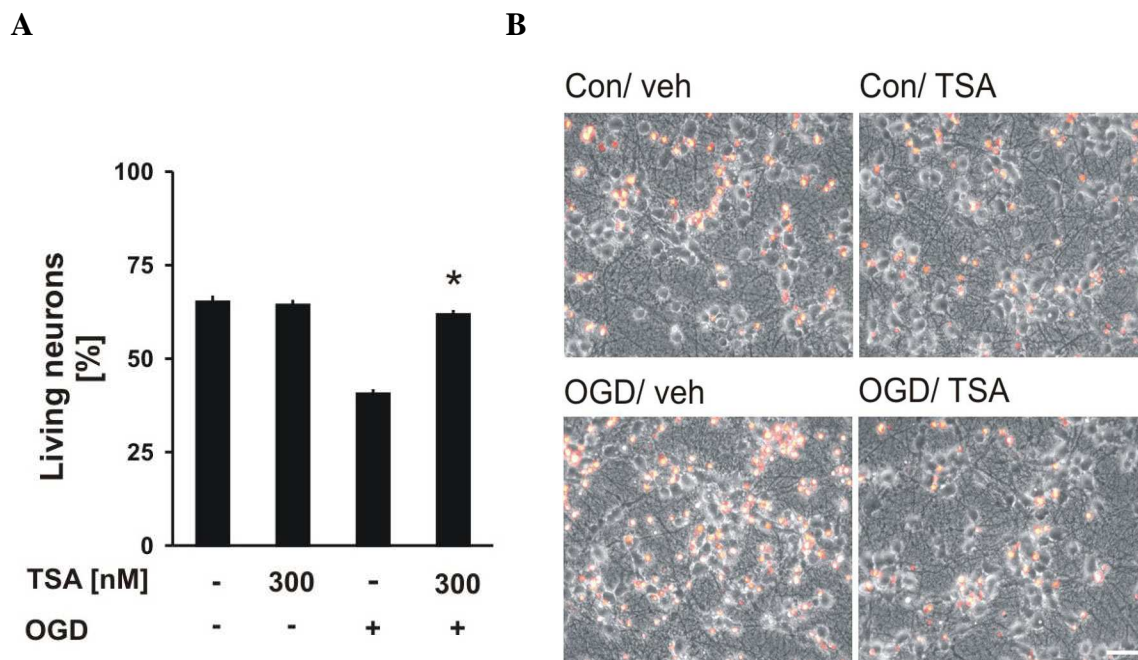


Figure 14 Trichostatin A pretreatment protects primary cortical cultures against combined oxygen-glucose deprivation (OGD). Cortical cultures were pre-treated with 300nM TSA for 12 h or 24 hours on DIV 8 and subsequently subjected to 2 to 3 hours of OGD on DIV9. (A) At 24 hours, cell counts were performed on merged phase contrast and propidium iodide (PI)-stained photomicrographs (B). Data are presented as the percentage of non-PI-stained vs. total number of neurons per high-power field; * $P < 0.001$ vs. vehicle. Scale bar, 30 μm .

4.3.2 Trichostatin A pre-treatment protects mice brain against ischemic injury

After the demonstration of its neuroprotective properties *in vitro*, we next tested whether TSA also afford neuroprotection in an *in vivo* model of cerebral ischemia. 129/Sv mice were treated with TSA, or vehicle, at a dose of 5mg/kg body weight for fourteen days by daily intraperitoneal injections, and went under surgery of filamentous middle cerebral artery occlusion for 1 hour. Animals were sacrificed after a reperfusion period of 24 hours and brains were snap-frozen. Cryostat sectioning of the mice brains, Hematoxylin staining of the sections and determination of cerebral lesion volumes by computer-assisted volumetry on serial coronal sections were subsequently carried out.

TSA pre-treatment conferred significant reduction in cerebral infarct volumes compared to vehicle treated group (figure 15A). Results were also similar when lesion volumes were

corrected for brain oedema with a different calculation ($58 \pm 4 \text{ mm}^3$ vs. $76 \pm 5 \text{ mm}^3$ in TSA vs. vehicle treated mice, $n=10$ per group, $P < 0.05$, Student's t-test). Cerebral lesion areas were smaller in all five anterior to posterior coronal brain sections (figure 15B). We also tested a lower TSA dose however treatment of mice with TSA at a dose of 1 mg/kg body weight for fourteen days did not afford protection in our model of ischemic stroke.

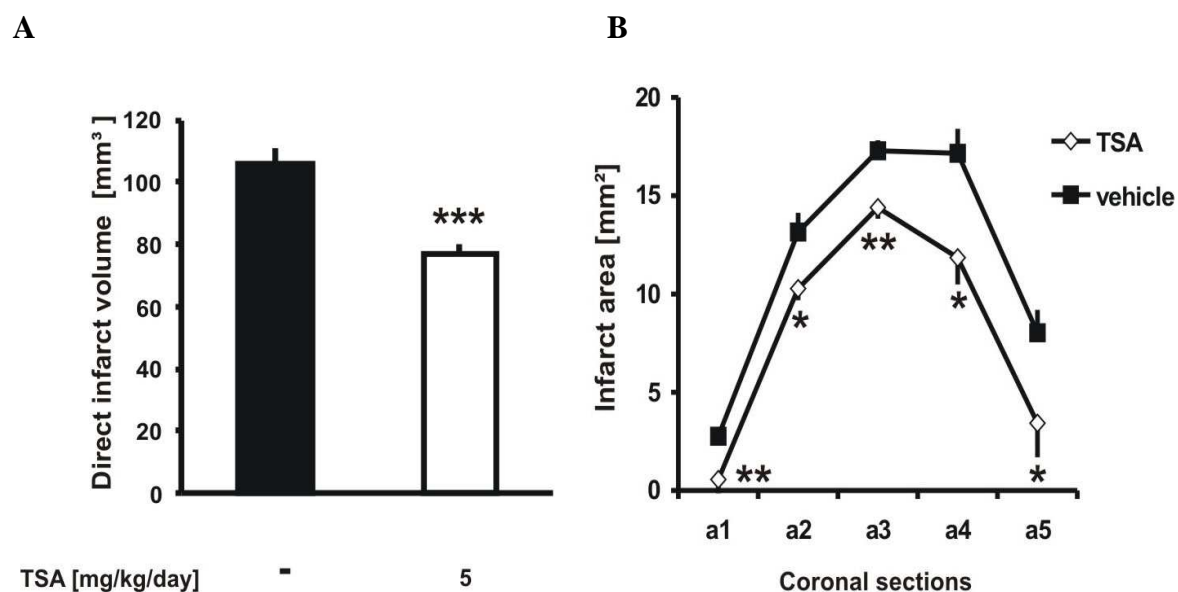


Figure 15 Trichostatin A pre-treatment protects mice from middle cerebral artery occlusion and reperfusion. The effect of trichostatin A (TSA) pre-treatment on cerebral infarct volume (A) and area (B) following 1 hour filamentous MCA occlusion and 24 hours of reperfusion compared with vehicle-injected 129/Sv mice. Cerebral infarction volume was determined quantitatively on $20 \mu\text{m}$ thick, hematoxylin stained brain cryostat section as described (Endres et al., 1999); $n=10$ animals per group; Student's t-test; $*P < 0.05$, $**P < 0.01$; and $***P < 0.005$.

Table 1 Physiological parameters in 129/Sv mice

Parameter	Vehicle	TSA
MABP [mmHg]	94.3 ± 2.8	94.6 ± 3.1
PH	7.31 ± 0.01	7.36 ± 0.02
$P_a\text{CO}_2$ [mmHg]	42.7 ± 1.0	43.1 ± 1.2
$P_a\text{O}_2$ [mmHg]	120.7 ± 1.8	117.6 ± 3.7

Mean arterial blood pressure was measured via a femoral artery catheter. Fifty microliters of blood were withdrawn for blood gas determination. Animals were weighted and rectal (core) temperature was measured. $N = 5$ animals per group. There were no statistically significant differences between groups.

Neuroprotective effects of TSA were not due to changes in physiological parameters, which might influence the course of brain ischemia/reperfusion. Table 1 shows that blood pressure, blood gases (PaO₂, PaCO₂, pH) and temperature did not differ between TSA vs. vehicle treated mice.

Bederson neurological sensorimotor deficit scores were taken 24 hours after the ischemic stroke, before the sacrifice of mice. As Table 2 demonstrates TSA treated animals displayed better scores compared to vehicle treated group, however this effect was not significant (P=0.12), which might well be due to the low number of animals used in the study (n=10). There was no difference in Bederson scores between mice treated with vehicle or 1mg/kg TSA, a treatment protocol which was also not protective.

Table 2 Neurological Sensorimotor Deficit Score

Group	N	SCORE						
		0	1	2	3	median	25%	75%
Vehicle	10	0	2	7	1	2.0	2.0	2.0
TSA	10	1	4	5	0	1.5	1.0	2.0

Wildtype 129/Sv mice were pre-treated with trichostatin A (TSA) or vehicle (5 mg/kg body weight given daily by intraperitoneal injection for 14 days; see Methods). Neurological scoring was performed by the use of a previously published method performed at 24 hours after 1-hour MCA occlusion/reperfusion (Bederson et al., 1986). The numeral scores are as follows: 0, normal motor function; 1, flexion of contralateral torso on lifting the whole animal by the tail; 2, circling to the contralateral side; 3, loss of walking or righting reflex.

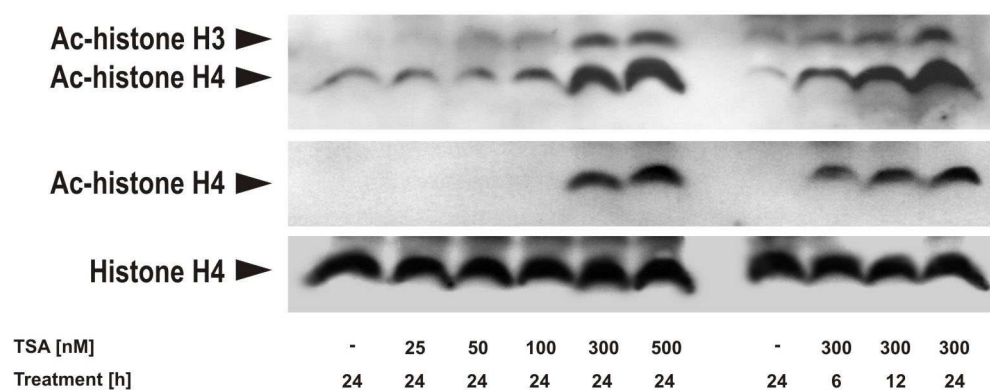
4.3.3 Trichostatin A treatment increases histone acetylation levels in primary cortical cultures and in mice brain

Next, whether the neuroprotective TSA treatment regimes enhance histone acetylation patterns was examined in neuronal cultures. For this aim, primary cortical cultures were treated with increasing concentrations of TSA for 24 hours and with 300nM TSA for different durations. Nuclear extracts were subsequently subjected to SDS-PAGE and antibodies against histone H4, acetyl-histone H4 and acetyl-Lysin, recognising both acetyl-histone H4 and H3, were used for western immunoblotting. Figure 16A demonstrates that 300 and 500nM TSA

increased histone H4 as well as H3 acetylation, whilst lower doses or shorter treatment protocols, which also did not afford neuroprotection against OGD, did not enhance acetylation of histones. Anti-histone H4 antibody was employed for the demonstration of equal loading.

To investigate whether the neuroprotective TSA treatment regimes also enhance histone acetylation patterns in mice brain, we treated 129/Sv mice with TSA at doses of 1 and 5 mg/kg body weight for fourteen days by daily intraperitoneal injections. After the last injections, total brain nuclear extracts were subjected to SDS-PAGE and acetylation of histone H4 was determined by western immunoblotting. Figure 16B shows the increase of histone H4 acetylation by 5 mg/kg TSA. TSA at 1mg/kg dose nor conferred neuroprotection against middle cerebral artery occlusion, neither did it increase histone H4 acetylation. Actin antibody was employed for the demonstration of equal loading. In addition, immunohistochemical stainings were performed on coronal brain sections of vehicle- or TSA (5 mg/kg)-treated mice using anti-acetyl histone H4 antibody. Representative photomicrographs shows enhanced stainings with acetyl-histone H4 antibody within the striatum/corpus callosum/cortex and hippocampus regions, and confirms the western immunoblotting results (Figure 16C). Noteworthy, a neuronal expression pattern for acetylated histone H4 was observed in our stainings.

A



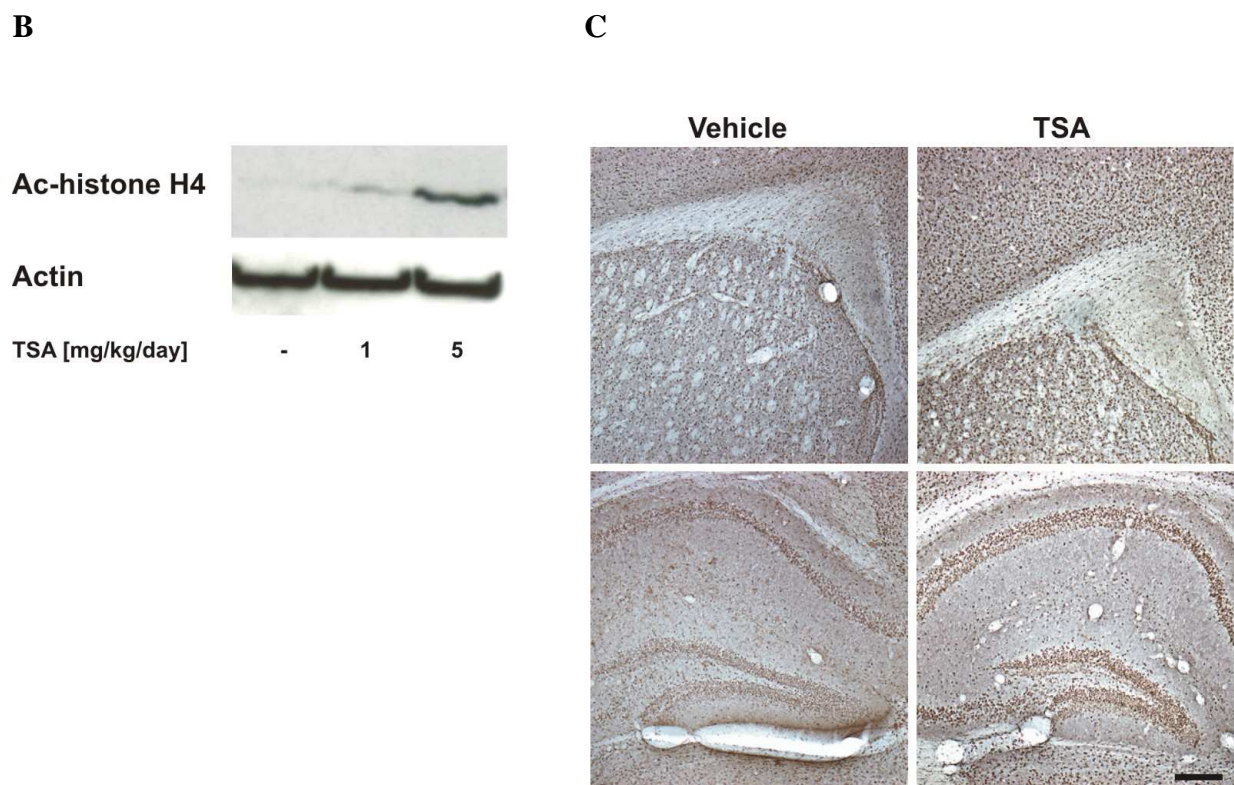


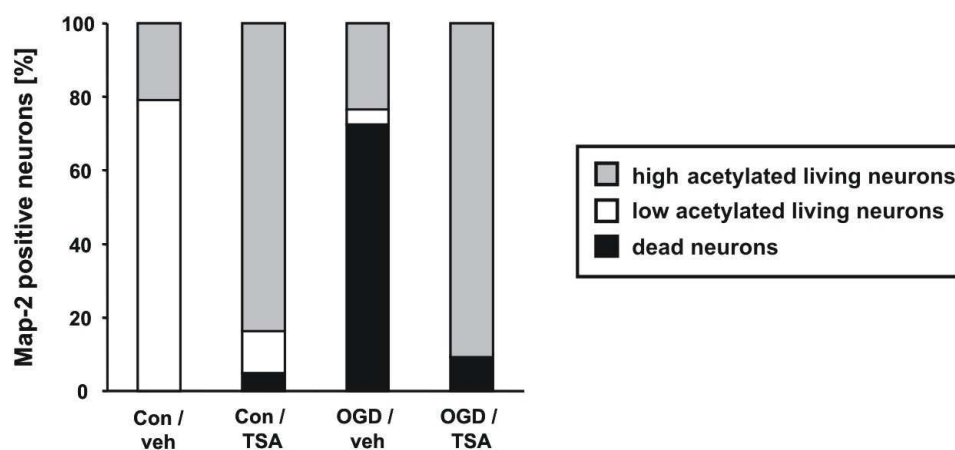
Figure 16 Trichostatin A enhances histone acetylation in primary cortical cultures and in mice brain. (A) Primary cortical neurons were treated with different concentrations of TSA for the indicated durations and subsequently nuclear protein extraction was carried out for western blotting. Twenty μg of protein was subjected to sodium dodecyl sulphate-polyacrylamide gel electrophoresis (SDS-PAGE) and incubated with polyclonal antibodies against acetyl-lysine (top panel; recognizing Ac-histone H3 and H4), Ac-histone H4 and histone H4 after stripping and reprobing the same membrane. (B, C) Immunoblots and immunocytochemical stainings showing the effect of TSA treatment on histone acetylation patterns in brains of 129/Sv mice treated with TSA at 1 and 5 mg/kg body weight daily given intraperitoneally for 14 days. (B) Brain tissue lysates were subjected to SDS-PAGE and acetylation of histone H4 was analyzed by immunoblotting. Actin was used as internal loading control. (C) Paraformaldehyde-fixed 40 μm -thick coronal brain sections of vehicle- or TSA (5 mg/kg)-treated mice were subjected to anti- Ac-histone H4 immunostaining. Photomicrographs show expression in the striatum/cortex and hippocampus regions, respectively. Scale bar, 200 μm . Representative results of three independent experiments with similar results are shown.

4.3.4 Enhancement of histone acetylation by Trichostatin A renders neurons more resistant to ischemic injury

The following experiment was performed to investigate whether enhancement of histone H4 acetylation by TSA is causally linked to its neuroprotective effects. Rat primary cortical

neurons were pre-treated with 300nM TSA for 24 hours and then subjected to 120min OGD. Immunocytochemical staining was performed after 24 hours, with antibodies for the neuronal marker microtubule associated protein MAP2 (green), acetylated (Ac) histone H4 (red) and nuclear Hoechst 33258 dye (blue). As presented in the photomicrographs of Figure 17B different levels of histone H4 acetylation was observed in individual neurons. Neurons were counted and classified in groups according to the acetylation levels of histone H4 in their nuclei, low- vs. high-acetylated, and the result was presented as the figure 17A. Naive neuronal cultures displayed less than 20% high-acetylated neurons, upon TSA treatment this number was dramatically increased to more than 80%. MAP2 is a neuronal marker which has been previously reported to be very sensitive to ischemic insult (Harms et al. 2001). Following OGD the number of MAP2-positive, healthy, neurons was three-fold higher in TSA pre-treated cultures, demonstrating once again TSA's neuroprotective properties. Nevertheless, the most important finding of this experiment was that neurons surviving the ischemic insult both in vehicle- and TSA pre-treated cultures had high histone H4 acetylation levels in their nuclei. Noteworthy, dead neurons which show morphology characteristic to apoptosis also presented an intense signal after acetylated histone H4 staining. Taken all together, these data however suggest that high-acetylated neurons are more likely to survive an ischemic insult.

A



B

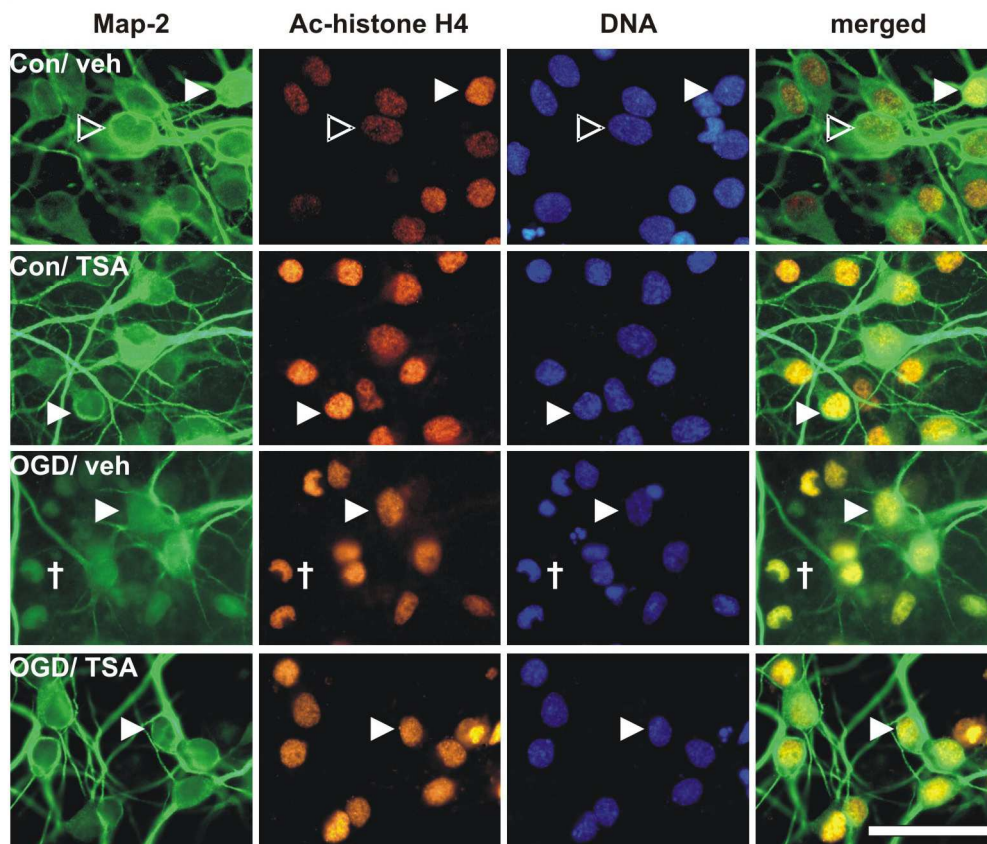


Figure 17 Trichostatin A enhances histone acetylation levels in cortical neurons. (A, B) Primary cortical neurons were pre-treated with 300 nM TSA for 24 hours and then subjected to 150 min of oxygen-glucose deprivation (OGD). At 24 hours, immunocytochemical staining was performed with antibodies raised against the neuronal marker microtubule-associated protein Map-2 (green), acetylated (Ac)-histone H4 (red) and Hoechst 33258 (blue). The fractions of dead Map-2-positive neurons (dagger), low-acetylated living Map-2-positive neurons (open arrow) and high-acetylated living Map-2-positive neurons (filled arrow) were determined. Two hundred Map-2-positive neurons per group were evaluated and divided into three different groups (high-acetylated living neurons, low-acetylated living neurons and dead neurons) using a fluorescence microscope and a digital camera without changing the lightexposure time during the process. The acetylation status was evaluated in Map-2-positive viable neurons with dendrites and intact nuclear morphology (visualized by Hoechst DNA counterstaining), whereas dead neurons and those exhibiting nuclear shrinkage, blebbing or chromatin condensation were not considered. Counts were performed in two independent experiments with at least three different cover slips per group. Scale bar, 30 μ m.

4.3.5 Trichostatin A up-regulates gelsolin expression in cortical neurons and in mice brain

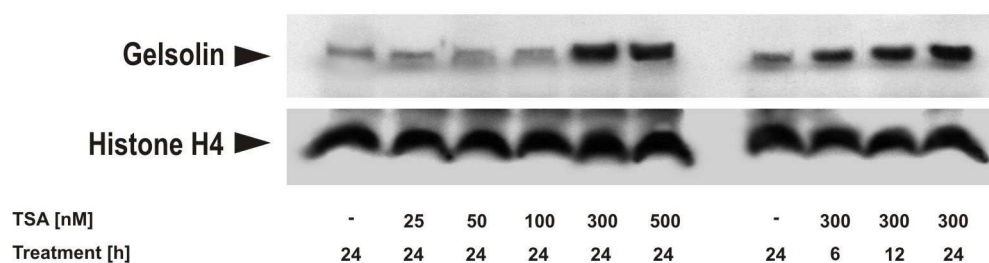
Our group has previously reported anti-apoptotic and anti-excitotoxic properties for gelsolin protein (Harms et al. 2004). Previously, my MSc thesis presented that TSA enhanced histone H4 acetylation levels at gelsolin gene promoter region in primary cortical cultures and that the subsequent result of this event was increase in gelsolin mRNA levels (Meisel et al. 2006). Here, to test whether TSA's effect on gelsolin transcription is also translated into its protein levels, rat primary cortical cultures were treated with different concentrations of TSA for 24 hours and with 300nM TSA for different durations. Cellular protein extracts were subjected to SDS-PAGE, followed by western immunoblotting using antibodies against murine gelsolin and histone H4. TSA up-regulated gelsolin protein levels in a time and concentration dependent manner (Figure 18A). Importantly, these increases were in agreement with the enhancement of histone H4 as well as histone H3 acetylation by TSA treatment (Figure 16). A significant up-regulation of gelsolin was observed with TSA only at the doses of 300nM and 500nM and with the treatment durations for 12 and 24 hours. TSA treatment with lower doses, 25nM-100nM, as well as for shorter time duration, 6 hours, did not result in any prominent up-regulation of gelsolin protein, neither did they afford neuroprotection against OGD. Anti-histone H4 antibody was utilized for the demonstration of equal protein loading.

To address the question of whether up-regulation of gelsolin protein and enhancement of histone acetylation levels occur within the same individual neurons, immunocytochemistry was performed on cortical cultures treated with 300nM TSA for 24 hours and antibodies against gelsolin (green), acetylated (Ac) histone H4 (red) and Hoechst 33258 dye (blue) were used. Immunocytochemistry followed by high resolution confocal laser scanning microscopy demonstrated that individual neurons with high histone H4 acetylation pattern in their nuclei also expressed increased gelsolin levels in their cell body (Figure 18B).

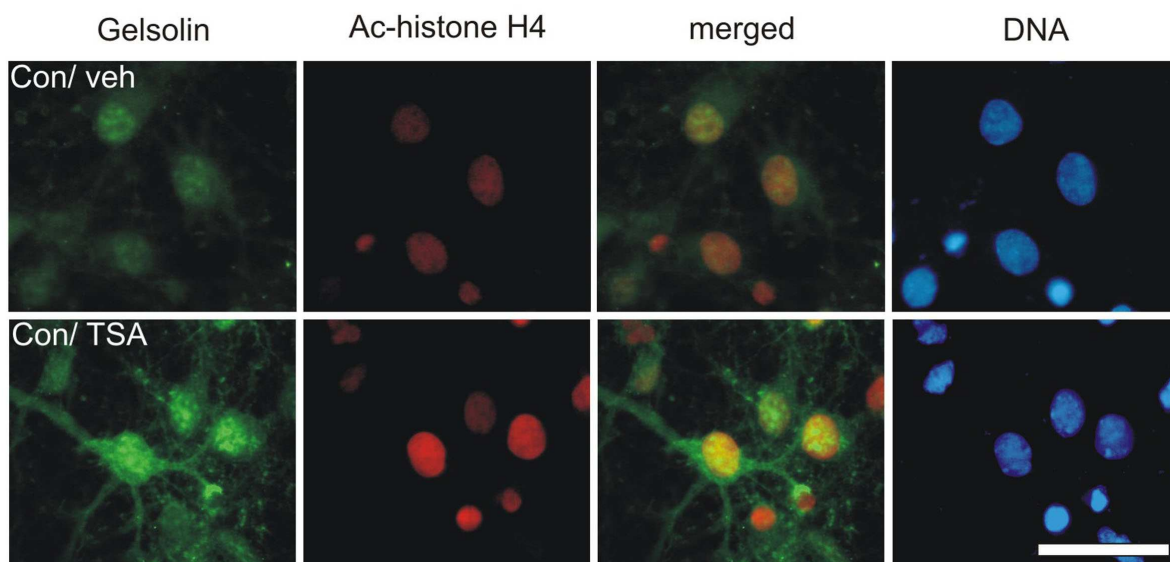
To examine whether TSA exerts a similar effect on gelsolin expression also in mice brain, 129/Sv mice were treated with TSA at the doses of 1 and 5mg/kg body weight for fourteen days, by daily intraperitoneal injections. Thereafter, whole brain cellular extracts were used for western immunoblotting. Figure 18C shows dose dependent up-regulation of gelsolin protein in mice brain upon TSA treatment. Importantly 1mg/kg TSA, a dose which neither

afforded neuroprotection nor enhanced histone H4 acetylation in vivo, did not up-regulate gelsolin protein in mice brain. Anti-actin antibody was utilized for the demonstration of equal protein loading. Immunohistochemistry was carried out on brain slices of mice confirmed the up-regulation of gelsolin after the neuroprotective TSA treatment and suggested a neuron specific expression pattern (Figure 18D). Double-labeling fluorescent immunohistochemistry indeed demonstrated the up-regulation of gelsolin in neuronal marker (NeuN+) positive neurons (Figure 18E). The photomicrographs were taken from a neuron-rich brain region, hippocampus, to better present up-regulation of gelsolin protein by TSA.

A



B



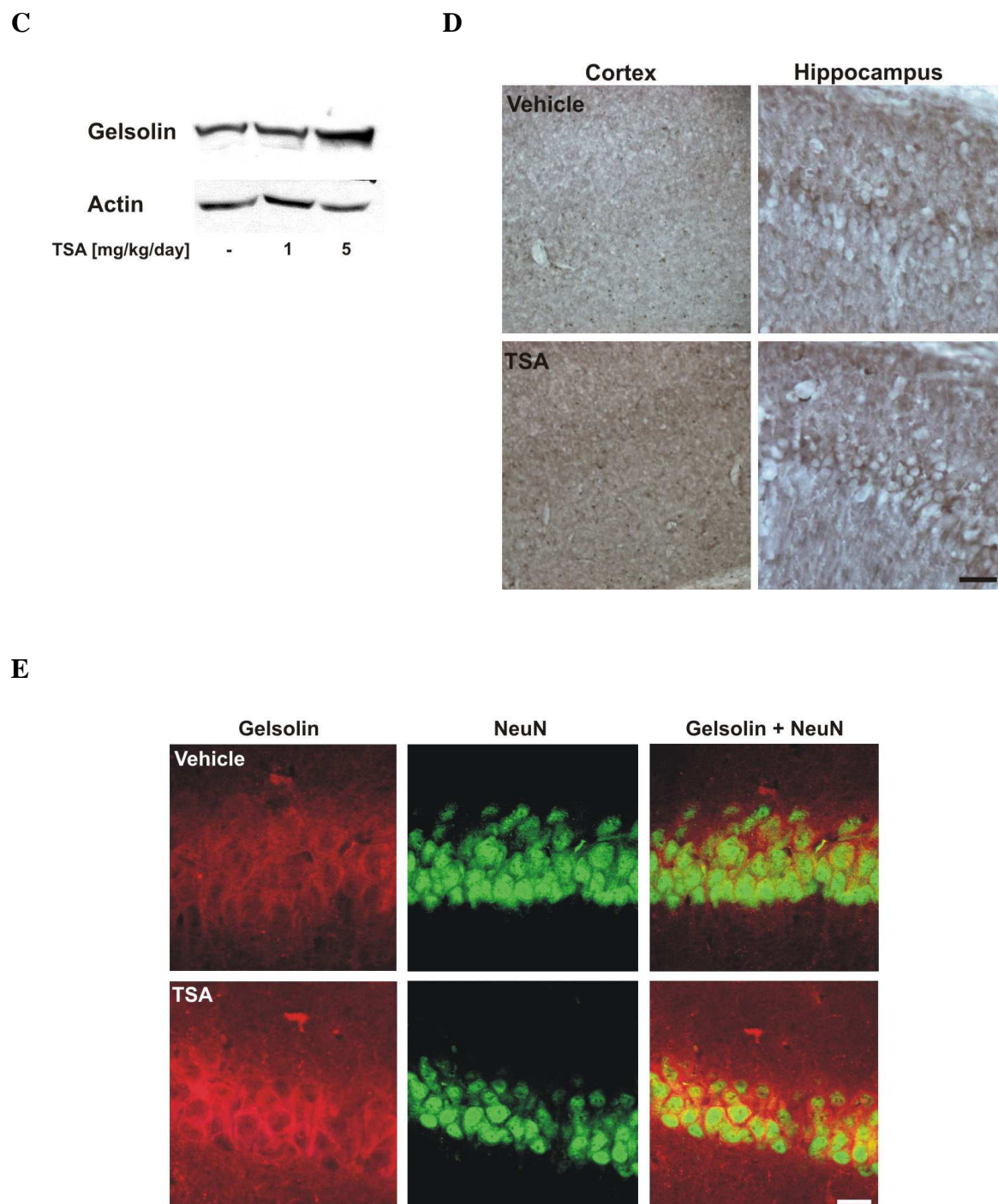


Figure 18 Trichostatin A up-regulates gelsolin expression in cortical cultures and in mice brain. Primary cortical neurons were treated with different concentrations of TSA for the indicated durations and were subjected to western immunoblotting. (A) Twenty μ g of protein was subjected to sodium dodecyl sulphate-polyacrylamide gel electrophoresis (SDS-PAGE) and incubated with polyclonal antibodies against murine gelsolin and histone H4 after stripping and reprobing the same membrane. (B) Primary cortical neurons were seeded on glass cover slips and treated with 300 nM TSA on the ninth day in vitro (DIV9). Cells were fixed after 24 hours and immunocytochemistry was performed. Gelsolin (green), ac-histone H4 (red) and Hoechst staining (blue) were shown in the same cells after treatment with vehicle or TSA. Scale bar, 30 μ m. (C) Immunoblots and (D)

immunohistochemical stainings of sections from frontoparietal cortex and hippocampus showing the effect of TSA treatment on gelsolin expression in brains of 129/Sv mice treated with TSA at 1 and 5 mg/kg body weight daily given intraperitoneally for 14 days. (E) Up-regulation of gelsolin (red) by TSA in neurons of hippocampal CA1 region. Neuronal marker NeuN (green). Scale bars, (D) 100 μm (cortex) and 25 μm (hippocampus), (E) 20 μm . Representative results of three independent experiments with similar results are shown.

4.3.6 Trichostatin A confers actin filament remodelling

Gelsolin was previously reported to sever actin microfilaments, conferring remodelling of actin cytoskeleton (Kwiatkowski et al. 1988, Harms et al. 2004). We therefore examined whether filamentous actin dynamics are altered upon TSA-induced gelsolin up-regulation. Rat cortical cultures were treated with 300nM TSA for different durations, followed by phalloidin-fluorescein staining. The photomicrographs indeed revealed that filamentous actin levels were reduced in parallel to enhancement of histone H4 acetylation after TSA treatment (Figure 19A). Importantly, these two events occurred within the same individual neurons as the merged photomicrographs clearly demonstrate. Methanol extraction of bound phalloidin and subsequent photometric quantification, using a fluorescence plate reader, revealed significant decrease in filamentous actin levels by 300nM TSA treatment (Figure 19B). Noteworthy is that the decrease in filamentous actin levels reached statistical significance only after TSA treatments for 12 hours or longer.

We further tested whether TSA's effect on actin cytoskeleton still persists in neurons after their exposure to oxygen glucose deprivation (OGD). For this purpose, rat primary cortical cultures were pre-treated with 300nM TSA for 12 hours, subjected to OGD and subsequently cells were fixed at different time intervals. Phalloidin-fluorescein staining of actin cytoskeleton was followed by methanol extraction of F-actin bound phalloidin. Data obtained from photometric quantification is presented as figure 19C. OGD decreased actin microfilament levels to approximately 80% of baseline, yet TSA-induced differences in filamentous actin levels were sustained at all time points following OGD.

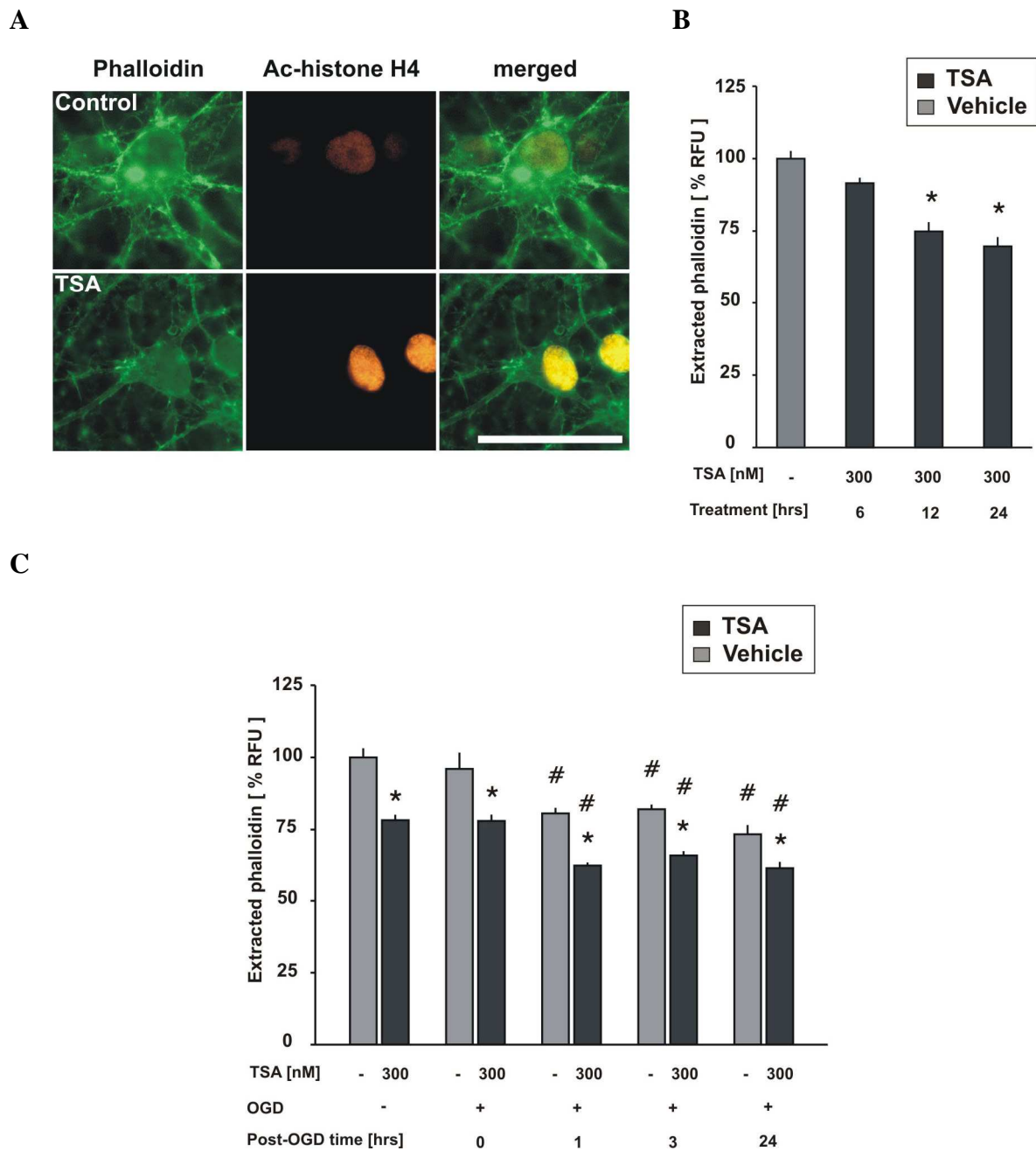


Figure 19 Effects of Trichostatin A on filamentous actin. Primary cortical neurons were seeded on glass cover slips and pre-treated with 300 nM TSA or vehicle (control) for 12 hours (A, C) or 6, 12 and 24 hours (B). (A) Following end of the treatment, neurons were fixed with 4% paraformaldehyde, stained with phalloidin–fluorescein (green) and immunostained against acetylated (Ac)-histone H4 (red). Scale bar, 30 μ m. (B) Phalloidin–fluorescein was extracted and fluorescence was quantified. * $P < 0.001$ vs. vehicle treatment. (C) In a different subset of experiments, at 12 hours following TSA or vehicle (control) treatment, cultured neurons were subjected to oxygen-glucose deprivation (OGD) or normoxia as control treatment, and subsequently fixed with 4% paraformaldehyde at the indicated time points, and stained with phalloidin–fluorescein. Phalloidin–fluorescein was then extracted by methanol and fluorescence signal was quantified. * $P < 0.0001$ vs. vehicle treatment, # $P < 0.0001$ vs. OGD control. RFU; Relative fluorescence units

4.3.7 Trichostatin A reduces intracellular calcium overload caused by ischemic injury

Intracellular calcium overload is considered to be a central player in ischemic neuronal cell death (Choi, 1995). Our group has previously reported that gelsolin exerts anti-excitotoxic effects following cerebral ischemia via remodelling actin cytoskeleton and also stabilising calcium channels (Endres et al. 1999). Here, whether TSA has effect on intracellular calcium overload triggered by oxygen-glucose deprivation was investigated. Rat primary cortical cultures were pre-treated with 300nM TSA for 12 hours and subjected to OGD on in vitro day 9 (DIV9). It is well known that major calcium influx take place both during the ischemic event and also directly after reperfusion/re-oxygenation. Thus the cultures were loaded with calcium binding fluorescent dye Fluo-4 AM either during OGD or immediately after OGD

and subsequently measured the fluorescent signal after a dye incubation period of 45min. In either paradigm significantly lower intracellular calcium levels were observed when the cultures received TSA treatment prior to OGD (figure 20A and 20B). Moreover, the differences in fluorescence signal intensities between TSA and vehicle pre-treated cultures persisted throughout subsequent repetitive measurements at 10min intervals for one hour after the first measurement (data not shown).

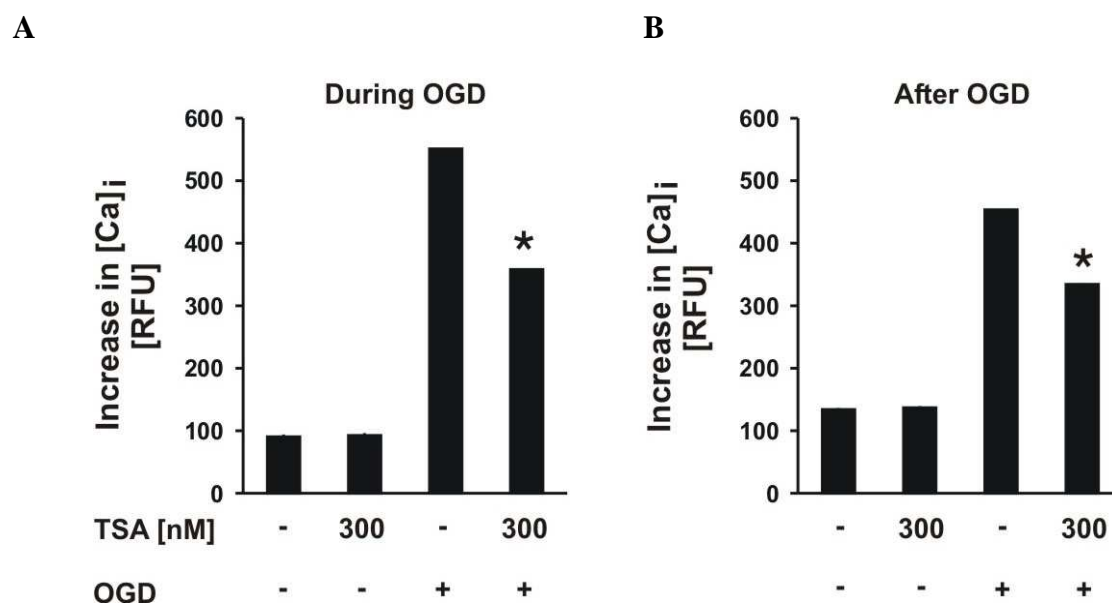
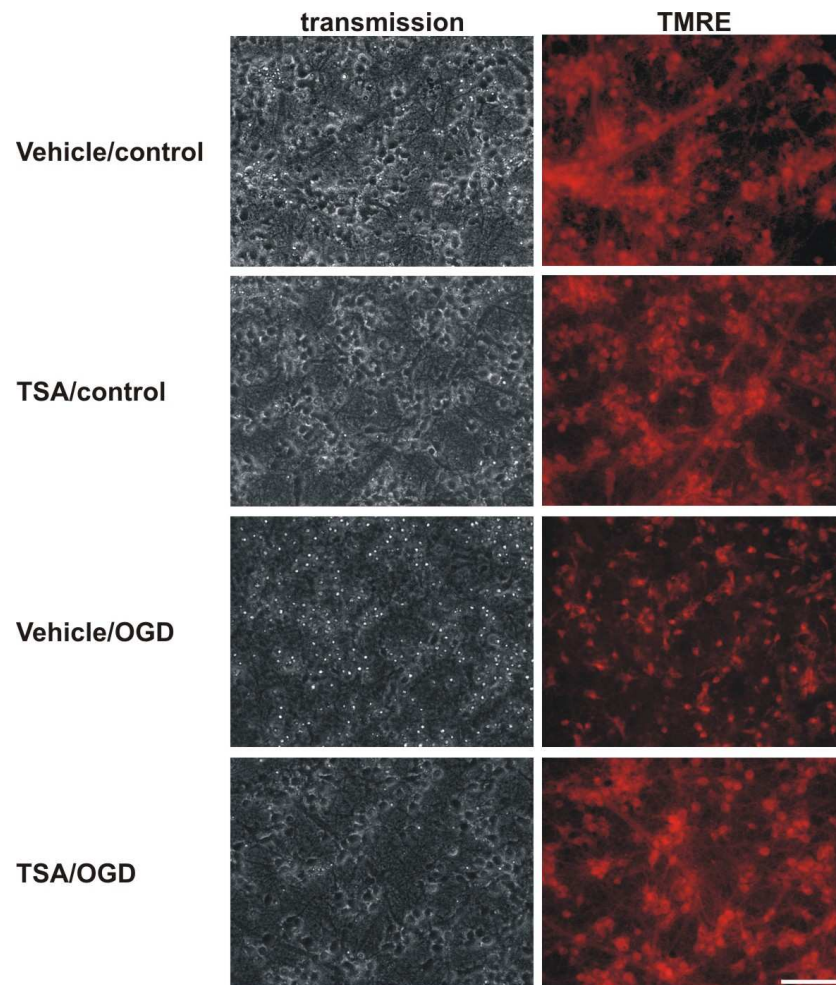


Figure 20 Trichostatin A decreases calcium influx following combined oxygen-glucose deprivation. Primary cortical neurons were pre-treated with 300 nM TSA for 24 hours and subjected to 150 min OGD. Calcium indicator fluorescent dye Fluo-4 AM was loaded either during (A) or immediately after (B) OGD. Fluorescent signal intensities were measured following an incubation period of 45 min. Values (mean±SEM) in relative fluorescence units (RFU) are 90.4±3.7, 92.4±3.9, 550.9±1.3, and 358.1±1.6 in (A), and 133.9±2.3, 136.8±2.5, 453.6±1.2, and 334.2±1.1 in (B) * $P < 0.001$ for TSA vs. vehicle.

4.3.8 Trichostatin A prevents loss of mitochondrial membrane potential caused by ischemic injury

After assessment of intracellular calcium levels, we measured loss of mitochondrial membrane potential by tetramethyl rhodamine ethyl ester (TMRE) fluorescence, which is an event implicated in cell death cascades mediated by the mitochondria. For this purpose, rat primary cortical cultures were pre-treated with 300nM TSA for 12 hours and subjected the cultures to oxygen-glucose deprivation on in vitro day 9 (DIV9). Twenty-four hours afterwards TMRE was added into culture medium and photomicrographs were taken following an incubation period of 40min. Figure 21A demonstrates the loss of mitochondrial membrane potential, by means of loss of fluorescence signal intensity, however this loss was clearly prevented in cultures which were treated with TSA prior to OGD. Subsequent measurements of fluorescent signals are presented as figure 21B. Four different OGD durations carried out on sister cultures yielded the result that only longer durations of OGD caused statistically significant loss of mitochondrial membrane potential, although the loss was detectable after all four OGD durations. Importantly, OGD-caused mitochondrial dysfunction was prevented when cultures were pre-treated with TSA. TSA's effect was evident in all durations of OGD, milder as well as more severe forms of the ischemic insult. Neuroprotection by TSA was also confirmed in experiments by measurement of lactate dehydrogenase (LDH) release into the medium (data not shown).

A



B

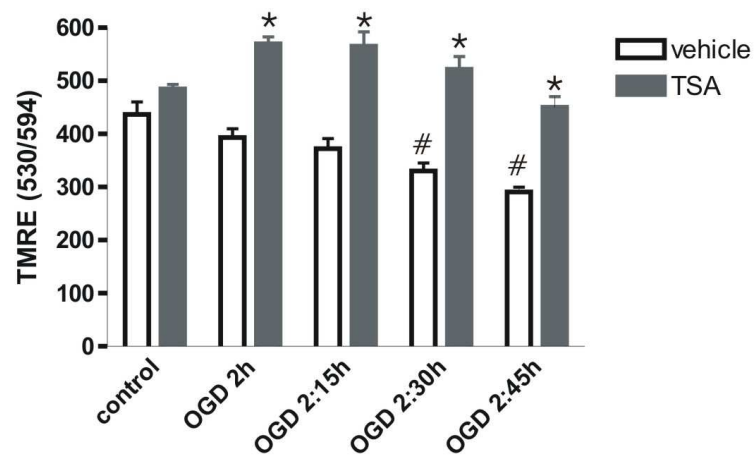


Figure 21 Trichostatin A decreases loss of mitochondrial membrane potential following combined oxygen/glucose deprivation. Primary cortical neurons were pre-treated with 300 nM TSA for 12 hours and

subjected to various durations of OGD. (A) Loss of mitochondrial membrane potential was measured 24 hours after OGD. TMRE was added into the culture wells and photomicrographs were taken after an incubation period of 40 min. (B) Subsequently fluorescent signal was measured in a multiwell fluorescence plate reader. There were no significant differences between TSA vs. vehicle pre-treated cultures in the control conditions. $n=8$. $*P<0.001$ for TSA vs. vehicle in each OGD condition. $\#P<0.05$ for corresponding vehicles in control vs. OGD 2:30 hours and control vs. OGD 2:45 hours. Scale bar, 100 μ m.

4.3.9 Trichostatin A pre-treatment does not protect gelsolin-deficient mice against brain ischemic injury

My MSc thesis has previously presented TSA's failure in protecting gelsolin-deficient murine neuronal cultures against ischemic insult, underscoring gelsolin as an integral perpetrator of TSA's neuroprotective effects (Meisel et al., 2006). Here, we tested whether gelsolin has a similar role in neuroprotection by TSA in vivo. For this purpose, gelsolin-deficient and wild-type mice were pre-treated with the neuroprotective TSA pre-treatment regime, 5mg/kg body weight of TSA for fourteen days by daily intraperitoneal injections. Subsequently mice underwent operation of filamentous middle cerebral artery occlusion for 1 hour. After a reperfusion period of 24 hours, animals were sacrificed and brains were snap-frozen. Cryostat sectioning of the brains and hematoxylin staining of the sections were followed by determination of cerebral lesion volumes by computer-assisted volumetry on serial coronal brain sections.

TSA pre-treatment did not afford neuroprotection of gelsolin-deficient mice against MCAo for 1 hour. TSA as well as vehicle pre-treated mice had similar cerebral lesion volumes and anterior to posterior lesion areas (Figure 22A and B). An indirect method for measuring lesion volume, corrected for brain oedema, did not change the lack of protection by TSA in gelsolin-deficient mice (60 \pm 14 vs 58 \pm 8 mm³ in TSA vs. vehicle pre-treated mice, $n=10$ per group).

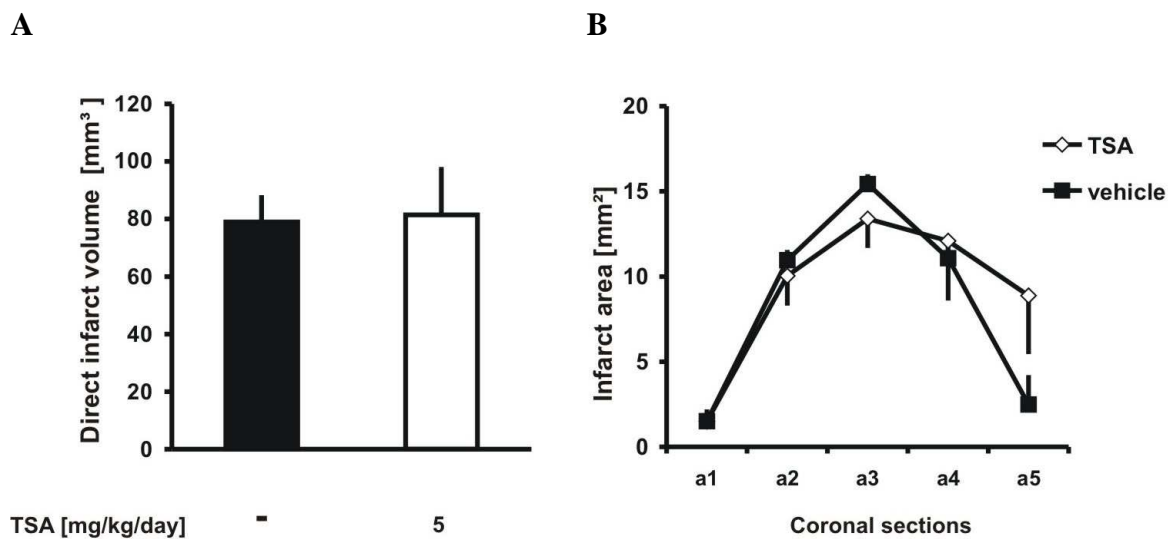


Figure 22 Trichostatin A does not protect gelsolin knockout mice against MCAo/reperfusion. The effect of Trichostatin A (TSA) pre-treatment (5 mg/kg body weight daily for 14 days given intraperitoneally) on cerebral infarct volume (A) and area (B) following 1 hour filamentous MCA occlusion and 24 hours of reperfusion compared with vehicle-injected gelsolin knockout mice. Cerebral infarction volume was determined quantitatively on 20 μ m-thick, hematoxylin stained brain cryostat sections, as described previously (Endres et al., 1999). n=10 animals per groups.

4.3.10 TSA confers actin remodelling in wild-type but not in gelsolin-deficient mice brain

Gelsolin severs actin microfilaments, conferring remodelling of actin cytoskeleton (Kwiatkowski et al. 1988, Harms et al. 2004). As presented above, Trichostatin A up-regulation of gelsolin protein was followed by significantly reduced levels of filamentous actin in rat primary cortical neurons (figure 19). Here, we examined whether TSA's modulatory effect on actin cytoskeleton is present also in brains of wild-type vs. gelsolin-deficient mice.

Wild-type and gelsolin-deficient mice were treated with 5mg/kg body weight of TSA, or vehicle, for fourteen days by daily intraperitoneal injections. After last injections, animals were sacrificed and brains were snap-frozen. Phalloidin-fluorescein as well as nuclear Hoechst 33258 staining was carried out on coronal brain sections. Representative photomicrographs which were chosen from a neuron-rich brain region, hippocampal CA1

area, are presented as figure 23. In wild-type mice TSA reduced filamentous actin levels, by means of reduction in fluorescent signal intensity, confirming our *in vitro* results. As expected, vehicle treated gelsolin-deficient mice appeared to have higher levels of filamentous actin in comparison to vehicle treated wild-type mice. Unlike in wild-type mice, however, TSA treatment did not reduce filamentous actin levels in gelsolin-deficient mice.

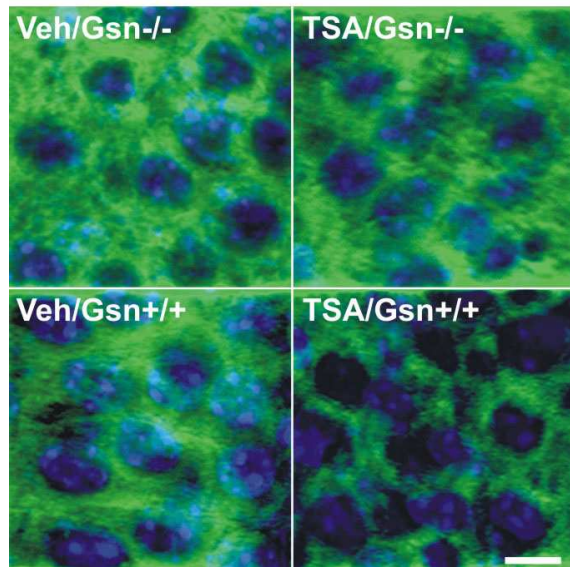


Figure 23 Effects of Trichostatin A on filamentous actin levels in mice brain tissue.

Phalloidin stainings (green) on 20 μm -thick coronal brain sections from wild-type and gelsolin-deficient mice treated with TSA 5mg/kg body weight for 14 days. The images show neurons from hippocampal CA1 region, counterstained with Hoechst 33258 nuclear dye (blue). Scale bar, 10 μm .

5 DISCUSSION

5.1 HISTONE ACETYLATION AND NEURONAL ISCHEMIC INJURY

In recent years, numerous publications demonstrated dramatic impairment in histone acetylation balance during neurodegenerative conditions and neurodegeneration-coupled histone acetyltransferase (HAT) loss, in particular loss of CREB-binding protein (CBP), was proposed to be the main molecular event underpinning the forfeiture of neuronal acetylation homeostasis. Yet, involvement of histone acetylation as well as histone acetylation machinery in the pathophysiological cascades triggered by brain ischemic damage was not clearly studied. Here, the present work not only demonstrates rapid decrease in histone acetylation and CBP protein levels in neurons after ischemic insult, but it also evidences causal involvement of these events in the deterioration processes following neuronal ischemic injury.

5.1.1 Histone acetylation and CREB-binding protein (CBP) levels rapidly decrease in neurons following ischemic injury

A central role has been attributed to CBP loss of function during manifestation of neurodegenerative conditions such as polyglutamine (polyQ) diseases (Hughes et al., 2002; Taylor et al., 2003; Jiang et al., 2006), spinocerebellar ataxia type 7 (SCA7) (Takahashi et al., 2002), spinal and bulbar muscular atrophy (SBMA) (McCampbell et al., 2000) and Huntington's disease (HD) (Steffan et al., 2000). In an apoptotic model of primary neurons, Boutillier and colleagues described CBP as a substrate of apoptotic caspases, alternatively to its classical proteasomal degradation (Rouaux et al., 2003). In this neuronal death context, histone acetylation levels were also decreased. Here, we demonstrate histone hypo-acetylation and CBP's rapid depletion in the context of neuronal ischemic injury. Acetylation levels of core histones, histone H4 and histone H3, as well as CBP protein levels rapidly decreased in neuronal cultures after their exposure to damaging combined oxygen-glucose deprivation, and this decrease sustained throughout later time points after the ischemic insult. Histone H4 and histone H3 being the preferred substrates of CBP's HAT function, yet to this date we still do not know whether decrease in histone H4 and histone H3 acetylation levels after neuronal ischemia is the consequence of loss of CBP HAT activity or whether other HATs and/or

HDACs are also involved. Our data is also consistent with reports showing reduction in histone acetylation levels after cerebral ischemic injury in mice (Ren et al., 2004; Faraco et al., 2006). Yet, any involvement of HAT or HDAC enzymes was not indicated in these investigations. In full agreement with a previous report (Jin et al., 2001), our immunocytochemical staining revealed that CBP protein was particularly absent in neurons with characteristic apoptotic nuclei indicative of irreversibly damaged neurons following ischemic injury (see arrows in figure 7B).

5.1.2 Loss of CREB-binding protein (CBP) is causally associated to extent of damage caused by neuronal ischemia

Heterozygous mutations of CBP gene leads to Rubinstein-Taybi Syndrome (RTS) in humans. While homozygous mutations of either CBP or p300 results in mouse lethality at embryonal stages, mice carrying a heterozygous mutation of CBP on one allele showed deficits in LTP and memory consolidation (Korzus et al., 2004; Alarcon et al., 2004). CBP's exogenous expression reversed neurotoxicity in several neurodegenerative disease models, where its endogenous levels were depleted, indicating a causative link rather than an end-effect in the pathological scenario (Taylor et al., 2003; Jiang et al., 2006). Here, we present data suggesting importance of CBP's intact function for neuronal survival following ischemic injury. Curcumin, a specific inhibitor of CBP and p300 HAT activities (Balasubramanyam et al., 2004) exacerbated neuronal damage caused combined oxygen-glucose deprivation. Significantly, curcumin at 4 μ M and 16 μ M doses, the doses which prominently reduced acetylation levels of histone H4 and histone H3, further enhanced neuronal ischemic damage. Unlike HDAC inhibitors, currently available HAT inhibitors are poor in specificity and curcumin might exert pleiotropic effects apart from its CBP and p300 HAT inhibitory function. Therefore, we utilized CBP-deficient (heterozygous) mice to confirm that CBP's protein availability and/or functionality is indeed important for neuronal survival following ischemic injury. Here, we present that primary cortical cultures from CBP-deficient mice show drastic enhancement of susceptibility to injury by oxygen-glucose deprivation, compared to wild-type cultures. Our ischemia model, particularly more severe oxygen-glucose deprivations for 95 minutes and 115 minutes, caused damage to cortical cultures. Yet, the damage was much higher when the cultures were heterozygous for CBP, underscoring

once again a causal link, rather than a simple correlation, between reduced CBP protein availability and increased neuronal injury after ischemia. We also show that acetylation levels of histone H4 and histone H3 are clearly reduced in CBP-deficient neurons, compared to wild-type littermate cultures. Importantly under normal conditions (in OGD control cultures), cultures of both genotype presented similar LDH levels in media, indicating comparable cellular health in culture. In fact, CBP's restricted functionality and subsequent histone hypoacetylation was shown to occur in parallel with the pathological deterioration processes in a Huntington Disease model, where its exogenous expression restored histone acetylation levels and reversed neurotoxicity (Jiang et al., 2006). Whether its exogenous expression could rescue CBP-deficient cultures from ischemic damage in our model is currently under investigation.

5.2 HISTONE ACETYLATION AND BRAIN ISCHEMIC PRECONDITIONING

Many different mechanisms have been so far proposed to be involved in the development of brain ischemic preconditioning, including early events involving opening of neuronal membrane channels and delayed events like expression of neuroprotective genes. Yet, once the ischemic preconditioning stimulus is perceived by the cell, little is known on the nature of events occurring at the epigenome level, eventually leading to the induction of neuroprotective gene expression. Histone acetylation is an integral switch for active gene expression processes, thus is a diagnostic feature of ongoing gene expression activities. The present work provides the first demonstration of histone acetylation involvement in brain ischemic preconditioning. Here, we show that ischemic preconditioning leads to enhancement of histone acetylation in rat primary cortical cultures as well as in mice brain and suggest that this epigenetic modification might be a tool utilized by neuronal endogenous protective programs to up-regulate neuroprotective gene expression in response to brief ischemia.

5.2.1 Brief ischemia protects mice brain against subsequent ischemic injury

A wide range of animal models have so far been developed in the field of cerebral ischemic preconditioning. Reduced atmospheric pressure in combination with reduced oxygen

concentration was used to precondition neural tissue, a model which was also established and utilised previously in our lab (Prass et al., 2003, Miller et al., 2001; Romanovskii et al., 2001). Choice of the experimental model is of obvious importance to differentiate between experimental phenomena and potential clinical relevance, and clinically seen multiple transient ischemic attacks are most likely to be analogous to the experimental tolerance to focal ischemia induced by prior exposure to transient focal ischemia. Accordingly, in our focal-focal ischemic preconditioning model, mice had an initial 5 minutes occlusion of left middle cerebral artery which was followed by 30 minutes occlusion of the same artery 24 hours later. Although most animals were scored with Grade II according to Bederson neurodeficit scoring, cerebral lesion volumes were significantly smaller in the group which had brief occlusion of MCA previously. Control (sham-operated) mice underwent the same operational procedure except for the actual 5 minutes occlusion of MCA.

5.2.2 Brief ischemia protects neuronal cultures against subsequent ischemic injury

Apart from the wide range of *in vivo* models developed for the investigation of ischemic preconditioning in brain, there have been also important reports derived from works in cell culture models. Grabb demonstrated that murine cortical cultures, containing both neurons and glia, exhibited 30–50% less neuronal death than controls following a 45–55 min period of oxygen–glucose deprivation, when the cultures were exposed to 5–30 minutes of oxygen–glucose deprivation 24 hours previously (Grabb et al., 1999). Neuroprotection was lost if the time between preconditioning stimulus and severe insult was decreased to 7 hours or increased to 72 hours. In our model, we subjected rat primary cortical cultures to brief preconditioning oxygen-glucose deprivation of 30 to 60 minutes, followed by an injurious prolonged oxygen-glucose deprivation of 2 to 3 hours, with an interval of 24 or 48 hours. Experiments with either intervals conferred significant neuroprotection. Differences in the durations of preconditioning and injurious ischemia in different studies are likely to be due to the experimental system variables such as neuronal cultures from murine *vs.* rat, age of cultures, and use of near-pure neuronal *vs.* mixed neuronal-glial cultures. According to personal experience, murine primary neuronal cultures are more susceptible to ischemic

damage in comparison to neuronal cultures of rat. Indeed, use of near-pure neuronal cultures, with less than 10% astroglial contamination on in vitro day 14 (Lautenschlager et al., 2000), underscored that neuroprotection achieved in our model was probably due to intrinsic neuronal properties. Demonstration of ischemic preconditioning in vitro in near-pure neuronal cultures is consistent with the view that ischemic preconditioning in vivo could be predominantly explained by alterations in brain parenchyma rather than alterations in blood flow or systemic response to ischemia, and this view is also further supported by reports showing that preconditioning does not alter regional cerebral blood flow associated with a subsequent lethal ischemic insult (Matsushima and Hakim, 1995; Chen et al., 1996).

5.2.3 Mechanisms of brain ischemic preconditioning

The requirement of 24 hours interval for the acquisition of ischemic preconditioning underpins the novel gene expression dependent delayed pattern of ischemic tolerance in our experimental systems. Many research papers have so far described pivotal effectors of delayed ischemic preconditioning in brain, some of which include heat-shock proteins, Bcl-2, BCL-xL, brain derived neurotrophic factor (BDNF), adrenomedullin, iNOS, VEGF, erythropoietin, p21 and hexokinases (Sharp et al., 2004; Chen et al., 1997; Ruscher et al., 2002; Prass et al., 2003; Yanamoto et al., 2004). In the genomic arena, evidence strongly suggest that transcription factors such as hypoxia inducible factor (HIF), cAMP response element binding protein (CREB) and nuclear factor- κ B (NF- κ B) are driving the expression of these neuroprotective genes for the acquisition of ischemic tolerance (Blondeau et al., 2001; Simakajornboon et al., 2001; Digicaylioglu et al., 2001; Hara et al., 2003; Meller et al., 2005).

With a genome-wide approach, Stenzel-Poore analyzed cerebral gene expression alterations after ischemic preconditioning. Micro-array analysis revealed changes in gene expression patterns with little overlap among the conditions of injurious ischemia, ischemic preconditioning, or both. Authors suggested that preconditioning may lead to a fundamental reprogramming of the transcriptional response to ischemic injury, ultimately conferring a neuroprotective phenotype (Stenzel-Poore et al., 2003; Stenzel-Poore et al., 2004; Stenzel-Poore et al., 2007).

5.2.4 Involvement of histone acetylation in brain ischemic preconditioning

Despite numerous reports indicating major transcriptional activity following ischemic preconditioning, our current knowledge on the epigenomic cooperation towards the induction of neuroprotective gene expression is fragmentary. Certainly, the switching “on–off” of gene expression is the province of transcription factors and we now know the major transcription factors in the context of neuronal ischemic preconditioning, yet we are still at the brink of comprehending how factors other than the primary DNA sequence regulate the ability of these transcription factors to activate gene expression machinery. It is presently well-known that histone acetylation is a master epigenetic mechanism for the regulation of gene expression and enhanced histone acetylation patterns could be referred to as diagnostic signs of “genomic fertility”, indicating ongoing active gene expression processes. Here, our work provides the first demonstration of enhancement of histone acetylation after cerebral ischemic preconditioning. In our *in vitro* model, brief preconditioning ischemic episode increased acetylation levels of histone H4, histone H3 and histone H2B in neuronal cultures. Ischemic preconditioning induced increase in histone acetylation levels followed a dynamic pattern, suggesting that the rapid increases in histone acetylation levels following brief ischemia might be due to increased HAT and/or decreased HDAC enzyme activity, while the delayed increase at 24 hours could also be due to an increase of HAT and/or decrease of HDAC enzyme expressions.

In our *in vivo* system, brief preconditioning ischemic episode increased acetylation levels of histones in mice brain. Five minutes occlusion of left middle cerebral artery increased acetylation levels of histone H3 and histone H2B in mice brain one hour after the preconditioning stimulus. Strikingly, in brains of preconditioned animals, acetylation of the both histones was increased to a similar extent in both ipsilateral and also in contralateral hemispheres. Unlike the *in vitro* findings, acetylation levels of histone H4 was not altered at any of the time points examined after preconditioning. Certainly, this discrepancy in the induction of histone acetylation by ischemic preconditioning stimuli *in vitro* vs. *in vivo* could be attributed to several factors. Firstly, our *in vitro* system consists of near-pure neuronal cultures, while protein samples from mice brain are rather heterogenous in origin, having neuronal as well as glial and endothelial components. Although the exact cellular proportion, neuronal vs. glial and endothelial, is not known, it is expected that slight alterations of any

protein or posttranslational modification level restricted to only one cellular population is not easily detected by western immunoblotting technique using whole hemisphere protein lysates. Furthermore, we evidence that brief preconditioning ischemia enhances histone acetyltransferase activity in neuronal cultures. Total cellular histone acetyltransferase activity was increased in rat primary cortical cultures one hour after the preconditioning stimulus. However, we still do not know which HAT family might specifically be responsible for this alteration. On the other hand, while involvement of histone acetylation in brain ischemic preconditioning phenomenon has not been reported previously, HAT enzyme CBP was already linked to neuronal ischemic preconditioning by others (Meller et al., 2005). Using chromatin immunoprecipitation assay, Simon and colleagues strikingly revealed that it was not the binding of CREB, but of CBP to bcl-2 CRE site that increased after preconditioning ischemia, and blocking CBP binding to the bcl-2 CRE with U0126 (a kinase inhibitor) reduced bcl-2 expression and abrogated ischemic tolerance. Investigations for CBP's involvement in our ischemic preconditioning models are underway. It could be also equally interesting to test whether histone acetylation levels are altered at bcl-2 promoter region, as well as at the promoters of other prominent neuroprotective genes, following ischemic preconditioning stimulus. Moreover, whether reduced HDAC enzyme activity could also be involved in ischemic preconditioning-induced histone acetylation enhancements remain to be investigated.

5.3 NEUROPROTECTION BY TRICHOSTATIN A PRE-TREATMENT

Here, we present that HDAC inhibitor Trichostatin A (TSA) increases histone acetylation levels, up-regulates neuroprotective protein gelsolin and ultimately confers neuroprotection against ischemic injury in mice brain as well as in primary cortical cultures of rat. In an *in vivo* model, TSA increased levels of histone acetylation and gelsolin expression, an anti-apoptotic and anti-excitotoxic protein, in mice brain and significantly reduced cerebral infarct volumes after middle cerebral artery occlusion (MCAo). In rat primary cortical cultures, TSA increased histone acetylation levels, up-regulated gelsolin protein and subsequently led to neuroprotection against combined oxygen-glucose deprivation (OGD). Previously, it was presented in my MSc thesis that TSA failed in protecting gelsolin-deficient cortical cultures from oxygen-glucose deprivation. Here, we show that TSA does not afford protection of

gelsolin-deficient mice against middle cerebral artery occlusion, further underscoring gelsolin's integral role for TSA-induced neuroprotection against cerebral ischemic damage. Alterations of filamentous actin cytoskeleton, reduction in ischemia-led intracellular calcium overload and stabilization of mitochondrial membrane potential were the underlying downstream mechanisms of neuroprotection by TSA.

5.3.1 Histone deacetylase inhibitors are already in clinical use

Histone deacetylase inhibitors, like TSA, reside among the most promising anticancer agents that are potent inducers of growth arrest, differentiation, apoptosis of transformed cells and inhibition of angiogenesis (Liu et al. 2006). In October 2006, the US Food and Drug Administration (FDA) approved the first drug of this new class, SAHA, vorinostat (1, Zolinza, Merck) for the treatment of cutaneous T cell lymphoma. Several other HDAC inhibitors are currently investigated in clinical trials. HDAC inhibitors have shown significant activity against a variety of hematological and solid tumors at doses that are well tolerated by patients, both in monotherapy as well as in combination with other drugs. Activities of both histone acetyltransferases and histone deacetylases have been reported to affect angiogenesis, cell-cycle arrest, apoptosis, terminal differentiation of different cell types, and the pathogenesis of malignant disease (Chung et al., 2002). Therefore, functions of histone deacetylase inhibitors as anticancer agents are manifold.

5.3.2 HDAC inhibition in experimental models of neurodegenerative and psychiatric diseases

Recent years have witnessed a tremendous increase in the number of studies suggesting HDAC inhibitors as novel treatment strategies against neurological diseases. Pharmacological inhibition of HDAC activity was shown to protect neurons in numerous models of neurodegeneration including spinal muscular atrophy (Avila et al., 2007), Huntington's disease (Ferrante et al., 2003; Hockly et al., 2003; Ryu et al., 2003), amyotrophic lateral sclerosis (Ryu et al., 2005; Petri et al., 2006), experimental autoimmune encephalitis (Camelo et al., 2005) and neuronal oxidative stress (Langley et al., 2005; Langley et al., 2008) which is

a common pathological event in many neurodegenerative conditions, independent of different aetiologies. Mutant htt and other polyglutamine-expansion proteins have been reported to sequester CREB-binding protein (CBP), causing inhibition of its HAT activity. Consequent histone hypoacetylation was reported to be reversed by HDAC inhibitor administration in *Drosophila* as well as in mouse models of polyglutamine pathogenesis (Steffan et al., 2001). SAHA and sodium butyrate were shown to ameliorate motor impairments, improve body weight, delay neuropathological effects and extend survival (Ryu et al., 2003; Hockly et al., 2003). Sodium butyrate appears to be a potential therapeutic agent for two other polyglutamine-expansion diseases, namely spinal and bulbar muscular atrophy (SBMA) and dentatorubral-pallidoluysian atrophy (DRPLA) (Minamiyama et al., 2004; Ying et al., 2006). HDAC inhibitors were also suggested to be effective against several psychiatric disorders. Depression is one of these pathological conditions in which there is strong evidence suggesting histone acetylation as a valid therapeutic target (Tsankova et al., 2007). Furthermore, some anti-depressant agents such as valproic acid, an anti-convulsant and mood-stabilizing drug, were reported to exert HDAC inhibitory functions (Faraco et al., 2006). Eric Nestler and co-workers reported that the tricyclic anti-depressant imipramine, partly by reducing levels of HDAC 5, increased histone acetylation at BDNF promoter region in the hippocampus. Imipramine overcame chronic social defeat stress, prevented hypermethylation of the BDNF locus and reversed its subsequent downregulation (Tsankova et al., 2006). Sodium butyrate improved performance in tail suspension test, a mouse model of antidepressant efficacy, and further enhanced the efficacy of selective serotonin re-uptake inhibitor fluoxetine (Schroeder et al., 2007).

5.3.3 Induction of cell death vs. cell protection by HDAC inhibitors

The apparent paradox between the cell death inducing effect of HDAC inhibition in cancer cells and the protective effect in the central nervous system may be explained by differences in the signalling pathways of cell death vs. survival in cancer cells vs. differentiated post-mitotic neurons. Moreover, acetylation patterns at neuronal genes are strikingly different in neuronal vs. non-neuronal tissues (Huang et al., 1999, Roopra et al., 2001). The situation within the CNS, however, maybe even more complex, as a number of studies that have used HDAC inhibitors to ascertain HDAC involvement in neuronal survival have provided

conflicting results. For instance, while inhibition of HDACs were shown to block neuronal loss in *Drosophila* and mouse models of HD (Steffan et al., 2001; Hockly et al., 2003; Ferrante et al., 2003), there were reports suggesting that treatment of cerebellar granule neurons (CGNs) with HDAC inhibitors actively induced apoptosis (Salminen et al., 1998; Boutillier et al., 2002; Boutillier et al., 2003). However, it should be pointed out that the HDAC inhibitor doses used in these studies were much higher than the neuroprotective TSA doses we utilized in our study. Other studies in CGNs have reported that VPA causes induction of alpha-synuclein and confers neuroprotection against glutamate excitotoxicity (Leng et al., 2006). It was also demonstrated that HDAC inhibitors enhance neuronal cell death by neurotoxins (Kim et al. 2004).

The opposing effects of HDAC inhibitors amongst various neurodegeneration paradigms may well be explained by the tissue and stage-specific expression of different classes of HDACs. In this connection, it is noteworthy to point out that HDACs are non-redundant in their biological function (De Ruijter et al., 2003; Lehrmann et al., 2002; Glaser et al., 2003; Verdin et al., 2003; Marks et al., 2004). HDACs targets include histones and non-histone proteins which regulate gene expression and proteins involved in regulation of cell cycle progression, and cell death (Lehrmann et al., 2002; Johnstone and Licht, 2003; Warrener et al., 2003; Di Gennaro et al., 2004; Marks et al., 2004; Rosato and Grant, 2004; Drummond et al., 2005). Different HDACs associate with different co-repressors and activators. The expression of different HDACs through embryonic development changes with different stages of embryogenesis, and targeted disruption of different HDAC family members, therefore, result in different pathologies (Marks et al., 2004; Sengupta and Seto, 2004; Drummond et al., 2005). Evidence suggests that members of HDAC family may have opposing actions, even within the CNS, as is the case for HDAC 5 and 9 in mammalian neuronal survival and HDAC 1 and 3 in *C. elegans* neuronal survival (Morrison et al., 2007). Therefore, it is not surprising that broad spectrum HDAC inhibitors could yield confusing results, and such inhibition could conceivably cause undesirable side effects. Synthesis of inhibitors against specific HDACs is currently a major focus of the studies conducted in the field.

5.3.4 Trichostatin A protects against cerebral ischemia

Here, we successfully utilized TSA against *in vitro* and *in vivo* models of cerebral ischemia. TSA caused a significant reduction in cerebral infarct volumes after filamentous middle cerebral artery occlusion (MCAo) for one hour. TSA was given to mice at a dose of 5mg/kg body weight by daily intra-peritoneal injections for 14 days prior to the experimental stroke. In agreement with this result, TSA pre-treatment at a concentration of 300nM for 12 or 24 hours protected rat primary cortical cultures against combined oxygen-glucose deprivation (OGD). Measurement of lactate dehydrogenase (LDH) in medium conferred that neuroprotective TSA pre-treatment regimes did not cause any basal toxicity to neurons in cell culture conditions. In line, there was no evidence of intoxication of mice following 14 days of TSA treatment at 5mg/kg body weight dose. Neuroprotective TSA treatment regimes enhanced acetylation of histone H4 in mice brain, acetylation of histone H4 as well as histone H3 in primary cortical cultures, and consequently up-regulated neuroprotective protein gelsolin both in mice brain and in rat primary cortical cultures. Gelsolin is an actin-severing protein which was reported, by our group as well as by others, to exert anti-apoptotic and anti-excitotoxic effects (Harms et al., 2004). In my MSc thesis, I had already demonstrated that TSA enhanced histone H4 acetylation levels at gelsolin promoter region and consequently increased gelsolin mRNA levels in rat primary cortical cultures. This data not only evidenced a causal link between histone acetylation enhancement and increased gelsolin expression, but it also underscored the targeted neuroprotective gene induction by TSA. Here, we present that gelsolin mRNA increase is also translated into its protein levels *in vitro* as well as *in vivo*. Immunocytochemical approach demonstrated that neurons which had high histone acetylation levels in their nuclei also displayed increased gelsolin immunoreactivity in their cell body. My MSc thesis previously showed that primary cortical cultures of gelsolin-deficient mice were not protected by TSA against oxygen-glucose deprivation. In line, here we demonstrate that TSA did not afford protection of gelsolin-deficient mice against middle cerebral artery occlusion, further highlighting gelsolin's integral role for TSA-induced neuroprotection against cerebral ischemic injury. Besides, our immunocytochemical stainings revealed a heterogenous histone acetylation pattern in cortical cultures, with or without TSA treatment, and neurons with highly acetylated nuclei appeared to survive ischemic insult better, suggesting once again a causal link between histone acetylation and neuronal susceptibility to ischemic damage. We suggest that, in addition to gelsolin-mediated neuroprotection, TSA by

increasing number of neurons with highly-acetylated nuclei could increase the number of neurons surviving the injury caused by combined oxygen-glucose deprivation.

5.3.5 Other HDAC inhibitors are also beneficial against cerebral ischemia

Neuroprotective effects against cerebral ischemic injury were also suggested for other HDAC inhibitors such as valproic acid (VPA), sodium butyrate, sodium phenyl butyrate and SAHA. Subcutaneous injection of VPA at a dose of 300 mg/kg immediately after ischemia was found to decrease infarct size and reduce ischemia-induced neurological deficit scores measured at 24 and 48 hours after the ischemic onset (Ren et al., 2004). VPA treatments resulted in a time-dependent increase in acetylated histone H3 and heat shock protein 70 (HSP70) expression in the cortex and striatum of rat. Although reported to be well-tolerated by rats, admittedly 300mg/kg VPA used in this study is much higher than 5mg/kg TSA dose we used in our study, underscoring the potency of TSA as an HDAC inhibitor. Using VPA in experiments could obviously be advantageous that it is already a clinically available drug, on the other hand, the dose 300mg/kg body weight in rats once again appears to be far higher than the dose used for the treatment of epileptic, bipolar and/or headache patients, which ranges from 500mg to 3000mg for 70kg average human body weight. These dose discrepancies of VPA in rats *vs.* humans may well be explained by different pharmacokinetics in two species. Nevertheless whether VPA inhibits HDACs in humans at its currently used therapeutic doses and what dose could be required for achievement of neuroprotection against stroke by VPA in humans remain to be investigated.

In another study SAHA reduced infarct size in a mouse model of focal cerebral ischemia when administrated intraperitoneally twice, immediately and 6 hours after the ischemic onset (Faraco et al., 2006). Similar to our *in vitro* findings, histone H3 acetylation levels were markedly decreased in the ischemic brain tissue subjected to 6 hours of middle cerebral artery occlusion. SAHA treatment of mice not only increased histone H3 acetylation levels but also led to upregulation of neuroprotective proteins Hsp70 and bcl-2 in mice brain. Sodium phenyl butyrate (4-PBA) is another clinically available drug which was also shown to confer neuroprotection in a mouse model of hypoxia-ischemia (Qi et al., 2004). The underlying

mechanisms of neuroprotection by 4-PBA were suggested to be via inhibition of ER stress-mediated apoptosis and inflammation. Recently, an anti-inflammatory effect in association with protection against cerebral ischemia was also attributed to TSA in a rat permanent middle cerebral artery occlusion (pMCAo) model. Post-pMCAo injections with three HDAC inhibitors, trichostatin A (0.5 mg/kg), VPA (300mg/kg) and sodium butyrate (300mg/kg) decreased brain infarct volume (Kim et al., 2007). Similar to our in vitro results and findings of others, authors reported a marked decrease in the acetylation levels of histone H3 in the ischemic brain (Ren et al., 2004; Faraco et al., 2006), which was prevented by treatment with VPA, sodium butyrate or TSA. In addition to induction of neuroprotective genes such as heat-shock protein 70 and bcl-2, post-insult treatment with VPA or sodium butyrate also suppressed microglial activation, reduced the number of microglia and inhibited other inflammatory markers in the ischemic brain. We currently do not know whether any anti-inflammatory effect of TSA plays a role in the neuroprotection achieved in our study.

In the present study, we employed TSA, a potent inhibitor of HDAC class I and II families. It inhibits HDACs at nanomolar concentrations in vitro and in vivo at much lower doses compared to other HDAC inhibitors. Side effects of high-dose drug intake might thereby be avoided, increasing tolerability in living organisms. It is probably due to this reason that chemical structure of TSA was taken as a template to develop novel potent and specific HDAC inhibitors for potential therapeutic use (Furumai et al., 2001). TSA was first isolated in 1976 as an anti-fungal antibiotic (Tsuji et al. 1976) and like suberoylanilide hydroxamic acid (SAHA) it belongs to the hydroxamic acid family of HDAC inhibitors. Interestingly both TSA and SAHA appear to have relatively brief effects on histone acetylation in vivo. In humans, oral SAHA has been shown to induce a rapid increase in acetylated histones in blood within 2 hours, with a return to baseline levels by 8 hours (O'Connor et al., 2006). Avila and co-workers observed transient increases in gene expression 2-6 hours after TSA dosing in a mouse model of spinal muscular atrophy (Avila et al., 2007). Similarly, Faraco reported that a single dose of SAHA transiently increased histone acetylation within the normal brain with a ~8-fold increase within 6 hours, maintained up to 12 hours and returned back to baseline by 48 hours (Faraco et al., 2006). In our current experimental system, only 5 mg/kg for 14 days TSA conferred relevant changes in histone acetylation and gelsolin expression while 1 mg/kg for 14 days TSA failed to do so. Accordingly only 5 but not 1 mg/kg TSA provided stroke protection. We previously followed pre-treatment protocols with single dose TSA treatment

or pre-treatment for up to 4 days. These treatment regimes neither increased histone acetylation nor did they afford neuroprotection (data not shown), which might be explained by the dynamic and reversible nature of histone acetylation. Therefore, a protocol of 14 days continuous TSA pre-treatment of mice was chosen in this project. We had no possibility to measure TSA levels in plasma and CNS tissue, yet there was no evidence of intoxication and the behaviour of the animals was apparently normal. Physiological parameters in TSA-treated animals were within normal limits. Due to the differences in metabolism between mouse and man, however, it is not clear which dose would be necessary to achieve augmentation of histone acetylation and up-regulation of gelsolin expression in human brain.

5.3.6 Induction of gelsolin by Trichostatin A and subsequent down-stream events

Our data suggests that up-regulation of actin-severing protein gelsolin is an integral mediator of neuroprotection by TSA against experimental cerebral ischemia. Gelsolin-deficient (gsn *-/-*) mice or cortical cultures from gelsolin-deficient mice were not protected against ischemic injury by the neuroprotective TSA pre-treatment protocols. Gelsolin is an 85 kDa protein widely expressed throughout the nervous system which has a critical role in actin filament dynamics (Kwiatkowski et al., 1988; Witke et al., 1995). It severs actin filaments and caps the growing ends of filaments thereby leading to net actin filament disassembly. It should be noted that the induction observed with the 1 mg/kg/day TSA dose was somewhat less pronounced (but clearly evident) for histone acetylation than for gelsolin, while 5 mg/kg/day TSA dose induced strong increase in the levels of both acetylated histone and gelsolin protein. Previously, my MSc thesis evidenced a causal link between enhancement of histone acetylation and up-regulation of gelsolin expression, by presenting that TSA enhanced histone acetylation levels at the gelsolin promoter region (Meisel et al., 2006). We and others previously identified the putative mechanism by which gelsolin provides stroke protection: Brain ischemia promotes neuronal depolarization, which activates voltage-dependent calcium channels and ligand-gated calcium channels via the release of glutamate. Subsequently, massive calcium influx into the cells leads to activation of death-promoting intracellular enzymes. Calcium also activates gelsolin, which in turn mediates dynamic changes, net depolymerisation, in the actin filament network. This actin remodeling event leads to channel rundown, inactivation and stabilization of intracellular calcium levels (Hoshikawa et al.,

1994; Furukawa et al., 1997; Endres et al., 1999). Similarly, agents that induce actin depolymerization such as cytochalasin A also provide stroke protection. Moreover, actin reorganization in the postsynaptic density leading to transient retraction of dendritic spines was recently proposed by Simon's group to be a novel mechanism underlying neuroprotection by rapid ischemic tolerance (Meller et al., 2008). Here, we demonstrate that TSA caused reduction in filamentous actin levels and that this reduction sustained even after exposure of cortical cultures to combined oxygen-glucose deprivation. In vivo, we showed that filamentous actin levels were decreased in brains of wildtype but not gelsolin-deficient mice by TSA treatment. Noteworthy, our group has previously reported increased levels of filamentous actin in gelsolin-deficient neurons (Harms et al., 2004). Other than filamentous actin cytoskeleton, we studied intracellular calcium levels and presented that neuroprotective TSA pre-treatment of primary cortical cultures significantly decreased oxygen-glucose deprivation-triggered intracellular calcium overload. Further, alterations in mitochondrial membrane potential was examined, as gelsolin is known to exert specific anti-apoptotic properties via stabilization of mitochondrial permeability transition which is also mediated by actin remodeling (Harms et al., 2004). Indeed, oxygen-glucose deprivation-caused loss of mitochondrial membrane potential was preserved when cortical neurons were pre-treated with TSA.

5.3.7 Other gene targets of HDAC inhibitors

Other authors also observed pronounced up-regulation of gelsolin amongst a large number of genes by several HDAC inhibitors, however, obviously gelsolin could not be the only gene induced by TSA (Hoshikawa et al., 1994; Mielnicki et al., 1999; Han et al., 2000). Heat shock protein 70 (HSP70) and Bcl-2 were prominently up-regulated by several HDAC inhibitors in brain tissue as well as in cultured neuronal cells and play a major role in cerebral ischemia-protection (Ren et al., 2004; Faraco et al., 2006; Kim et al., 2007). Other candidate genes induced by HDAC inhibition that were implicated in cell survival and maintenance and hence may contribute to stroke-protection include p21WAF/Cip1, e2f1, glutamate receptor 2 (GluR2), brain-derived neurotrophic factor (BDNF), glucose regulated protein 78 and glial cell line-derived neurotrophic factor (Langley B et al., 2008; Nakano et al., 1997; Sowa et al., 1997; Martinez-Balbas et al., 2000; Huang et al., 2002; Ryu et al., 2003; Bown et al., 2000).

In addition to enhancing acetylation of histones, TSA, VPA and sodium butyrate may exert their neuroprotective effects through acetylation of the transcription factor SP-1 which facilitates the expression of neuroprotective protein HSP70 (Ren et al., 2004). Overall, altered histone acetylation in response to cellular injury is a gene and promoter-specific regulatory event rather than a general phenomenon operating over large expanses in the genomic arena (Huang et al., 2002). In vitro studies have shown that only a small percentage (2%) of genes in the human genome become transcriptionally active in response to HDAC inhibition (Van Lint et al., 1996; Marks et al., 2001).

6 CONCLUSION

The most significant findings of my PhD thesis could be concluded as following:

1 Histone acetylation and HAT enzyme CBP levels are dramatically lost following neuronal ischemic injury. Constraint function and/or availability of CBP, by genetic as well as by pharmacological means, and consequent histone hypoacetylation resulted in increased susceptibility to neuronal ischemic injury. These findings underpin CBP's intact function and histone acetylation homeostasis as determinant factors for neuronal survival after ischemic injury. In addition to cerebral ischemia, given the diversity of the affected neuronal populations and aetiopathologies of the diseases, such as polyglutamine diseases, Alzheimers disease and amyotrophic lateral sclerosis, loss of CBP function and/or availability and subsequent histone hypoacetylation could be postulated as common traits of neurodegeneration. Thus, CBP activators and/or drugs that increase CBP stabilization could reveal as potent neuroprotective drugs.

2 In contrast to injurious ischemia, ischemic preconditioning stimuli increase histone acetylation levels in neuronal cultures and in mice brain and confer robust protection against in vivo and in vitro models of brain ischemic injury. Total cellular HAT activity was enhanced in neurons after ischemic preconditioning stimulus. I speculate that histone acetylation enzyme machinery might be part of an endogenous neuroprotective program which, in response to ischemic preconditioning stimulus, open chromatin environment for expression of neuroprotective genes necessary for the acquisition of ischemia tolerant state.

3 The HDAC inhibitor TSA enhances histone acetylation levels and confers robust neuroprotection against in vitro and in vivo models of brain ischemic injury. TSA up-regulated gelsolin protein levels in neuronal cultures and in mice brain, and the down-stream protective pathways involved dynamic actin remodelling, reduction in intracellular calcium overload and stabilisation of mitochondrial membrane potential. TSA did not protect gelsolin knockout mice against cerebral ischemia, a result which underscored gelsolin up-regulation as the predominant mechanism of neuroprotection by TSA. Altogether, these results suggest that HDAC inhibition and consequent up-regulation of gelsolin protein appear as an attractive

novel prophylactic treatment strategy for reducing brain injury following cerebral ischemia. Given that currently there is no effective treatment for stroke, HDAC inhibitors like TSA should be evaluated for their potential use for clinical trials in stroke patients.

7 REFERENCES

Alarcon JM, Malleret G, Touzani K, Vronskaya S, Ishii S, Kandel ER, Barco A (2004) Chromatin acetylation, memory, and LTP are impaired in CBP^{+/-} mice: a model for the cognitive deficit in Rubinstein-Taybi syndrome and its amelioration. *Neuron* 42:947-959.

Allfrey VG, Littau VC, Mirsky AE (1963) On the role of of histones in regulation ribonucleic acid synthesis in the cell nucleus. *Proc Natl Acad Sci U S A* 49:414-421.

Arboix A, Cabeza N, Garcia-Eroles L, Massons J, Oliveres M, Targa C, Balcells M (2004) Relevance of transient ischemic attack to early neurological recovery after nonlacunar ischemic stroke. *Cerebrovasc Dis* 18:304-311.

Avila AM, Burnett BG, Taye AA, Gabanella F, Knight MA, Hartenstein P, Cizman Z, Di Prospero NA, Pellizzoni L, Fischbeck KH, Sumner CJ (2007) Trichostatin A increases SMN expression and survival in a mouse model of spinal muscular atrophy. *J Clin Invest* 117:659-671.

Balasubramanyam M, Koteswari AA, Kumar RS, Monickaraj SF, Maheswari JU, Mohan V (2003) Curcumin-induced inhibition of cellular reactive oxygen species generation: novel therapeutic implications. *J Biosci* 28:715-721.

Balasubramanyam K, Swaminathan V, Ranganathan A, Kundu TK (2003) Small molecule modulators of histone acetyltransferase p300. *J Biol Chem* 278:19134-19140.

Balasubramanyam K, Varier RA, Altaf M, Swaminathan V, Siddappa NB, Ranga U, Kundu TK (2004) Curcumin, a novel p300/CREB-binding protein-specific inhibitor of acetyltransferase, represses the acetylation of histone/nonhistone proteins and histone acetyltransferase-dependent chromatin transcription. *J Biol Chem* 279:51163-51171.

Barone FC, White RF, Spera PA, Ellison J, Currie RW, Wang X, Feuerstein GZ (1998) Ischemic preconditioning and brain tolerance: temporal histological and functional outcomes,

protein synthesis requirement, and interleukin-1 receptor antagonist and early gene expression. *Stroke* 29:1937-1950; discussion 1950-1931.

Bederson JB, Pitts LH, Tsuji M, Nishimura MC, Davis RL, Bartkowski H (1986) Rat middle cerebral artery occlusion: evaluation of the model and development of a neurologic examination. *Stroke* 17:472-476.

Bernaudin M, Nedelec AS, Divoux D, MacKenzie ET, Petit E, Schumann-Bard P (2002) Normobaric hypoxia induces tolerance to focal permanent cerebral ischemia in association with an increased expression of hypoxia-inducible factor-1 and its target genes, erythropoietin and VEGF, in the adult mouse brain. *J Cereb Blood Flow Metab* 22:393-403.

Bird A (2002) DNA methylation patterns and epigenetic memory. *Genes Dev* 16:6-21.

Bird A (2007) Perceptions of epigenetics. *Nature* 447:396-398.

Blanco M, Aneiros A, Lema M, Castillo J. Transient ischemic attack (TIA): a clinical model of ischemic tolerance. *Cerebrovasc Dis* 1999; 9: 9.

Blondeau N, Widmann C, Lazdunski M, Heurteaux C (2001) Activation of the nuclear factor-kappaB is a key event in brain tolerance. *J Neurosci* 21:4668-4677.

Boutillier AL, Trinh E, Loeffler JP (2002) Constitutive repression of E2F1 transcriptional activity through HDAC proteins is essential for neuronal survival. *Ann N Y Acad Sci* 973:438-442.

Boutillier AL, Trinh E, Loeffler JP (2003) Selective E2F-dependent gene transcription is controlled by histone deacetylase activity during neuronal apoptosis. *J Neurochem* 84:814-828.

Bown CD, Wang JF, Young LT (2000) Increased expression of endoplasmic reticulum stress proteins following chronic valproate treatment of rat C6 glioma cells. *Neuropharmacology* 39:2162-2169.

Bruce AJ, Boling W, Kindy MS, Peschon J, Kraemer PJ, Carpenter MK, Holtzman FW, Mattson MP (1996) Altered neuronal and microglial responses to excitotoxic and ischemic brain injury in mice lacking TNF receptors. *Nat Med* 2:788-794.

Bruer U, Weih MK, Isaev NK, Meisel A, Ruscher K, Bergk A, Trendelenburg G, Wiegand F, Victorov IV, Dirnagl U (1997) Induction of tolerance in rat cortical neurons: hypoxic preconditioning. *FEBS Lett* 414:117-121.

Bruno V, Battaglia G, Copani A, D'Onofrio M, Di Iorio P, De Blasi A, Melchiorri D, Flor PJ, Nicoletti F (2001) Metabotropic glutamate receptor subtypes as targets for neuroprotective drugs. *J Cereb Blood Flow Metab* 21:1013-1033.

Camelo S, Iglesias AH, Hwang D, Due B, Ryu H, Smith K, Gray SG, Imitola J, Duran G, Assaf B, Langley B, Khoury SJ, Stephanopoulos G, De Girolami U, Ratan RR, Ferrante RJ, Dangond F (2005) Transcriptional therapy with the histone deacetylase inhibitor trichostatin A ameliorates experimental autoimmune encephalomyelitis. *J Neuroimmunol* 164:10-21.

Cao CX, Yang QW, Lv FL, Cui J, Fu HB, Wang JZ (2007) Reduced cerebral ischemia-reperfusion injury in Toll-like receptor 4 deficient mice. *Biochem Biophys Res Commun* 353:509-514.

Caplan LR (2000) Acute stroke: seeing the full picture. *Hosp Pract (Minneapolis)* 35:65-71; discussion 71-62; quiz 113.

Carapeti M, Aguiar RC, Watmore AE, Goldman JM, Cross NC (1999) Consistent fusion of MOZ and TIF2 in AML with inv(8)(p11q13). *Cancer Genet Cytogenet* 113:70-72.

Chen J, Graham SH, Zhu RL, Simon RP (1996) Stress proteins and tolerance to focal cerebral ischemia. *J Cereb Blood Flow Metab* 16:566-577.

Chen J, Graham SH, Nakayama M, Zhu RL, Jin K, Stetler RA, Simon RP (1997) Apoptosis repressor genes Bcl-2 and Bcl-x-long are expressed in the rat brain following global ischemia. *J Cereb Blood Flow Metab* 17:2-10.

Choi DW (1995) Calcium: still center-stage in hypoxic-ischemic neuronal death. *Trends Neurosci* 18:58-60.

Chung D (2002) Histone modification: the 'next wave' in cancer therapeutics. *Trends Mol Med* 8:S10-11.

Coyle JT, Puttfarcken P (1993) Oxidative stress, glutamate, and neurodegenerative disorders. *Science* 262:689-695.

Cregan SP, Fortin A, MacLaurin JG, Callaghan SM, Cecconi F, Yu SW, Dawson TM, Dawson VL, Park DS, Kroemer G, Slack RS (2002) Apoptosis-inducing factor is involved in the regulation of caspase-independent neuronal cell death. *J Cell Biol* 158:507-517

Dahl NA, Balfour WM (1964) Prolonged Anoxic Survival Due to Anoxia Pre-Exposure: Brain Atp, Lactate, and Pyruvate. *Am J Physiol* 207:452-456.

Danielisova V, Nemethova M, Gottlieb M, Burda J (2005) Changes of endogenous antioxidant enzymes during ischemic tolerance acquisition. *Neurochem Res* 30:559-565.

de Ruijter AJ, van Gennip AH, Caron HN, Kemp S, van Kuilenburg AB (2003) Histone deacetylases (HDACs): characterization of the classical HDAC family. *Biochem J* 370:737-749.

del Zoppo GJ (1997) Microvascular responses to cerebral ischemia/inflammation. *Ann N Y Acad Sci* 823:132-147.

del Zoppo G, Ginis I, Hallenbeck JM, Iadecola C, Wang X, Feuerstein GZ (2000) Inflammation and stroke: putative role for cytokines, adhesion molecules and iNOS in brain response to ischemia. *Brain Pathol* 10:95-112.

Di Gennaro E, Bruzzese F, Caraglia M, Abruzzese A, Budillon A (2004) Acetylation of proteins as novel target for antitumor therapy: review article. *Amino Acids* 26:435-441.

- Digicaylioglu M, Lipton SA (2001) Erythropoietin-mediated neuroprotection involves cross-talk between Jak2 and NF-kappaB signalling cascades. *Nature* 412:641-647.
- Dirnagl U, Iadecola C, Moskowitz MA (1999) Pathobiology of ischaemic stroke: an integrated view. *Trends Neurosci* 22:391-397.
- Dirnagl U, Simon RP, Hallenbeck JM (2003) Ischemic tolerance and endogenous neuroprotection. *Trends Neurosci* 26:248-254.
- Drummond DC, Noble CO, Kirpotin DB, Guo Z, Scott GK, Benz CC (2005) Clinical development of histone deacetylase inhibitors as anticancer agents. *Annu Rev Pharmacol Toxicol* 45:495-528.
- Eckner R, Ewen ME, Newsome D, Gerdes M, DeCaprio JA, Lawrence JB, Livingston DM (1994) Molecular cloning and functional analysis of the adenovirus E1A-associated 300-kD protein (p300) reveals a protein with properties of a transcriptional adaptor. *Genes Dev* 8:869-884.
- Endres M, Fink K, Zhu J, Stagliano NE, Bondada V, Geddes JW, Azuma T, Mattson MP, Kwiatkowski DJ, Moskowitz MA (1999) Neuroprotective effects of gelsolin during murine stroke. *J Clin Invest* 103:347-354.
- Endres M, Meisel A, Biniszkiwicz D, Namura S, Prass K, Ruscher K, Lipski A, Jaenisch R, Moskowitz MA, Dirnagl U (2000) DNA methyltransferase contributes to delayed ischemic brain injury. *J Neurosci* 20:3175-3181.
- Faraco G, Pancani T, Formentini L, Mascagni P, Fossati G, Leoni F, Moroni F, Chiarugi A (2006) Pharmacological inhibition of histone deacetylases by suberoylanilide hydroxamic acid specifically alters gene expression and reduces ischemic injury in the mouse brain. *Mol Pharmacol* 70:1876-1884.
- Ferrante RJ, Kubilus JK, Lee J, Ryu H, Beesen A, Zucker B, Smith K, Kowall NW, Ratan RR, Luthi-Carter R, Hersch SM (2003) Histone deacetylase inhibition by sodium butyrate

chemotherapy ameliorates the neurodegenerative phenotype in Huntington's disease mice. *J Neurosci* 23:9418-9427.

Finnin MS, Donigian JR, Cohen A, Richon VM, Rifkind RA, Marks PA, Breslow R, Pavletich NP (1999) Structures of a histone deacetylase homologue bound to the TSA and SAHA inhibitors. *Nature* 401:188-193.

Furukawa K, Fu W, Li Y, Witke W, Kwiatkowski DJ, Mattson MP (1997) The actin-severing protein gelsolin modulates calcium channel and NMDA receptor activities and vulnerability to excitotoxicity in hippocampal neurons. *J Neurosci* 17:8178-8186.

Furumai R, Komatsu Y, Nishino N, Khochbin S, Yoshida M, Horinouchi S (2001) Potent histone deacetylase inhibitors built from trichostatin A and cyclic tetrapeptide antibiotics including trapoxin. *Proc Natl Acad Sci U S A* 98:87-92.

Gayther SA, Batley SJ, Linger L, Bannister A, Thorpe K, Chin SF, Daigo Y, Russell P, Wilson A, Sowter HM, Delhanty JD, Ponder BA, Kouzarides T, Caldas C (2000) Mutations truncating the EP300 acetylase in human cancers. *Nat Genet* 24:300-303.

Gertz K, Priller J, Kronenberg G, Fink KB, Winter B, Schrock H, Ji S, Milosevic M, Harms C, Bohm M, Dirnagl U, Laufs U, Endres M (2006) Physical activity improves long-term stroke outcome via endothelial nitric oxide synthase-dependent augmentation of neovascularization and cerebral blood flow. *Circ Res* 99:1132-1140.

Glaser KB, Li J, Staver MJ, Wei RQ, Albert DH, Davidsen SK (2003) Role of class I and class II histone deacetylases in carcinoma cells using siRNA. *Biochem Biophys Res Commun* 310:529-536.

Gong C, Qin Z, Betz AL, Liu XH, Yang GY (1998) Cellular localization of tumor necrosis factor alpha following focal cerebral ischemia in mice. *Brain Res* 801:1-8.

Gonzalez RG (2006) Imaging-guided acute ischemic stroke therapy: From "time is brain" to "physiology is brain". *AJNR Am J Neuroradiol* 27:728-735.

Grabb MC, Choi DW (1999) Ischemic tolerance in murine cortical cell culture: critical role for NMDA receptors. *J Neurosci* 19:1657-1662.

Grant PA, Berger SL (1999) Histone acetyltransferase complexes. *Semin Cell Dev Biol* 10:169-177.

Grunstein M (1992) Histones as regulators of genes. *Sci Am* 267:68-74B.

Hacke W, Kaste M, Bluhmki E, Brozman M, Davalos A, Guidetti D, Larrue V, Lees KR, Medeghri Z, Machnig T, Schneider D, von Kummer R, Wahlgren N, Toni D (2008) Thrombolysis with alteplase 3 to 4.5 hours after acute ischemic stroke. *N Engl J Med* 359:1317-1329.

Halliwell B, Cross CE (1994) Oxygen-derived species: their relation to human disease and environmental stress. *Environ Health Perspect* 102 Suppl 10:5-12.

Han JW, Ahn SH, Park SH, Wang SY, Bae GU, Seo DW, Kwon HK, Hong S, Lee HY, Lee YW, Lee HW (2000) Apicidin, a histone deacetylase inhibitor, inhibits proliferation of tumor cells via induction of p21WAF1/Cip1 and gelsolin. *Cancer Res* 60:6068-6074.

Hansen JC, Tse C, Wolffe AP (1998) Structure and function of the core histone N-termini: more than meets the eye. *Biochemistry* 37:17637-17641.

Hara T, Hamada J, Yano S, Morioka M, Kai Y, Ushio Y (2003) CREB is required for acquisition of ischemic tolerance in gerbil hippocampal CA1 region. *J Neurochem* 86:805-814.

Harms C, Lautenschlager M, Bergk A, Katchanov J, Freyer D, Kapinya K, Herwig U, Megow D, Dirnagl U, Weber JR, Hortnagl H (2001) Differential mechanisms of neuroprotection by 17 beta-estradiol in apoptotic versus necrotic neurodegeneration. *J Neurosci* 21:2600-2609.

Harms C, Bosel J, Lautenschlager M, Harms U, Braun JS, Hortnagl H, Dirnagl U, Kwiatkowski DJ, Fink K, Endres M (2004) Neuronal gelsolin prevents apoptosis by enhancing actin depolymerization. *Mol Cell Neurosci* 25:69-82.

Hebbes TR, Thorne AW, Crane-Robinson C (1988) A direct link between core histone acetylation and transcriptionally active chromatin. *EMBO J* 7:1395-1402.

Heiskanen KM, Bhat MB, Wang HW, Ma J, Nieminen AL (1999) Mitochondrial depolarization accompanies cytochrome c release during apoptosis in PC6 cells. *J Biol Chem* 274:5654-5658.

Hockly E, Richon VM, Woodman B, Smith DL, Zhou X, Rosa E, Sathasivam K, Ghazi-Noori S, Mahal A, Lowden PA, Steffan JS, Marsh JL, Thompson LM, Lewis CM, Marks PA, Bates GP (2003) Suberoylanilide hydroxamic acid, a histone deacetylase inhibitor, ameliorates motor deficits in a mouse model of Huntington's disease. *Proc Natl Acad Sci U S A* 100:2041-2046.

Hoshikawa Y, Kwon HJ, Yoshida M, Horinouchi S, Beppu T (1994) Trichostatin A induces morphological changes and gelsolin expression by inhibiting histone deacetylase in human carcinoma cell lines. *Exp Cell Res* 214:189-197.

Huang Y, Myers SJ, Dingledine R (1999) Transcriptional repression by REST: recruitment of Sin3A and histone deacetylase to neuronal genes. *Nat Neurosci* 2:867-872.

Huang Y, Doherty JJ, Dingledine R (2002) Altered histone acetylation at glutamate receptor 2 and brain-derived neurotrophic factor genes is an early event triggered by status epilepticus. *J Neurosci* 22:8422-8428.

Huang J, Upadhyay UM, Tamargo RJ (2006) Inflammation in stroke and focal cerebral ischemia. *Surg Neurol* 66:232-245.

Hughes RE (2002) Polyglutamine disease: acetyltransferases awry. *Curr Biol* 12:R141-143.

Impey S, Fong AL, Wang Y, Cardinaux JR, Fass DM, Obrietan K, Wayman GA, Storm DR, Soderling TR, Goodman RH (2002) Phosphorylation of CBP mediates transcriptional activation by neural activity and CaM kinase IV. *Neuron* 34:235-244.

Janoff A (1964) Alterations in Lysosomes (Intracellular Enzymes) during Shock; Effects of Preconditioning (Tolerance) and Protective Drugs. *Int Anesthesiol Clin* 2:251-269.

Jenuwein T, Allis CD (2001) Translating the histone code. *Science* 293:1074-1080.

Jeppesen P, Turner BM (1993) The inactive X chromosome in female mammals is distinguished by a lack of histone H4 acetylation, a cytogenetic marker for gene expression. *Cell* 74:281-289.

Jiang H, Nucifora FC, Jr., Ross CA, DeFranco DB (2003) Cell death triggered by polyglutamine-expanded huntingtin in a neuronal cell line is associated with degradation of CREB-binding protein. *Hum Mol Genet* 12:1-12.

Jiang H, Poirier MA, Liang Y, Pei Z, Weiskittel CE, Smith WW, DeFranco DB, Ross CA (2006) Depletion of CBP is directly linked with cellular toxicity caused by mutant huntingtin. *Neurobiol Dis* 23:543-551.

Jin K, Mao XO, Simon RP, Greenberg DA (2001) Cyclic AMP response element binding protein (CREB) and CREB binding protein (CBP) in global cerebral ischemia. *J Mol Neurosci* 16:49-56.

Johnstone RW, Licht JD (2003) Histone deacetylase inhibitors in cancer therapy: is transcription the primary target? *Cancer Cell* 4:13-18.

Jones NM, Bergeron M (2004) Hypoxia-induced ischemic tolerance in neonatal rat brain involves enhanced ERK1/2 signaling. *J Neurochem* 89:157-167.

Katchanov J, Harms C, Gertz K, Hauck L, Waeber C, Hirt L, Priller J, von Harsdorf R, Bruck W, Hortnagl H, Dirnagl U, Bhide PG, Endres M (2001) Mild cerebral ischemia induces loss

of cyclin-dependent kinase inhibitors and activation of cell cycle machinery before delayed neuronal cell death. *J Neurosci* 21:5045-5053.

Kato H, Liu Y, Araki T, Kogure K (1991) Temporal profile of the effects of pretreatment with brief cerebral ischemia on the neuronal damage following secondary ischemic insult in the gerbil: cumulative damage and protective effects. *Brain Res* 553:238-242.

Kemp PJ, Peers C (2007) Oxygen sensing by ion channels. *Essays Biochem* 43:77-90.

Kim HS, Kim EM, Kim NJ, Chang KA, Choi Y, Ahn KW, Lee JH, Kim S, Park CH, Suh YH (2004) Inhibition of histone deacetylation enhances the neurotoxicity induced by the C-terminal fragments of amyloid precursor protein. *J Neurosci Res* 75:117-124.

Kim HJ, Rowe M, Ren M, Hong JS, Chen PS, Chuang DM (2007) Histone deacetylase inhibitors exhibit anti-inflammatory and neuroprotective effects in a rat permanent ischemic model of stroke: multiple mechanisms of action. *J Pharmacol Exp Ther* 321:892-901.

Kirino T, Tsujita Y, Tamura A (1991) Induced tolerance to ischemia in gerbil hippocampal neurons. *J Cereb Blood Flow Metab* 11:299-307.

Kirino T (2002) Ischemic tolerance. *J Cereb Blood Flow Metab* 22:1283-1296.

Kitagawa K, Matsumoto M, Tagaya M, Hata R, Ueda H, Niinobe M, Handa N, Fukunaga R, Kimura K, Mikoshiba K, et al. (1990) 'Ischemic tolerance' phenomenon found in the brain. *Brain Res* 528:21-24.

Kitagawa K, Matsumoto M, Kuwabara K, Tagaya M, Ohtsuki T, Hata R, Ueda H, Handa N, Kimura K, Kamada T (1991) 'Ischemic tolerance' phenomenon detected in various brain regions. *Brain Res* 561:203-211.

Koh JY, Choi DW (1987) Quantitative determination of glutamate mediated cortical neuronal injury in cell culture by lactate dehydrogenase efflux assay. *J Neurosci Methods* 20:83-90.

Korzus E, Rosenfeld MG, Mayford M (2004) CBP histone acetyltransferase activity is a critical component of memory consolidation. *Neuron* 42:961-972.

Kouzarides T (1999) Histone acetylases and deacetylases in cell proliferation. *Curr Opin Genet Dev* 9:40-48.

Kronenberg G, Wang LP, Synowitz M, Gertz K, Katchanov J, Glass R, Harms C, Kempermann G, Kettenmann H, Endres M (2005) Nestin-expressing cells divide and adopt a complex electrophysiologic phenotype after transient brain ischemia. *J Cereb Blood Flow Metab* 25:1613-1624.

Kuo MH, Allis CD (1998) Roles of histone acetyltransferases and deacetylases in gene regulation. *Bioessays* 20:615-626.

Kwiatkowski DJ (1988) Predominant induction of gelsolin and actin-binding protein during myeloid differentiation. *J Biol Chem* 263:13857-13862.

Langley B, Gensert JM, Beal MF, Ratan RR (2005) Remodeling chromatin and stress resistance in the central nervous system: histone deacetylase inhibitors as novel and broadly effective neuroprotective agents. *Curr Drug Targets CNS Neurol Disord* 4:41-50.

Langley B, D'Annibale MA, Suh K, Ayoub I, Tolhurst A, Bastan B, Yang L, Ko B, Fisher M, Cho S, Beal MF, Ratan RR (2008) Pulse inhibition of histone deacetylases induces complete resistance to oxidative death in cortical neurons without toxicity and reveals a role for cytoplasmic p21(waf1/cip1) in cell cycle-independent neuroprotection. *J Neurosci* 28:163-176.

Lau OD, Kundu TK, Soccio RE, Ait-Si-Ali S, Khalil EM, Vassilev A, Wolffe AP, Nakatani Y, Roeder RG, Cole PA (2000) HATs off: selective synthetic inhibitors of the histone acetyltransferases p300 and PCAF. *Mol Cell* 5:589-595.

- Lautenschlager M, Onufriev MV, Gulyaeva NV, Harms C, Freyer D, Sehmsdorf U, Ruscher K, Moiseeva YV, Arnswald A, Victorov I, Dirnagl U, Weber JR, Hortnagl H (2000) Role of nitric oxide in the ethylcholine aziridinium model of delayed apoptotic neurodegeneration in vivo and in vitro. *Neuroscience* 97:383-393.
- Lehnardt S, Lehmann S, Kaul D, Tschimmel K, Hoffmann O, Cho S, Krueger C, Nitsch R, Meisel A, Weber JR (2007) Toll-like receptor 2 mediates CNS injury in focal cerebral ischemia. *J Neuroimmunol* 190:28-33.
- Lehrmann H, Pritchard LL, Harel-Bellan A (2002) Histone acetyltransferases and deacetylases in the control of cell proliferation and differentiation. *Adv Cancer Res* 86:41-65.
- Leng Y, Chuang DM (2006) Endogenous alpha-synuclein is induced by valproic acid through histone deacetylase inhibition and participates in neuroprotection against glutamate-induced excitotoxicity. *J Neurosci* 26:7502-7512.
- Liu Y, Kato H, Nakata N, Kogure K (1992) Protection of rat hippocampus against ischemic neuronal damage by pretreatment with sublethal ischemia. *Brain Res* 586:121-124.
- Liu YZ, Chrivia JC, Latchman DS (1998) Nerve growth factor up-regulates the transcriptional activity of CBP through activation of the p42/p44(MAPK) cascade. *J Biol Chem* 273:32400-32407.
- Liu D, Lu C, Wan R, Auyeung WW, Mattson MP (2002) Activation of mitochondrial ATP-dependent potassium channels protects neurons against ischemia-induced death by a mechanism involving suppression of Bax translocation and cytochrome c release. *J Cereb Blood Flow Metab* 22:431-443.
- Liu B, Liao M, Mielke JG, Ning K, Chen Y, Li L, El-Hayek YH, Gomez E, Zukin RS, Fehlings MG, Wan Q (2006) Ischemic insults direct glutamate receptor subunit 2-lacking AMPA receptors to synaptic sites. *J Neurosci* 26:5309-5319.

-
- Liu T, Kuljaca S, Tee A, Marshall GM (2006) Histone deacetylase inhibitors: multifunctional anticancer agents. *Cancer Treat Rev* 32:157-165.
- Lo EH, Dalkara T, Moskowitz MA (2003) Mechanisms, challenges and opportunities in stroke. *Nat Rev Neurosci* 4:399-415.
- Lonze BE, Ginty DD (2002) Function and regulation of CREB family transcription factors in the nervous system. *Neuron* 35:605-623.
- Lonze BE, Riccio A, Cohen S, Ginty DD (2002) Apoptosis, axonal growth defects, and degeneration of peripheral neurons in mice lacking CREB. *Neuron* 34:371-385.
- Luger K, Rechsteiner TJ, Flaus AJ, Waye MM, Richmond TJ (1997) Characterization of nucleosome core particles containing histone proteins made in bacteria. *J Mol Biol* 272:301-311.
- Manteuffel-Cymborowska M (1999) Nuclear receptors, their coactivators and modulation of transcription. *Acta Biochim Pol* 46:77-89.
- Marambaud P, Wen PH, Dutt A, Shioi J, Takashima A, Siman R, Robakis NK (2003) A CBP binding transcriptional repressor produced by the PS1/epsilon-cleavage of N-cadherin is inhibited by PS1 FAD mutations. *Cell* 114:635-645.
- Marks P, Rifkind RA, Richon VM, Breslow R, Miller T, Kelly WK (2001) Histone deacetylases and cancer: causes and therapies. *Nat Rev Cancer* 1:194-202.
- Marks PA, Richon VM, Miller T, Kelly WK (2004) Histone deacetylase inhibitors. *Adv Cancer Res* 91:137-168.
- Martinez-Balbas MA, Bauer UM, Nielsen SJ, Brehm A, Kouzarides T (2000) Regulation of E2F1 activity by acetylation. *EMBO J* 19:662-671.

Matsushima K, Hakim AM (1995) Transient forebrain ischemia protects against subsequent focal cerebral ischemia without changing cerebral perfusion. *Stroke* 26:1047-1052.

McCampbell A, Taylor JP, Taye AA, Robitschek J, Li M, Walcott J, Merry D, Chai Y, Paulson H, Sobue G, Fischbeck KH (2000) CREB-binding protein sequestration by expanded polyglutamine. *Hum Mol Genet* 9:2197-2202.

McCampbell A, Taye AA, Whitty L, Penney E, Steffan JS, Fischbeck KH (2001) Histone deacetylase inhibitors reduce polyglutamine toxicity. *Proc Natl Acad Sci U S A* 98:15179-15184.

Meisel A, Harms C, Yildirim F, Bosel J, Kronenberg G, Harms U, Fink KB, Endres M (2006) Inhibition of histone deacetylation protects wild-type but not gelsolin-deficient neurons from oxygen/glucose deprivation. *J Neurochem* 98:1019-1031.

Meldrum DR, Cleveland JC, Jr., Rowland RT, Banerjee A, Harken AH, Meng X (1997) Early and delayed preconditioning: differential mechanisms and additive protection. *Am J Physiol* 273:H725-733.

Meller R, Minami M, Cameron JA, Impey S, Chen D, Lan JQ, Henshall DC, Simon RP (2005) CREB-mediated Bcl-2 protein expression after ischemic preconditioning. *J Cereb Blood Flow Metab* 25:234-246.

Meller R, Thompson SJ, Lusardi TA, Ordonez AN, Ashley MD, Jessick V, Wang W, Torrey DJ, Henshall DC, Gafken PR, Saugstad JA, Xiong ZG, Simon RP (2008) Ubiquitin proteasome-mediated synaptic reorganization: a novel mechanism underlying rapid ischemic tolerance. *J Neurosci* 28:50-59.

Mielnicki LM, Ying AM, Head KL, Asch HL, Asch BB (1999) Epigenetic regulation of gelsolin expression in human breast cancer cells. *Exp Cell Res* 249:161-176.

Miller BA, Perez RS, Shah AR, Gonzales ER, Park TS, Gidday JM (2001) Cerebral protection by hypoxic preconditioning in a murine model of focal ischemia-reperfusion. *Neuroreport* 12:1663-1669.

Minamiyama M, Katsuno M, Adachi H, Waza M, Sang C, Kobayashi Y, Tanaka F, Doyu M, Inukai A, Sobue G (2004) Sodium butyrate ameliorates phenotypic expression in a transgenic mouse model of spinal and bulbar muscular atrophy. *Hum Mol Genet* 13:1183-1192.

Minta A, Kao JP, Tsien RY (1989) Fluorescent indicators for cytosolic calcium based on rhodamine and fluorescein chromophores. *J Biol Chem* 264:8171-8178.

Moncayo J, de Freitas GR, Bogousslavsky J, Altieri M, van Melle G (2000) Do transient ischemic attacks have a neuroprotective effect? *Neurology* 54:2089-2094.

Morrison BE, Majdzadeh N, D'Mello SR (2007) Histone deacetylases: focus on the nervous system. *Cell Mol Life Sci* 64:2258-2269.

Murry CE, Jennings RB, Reimer KA (1986) Preconditioning with ischemia: a delay of lethal cell injury in ischemic myocardium. *Circulation* 74:1124-1136.

Nakano K, Mizuno T, Sowa Y, Orita T, Yoshino T, Okuyama Y, Fujita T, Ohtani-Fujita N, Matsukawa Y, Tokino T, Yamagishi H, Oka T, Nomura H, Sakai T (1997) Butyrate activates the WAF1/Cip1 gene promoter through Sp1 sites in a p53-negative human colon cancer cell line. *J Biol Chem* 272:22199-22206.

Namura S, Zhu J, Fink K, Endres M, Srinivasan A, Tomaselli KJ, Yuan J, Moskowitz MA (1998) Activation and cleavage of caspase-3 in apoptosis induced by experimental cerebral ischemia. *J Neurosci* 18:3659-3668.

Nawashiro H, Brenner M, Fukui S, Shima K, Hallenbeck JM (2000) High susceptibility to cerebral ischemia in GFAP-null mice. *J Cereb Blood Flow Metab* 20:1040-1044.

Ng HH, Bird A (2000) Histone deacetylases: silencers for hire. *Trends Biochem Sci* 25:121-126.

Nishi S, Taki W, Uemura Y, Higashi T, Kikuchi H, Kudoh H, Satoh M, Nagata K (1993) Ischemic tolerance due to the induction of HSP70 in a rat ischemic recirculation model. *Brain Res* 615:281-288.

Nishimura M, Sugino T, Nozaki K, Takagi Y, Hattori I, Hayashi J, Hashimoto N, Moriguchi T, Nishida E (2003) Activation of p38 kinase in the gerbil hippocampus showing ischemic tolerance. *J Cereb Blood Flow Metab* 23:1052-1059.

Nucifora FC, Jr., Sasaki M, Peters MF, Huang H, Cooper JK, Yamada M, Takahashi H, Tsuji S, Troncoso J, Dawson VL, Dawson TM, Ross CA (2001) Interference by huntingtin and atrophin-1 with cbp-mediated transcription leading to cellular toxicity. *Science* 291:2423-2428.

O'Connor OA, Heaney ML, Schwartz L, Richardson S, Willim R, MacGregor-Cortelli B, Curly T, Moskowitz C, Portlock C, Horwitz S, Zelenetz AD, Frankel S, Richon V, Marks P, Kelly WK (2006) Clinical experience with intravenous and oral formulations of the novel histone deacetylase inhibitor suberoylanilide hydroxamic acid in patients with advanced hematologic malignancies. *J Clin Oncol* 24:166-173.

Ogryzko VV, Schiltz RL, Russanova V, Howard BH, Nakatani Y (1996) The transcriptional coactivators p300 and CBP are histone acetyltransferases. *Cell* 87:953-959.

Peng PL, Zhong X, Tu W, Soundarapandian MM, Molner P, Zhu D, Lau L, Liu S, Liu F, Lu Y (2006) ADAR2-dependent RNA editing of AMPA receptor subunit GluR2 determines vulnerability of neurons in forebrain ischemia. *Neuron* 49:719-733.

Petri S, Kiaei M, Kipiani K, Chen J, Calingasan NY, Crow JP, Beal MF (2006) Additive neuroprotective effects of a histone deacetylase inhibitor and a catalytic antioxidant in a transgenic mouse model of amyotrophic lateral sclerosis. *Neurobiol Dis* 22:40-49.

Pogo BG, Allfrey VG, Mirsky AE (1966) RNA synthesis and histone acetylation during the course of gene activation in lymphocytes. *Proc Natl Acad Sci U S A* 55:805-812.

Prass K, Scharff A, Ruscher K, Lowl D, Muselmann C, Victorov I, Kapinya K, Dirnagl U, Meisel A (2003) Hypoxia-induced stroke tolerance in the mouse is mediated by erythropoietin. *Stroke* 34:1981-1986.

Qi X, Hosoi T, Okuma Y, Kaneko M, Nomura Y (2004) Sodium 4-phenylbutyrate protects against cerebral ischemic injury. *Mol Pharmacol* 66:899-908.

Redner RL, Wang J, Liu JM (1999) Chromatin remodeling and leukemia: new therapeutic paradigms. *Blood* 94:417-428.

Ren M, Leng Y, Jeong M, Leeds PR, Chuang DM (2004) Valproic acid reduces brain damage induced by transient focal cerebral ischemia in rats: potential roles of histone deacetylase inhibition and heat shock protein induction. *J Neurochem* 89:1358-1367.

Romanovskii DY, Tyul'kova EI, Samoilov MO (2001) Preconditioning hypobaric hypoxia prevents anoxia-induced inhibition of generation of focal potentials in slices of olfactory cortex from rat brain. *Bull Exp Biol Med* 132:1154-1156.

Roopra A, Huang Y, Dingleline R (2001) Neurological disease: listening to gene silencers. *Mol Interv* 1:219-228.

Rosato RR, Grant S (2004) Histone deacetylase inhibitors in clinical development. *Expert Opin Investig Drugs* 13:21-38.

Ross AM, Hurn P, Perrin N, Wood L, Carlini W, Potempa K (2007) Evidence of the peripheral inflammatory response in patients with transient ischemic attack. *J Stroke Cerebrovasc Dis* 16:203-207.

Rouaux C, Jokic N, Mbebi C, Boutillier S, Loeffler JP, Boutillier AL (2003) Critical loss of CBP/p300 histone acetylase activity by caspase-6 during neurodegeneration. *EMBO J* 22:6537-6549.

Ruscher K, Freyer D, Karsch M, Isaev N, Megow D, Sawitzki B, Priller J, Dirnagl U, Meisel A (2002) Erythropoietin is a paracrine mediator of ischemic tolerance in the brain: evidence from an in vitro model. *J Neurosci* 22:10291-10301.

Ryu H, Lee J, Olofsson BA, Mwidau A, Dedeoglu A, Escudero M, Flemington E, Azizkhan-Clifford J, Ferrante RJ, Ratan RR (2003) Histone deacetylase inhibitors prevent oxidative neuronal death independent of expanded polyglutamine repeats via an Sp1-dependent pathway. *Proc Natl Acad Sci U S A* 100:4281-4286.

Ryu H, Smith K, Camelo SI, Carreras I, Lee J, Iglesias AH, Dangond F, Cormier KA, Cudkovicz ME, Brown RH, Jr., Ferrante RJ (2005) Sodium phenylbutyrate prolongs survival and regulates expression of anti-apoptotic genes in transgenic amyotrophic lateral sclerosis mice. *J Neurochem* 93:1087-1098.

Salminen A, Tapiola T, Korhonen P, Suuronen T (1998) Neuronal apoptosis induced by histone deacetylase inhibitors. *Brain Res Mol Brain Res* 61:203-206.

Schiltz RL, Mizzen CA, Vassilev A, Cook RG, Allis CD, Nakatani Y (1999) Overlapping but distinct patterns of histone acetylation by the human coactivators p300 and PCAF within nucleosomal substrates. *J Biol Chem* 274:1189-1192.

Schroeder FA, Lin CL, Crusio WE, Akbarian S (2007) Antidepressant-like effects of the histone deacetylase inhibitor, sodium butyrate, in the mouse. *Biol Psychiatry* 62:55-64.

Sengupta N, Seto E (2004) Regulation of histone deacetylase activities. *J Cell Biochem* 93:57-67.

Sharp FR, Ran R, Lu A, Tang Y, Strauss KI, Glass T, Ardizzone T, Bernaudin M (2004) Hypoxic preconditioning protects against ischemic brain injury. *NeuroRx* 1:26-35.

Simakajornboon N, Gozal E, Gozal D (2001) Developmental patterns of NF-kappaB activation during acute hypoxia in the caudal brainstem of the rat. *Brain Res Dev Brain Res* 127:175-183.

Simon RP, Swan JH, Griffiths T, Meldrum BS (1984) Blockade of N-methyl-D-aspartate receptors may protect against ischemic damage in the brain. *Science* 226:850-852.

Simon RP, Niino M, Gwinn R (1993) Prior ischemic stress protects against experimental stroke. *Neurosci Lett* 163:135-137.

Snowden AW, Perkins ND (1998) Cell cycle regulation of the transcriptional coactivators p300 and CREB binding protein. *Biochem Pharmacol* 55:1947-1954.

Sowa Y, Orita T, Minamikawa S, Nakano K, Mizuno T, Nomura H, Sakai T (1997) Histone deacetylase inhibitor activates the WAF1/Cip1 gene promoter through the Sp1 sites. *Biochem Biophys Res Commun* 241:142-150.

Steffan JS, Kazantsev A, Spasic-Boskovic O, Greenwald M, Zhu YZ, Gohler H, Wanker EE, Bates GP, Housman DE, Thompson LM (2000) The Huntington's disease protein interacts with p53 and CREB-binding protein and represses transcription. *Proc Natl Acad Sci U S A* 97:6763-6768.

Steffan JS, Bodai L, Pallos J, Poelman M, McCampbell A, Apostol BL, Kazantsev A, Schmidt E, Zhu YZ, Greenwald M, Kurokawa R, Housman DE, Jackson GR, Marsh JL, Thompson LM (2001) Histone deacetylase inhibitors arrest polyglutamine-dependent neurodegeneration in *Drosophila*. *Nature* 413:739-743.

Stenzel-Poore MP, Stevens SL, Xiong Z, Lessov NS, Harrington CA, Mori M, Meller R, Rosenzweig HL, Tobar E, Shaw TE, Chu X, Simon RP (2003) Effect of ischaemic preconditioning on genomic response to cerebral ischaemia: similarity to neuroprotective strategies in hibernation and hypoxia-tolerant states. *Lancet* 362:1028-1037.

Stenzel-Poore MP, Stevens SL, Simon RP (2004) Genomics of preconditioning. *Stroke* 35:2683-2686.

Stenzel-Poore MP, Stevens SL, King JS, Simon RP (2007) Preconditioning reprograms the response to ischemic injury and primes the emergence of unique endogenous neuroprotective phenotypes: a speculative synthesis. *Stroke* 38:680-685.

- Strahl BD, Allis CD (2000) The language of covalent histone modifications. *Nature* 403:41-45.
- Sugawara T, Chan PH (2003) Reactive oxygen radicals and pathogenesis of neuronal death after cerebral ischemia. *Antioxid Redox Signal* 5:597-607.
- Takahashi J, Fujigasaki H, Zander C, El Hachimi KH, Stevanin G, Durr A, Lebre AS, Yvert G, Trottier Y, de The H, Hauw JJ, Duyckaerts C, Brice A (2002) Two populations of neuronal intranuclear inclusions in SCA7 differ in size and promyelocytic leukaemia protein content. *Brain* 125:1534-1543.
- Tamaru H, Selker EU (2001) A histone H3 methyltransferase controls DNA methylation in *Neurospora crassa*. *Nature* 414:277-283.
- Taniura H, Sng JC, Yoneda Y (2007) Histone modifications in the brain. *Neurochem Int* 51:85-91.
- Taylor JP, Taye AA, Campbell C, Kazemi-Esfarjani P, Fischbeck KH, Min KT (2003) Aberrant histone acetylation, altered transcription, and retinal degeneration in a *Drosophila* model of polyglutamine disease are rescued by CREB-binding protein. *Genes Dev* 17:1463-1468.
- Tsankova NM, Berton O, Renthal W, Kumar A, Neve RL, Nestler EJ (2006) Sustained hippocampal chromatin regulation in a mouse model of depression and antidepressant action. *Nat Neurosci* 9:519-525.
- Tsankova N, Renthal W, Kumar A, Nestler EJ (2007) Epigenetic regulation in psychiatric disorders. *Nat Rev Neurosci* 8:355-367.
- Tsuji N, Kobayashi M, Nagashima K, Wakisaka Y, Koizumi K (1976) A new antifungal antibiotic, trichostatin. *J Antibiot (Tokyo)* 29:1-6.
- Turner BM (2000) Histone acetylation and an epigenetic code. *Bioessays* 22:836-845.

- Van Lint C, Emiliani S, Verdin E (1996) The expression of a small fraction of cellular genes is changed in response to histone hyperacetylation. *Gene Expr* 5:245-253.
- Verdin E, Dequiedt F, Kasler HG (2003) Class II histone deacetylases: versatile regulators. *Trends Genet* 19:286-293.
- Warrener R, Beamish H, Burgess A, Waterhouse NJ, Giles N, Fairlie D, Gabrielli B (2003) Tumor cell-selective cytotoxicity by targeting cell cycle checkpoints. *FASEB J* 17:1550-1552.
- Wegener S, Gottschalk B, Jovanovic V, Knab R, Fiebach JB, Schellinger PD, Kucinski T, Jungehulsing GJ, Brunecker P, Muller B, Banasik A, Amberger N, Wernecke KD, Siebler M, Rother J, Villringer A, Weih M (2004) Transient ischemic attacks before ischemic stroke: preconditioning the human brain? A multicenter magnetic resonance imaging study. *Stroke* 35:616-621.
- Weih M, Kallenberg K, Bergk A, Dirnagl U, Harms L, Wernecke KD, Einhaupl KM (1999) Attenuated stroke severity after prodromal TIA: a role for ischemic tolerance in the brain? *Stroke* 30:1851-1854.
- Wiessner C, Gehrman J, Lindholm D, Topper R, Kreutzberg GW, Hossmann KA (1993) Expression of transforming growth factor-beta 1 and interleukin-1 beta mRNA in rat brain following transient forebrain ischemia. *Acta Neuropathol* 86:439-446.
- Witke W, Sharpe AH, Hartwig JH, Azuma T, Stossel TP, Kwiatkowski DJ (1995) Hemostatic, inflammatory, and fibroblast responses are blunted in mice lacking gelsolin. *Cell* 81:41-51.
- Wu C, Zhan RZ, Qi S, Fujihara H, Taga K, Shimoji K (2001) A forebrain ischemic preconditioning model established in C57Black/Crj6 mice. *J Neurosci Methods* 107:101-106.
- Yanamoto H, Xue JH, Miyamoto S, Nagata I, Nakano Y, Murao K, Kikuchi H (2004) Spreading depression induces long-lasting brain protection against infarcted lesion development via BDNF gene-dependent mechanism. *Brain Res* 1019:178-188.

Yao TP, Oh SP, Fuchs M, Zhou ND, Ch'ng LE, Newsome D, Bronson RT, Li E, Livingston DM, Eckner R (1998) Gene dosage-dependent embryonic development and proliferation defects in mice lacking the transcriptional integrator p300. *Cell* 93:361-372.

Ying M, Xu R, Wu X, Zhu H, Zhuang Y, Han M, Xu T (2006) Sodium butyrate ameliorates histone hypoacetylation and neurodegenerative phenotypes in a mouse model for DRPLA. *J Biol Chem* 281:12580-12586.

Yoshida M, Kijima M, Akita M, Beppu T (1990) Potent and specific inhibition of mammalian histone deacetylase both in vivo and in vitro by trichostatin A. *J Biol Chem* 265:17174-17179.
Zaremba J, Losy J (2001) Early TNF-alpha levels correlate with ischaemic stroke severity. *Acta Neurol Scand* 104:288-295.

Zhang W, Smith C, Monette R, Hutchison J, Stanimirovic DB (2000) Indomethacin and cyclosporin a inhibit in vitro ischemia-induced expression of ICAM-1 and chemokines in human brain endothelial cells. *Acta Neurochir Suppl* 76:47-53.

Ziegler G, Harhausen D, Schepers C, Hoffmann O, Rohr C, Prinz V, Konig J, Lehrach H, Nietfeld W, Trendelenburg G (2007) TLR2 has a detrimental role in mouse transient focal cerebral ischemia. *Biochem Biophys Res Commun* 359:574-579

Mein Lebenslauf wird aus Datenschutzgründen in der elektronischen Version meiner Arbeit nicht mit veröffentlicht.

PUBLICATIONS AND PRESENTATIONS

Publications

Meisel A, Harms C, **Yildirim F**, Bosel J, Kronenberg G, Harms U, Fink KB, Endres M (2006) Inhibition of histone deacetylation protects wild-type but not gelsolin-deficient neurons from oxygen/glucose deprivation. *J Neurochem* 98:1019-1031.

Yildirim F, Gertz K, Kronenberg G, Harms C, Fink KB, Meisel A, Endres M (2008) Inhibition of histone deacetylation protects wildtype but not gelsolin-deficient mice from ischemic brain injury. *Exp Neurol* 210:531-542.

Kronenberg G, Gertz K, Baldinger T, Eckart S, Ji S, **Yildirim F**, Heuser I, Schröck H, Kuschinsky W, Hörtnagl H, Djoufack PC, Hellweg R, Fink KB, Endres M Impact of actin filament stabilization on adult hippocampal and olfactory bulb neurogenesis in vivo (In revision)

Harms C, Hauck L, Katchanov J, Harms U, **Yildirim F**, Seidel K, Freyer D, Kronenberg G, Harsdorf R, Hörtnagl H, Endres M Loss of p130/E2F4 repressor complex initiates apoptosis in primary neurons (Manuscript in preparation)

Recent Presentations

Yildirim F, Ji S, Gertz K, Kronenberg G, Harms C, Barco A, Benito E, Olivares R, Endres M, Meisel A (2008) Histone acetylation and neuronal survival after experimental cerebral ischemia. Talk at Society of Neuroscience Meeting, Washington DC, USA

Yildirim F, Gertz K, Kronenberg G, Harms C, Fink KB, Endres M, Meisel A (2007) Neuroprotection by Trichostatin A-Involvement of histone acetylation in preconditioning against cerebral ischemia. Talk at Society of Neuroscience Meeting, San Diego, USA

Yildirim F, Gertz K, Ji S, Kronenberg G, Harms C, Endres M, Meisel A (2007) Epigenetic Mechanisms and Preconditioning against Experimental Models of Cerebral Ischemia. Poster presentation at Berlin Brain Days, Berlin, Germany

Yildirim F, Gertz K, Ji S, Kronenberg G, Harms C, Fink KB, Endres M, Meisel A (2007) Ischemic Tolerance and Epigenetic Mechanisms. Poster presentation at Neurizons Meeting, Göttingen, Germany

Yildirim F, Gertz K, Ji S, Kronenberg G, Harms C, Fink KB, Endres M, Meisel A (2007) Brain Ischemia and Epigenetics. Poster presentation at Epigenetics Meeting of European Molecular Biology Lab (EMBL), Heidelberg, Germany

Erklärung

Ich, Ferah Yildirim, erkläre, dass ich die vorgelegte Dissertation mit dem Thema: „Involvement of histone acetylation in neuroprotection against brain ischemic injury“ selbst verfasst und keine anderen als die angegebenen Quellen und Hilfsmittel benutzt, ohne die (unzulässige) Hilfe Dritter verfasst und auch in Teilen keine Kopien anderer Arbeiten dargestellt habe.

Berlin, den 01 Juli 2009

Ferah Yildirim